

*Republic of Iraq
Ministry of Higher Education
and Scientific Research
University of Kerbala
College of Engineering*



*Investigation of use of the Paraffin as a Phase
Change Material with Water in Solar Water
Heating Systems*

A Thesis

*Submitted to the College of Engineering / University of Kerbala in Partial
Fulfillment of the Requierments for the Degree of Master of Sience in
Mechanical Engineering –Thermal Fluids Field*

By

Hayder Sadoon Sachit

B.Sc. 1998

Supervised By

Prof. Dr. Abbas Sahi Shareef

Dr. Fadhel Noraldeen Abed Al-Mousawi

2020 A.D.

1440 A.H.

Supervisors' Certification

We certify that this thesis entitled (**Investigation of use of the Paraffin as a Phase Change Material with Water in Solar Water Heating Systems**) has been carried out under our supervision at the University of Kerbala / College of Engineering – Mechanical Engineering Department in partial fulfillment of the requirements for the degree of Master of Sciences in Mechanical Engineering /Thermal Fluids Field.

Signature:



Name: **Prof. Dr. Abbas Sahi Shareef**

Date: / / 2020

Signature:



Name: **Dr. Fadhel Noraldeen Abed Al-Mousawi**

Date: / / 2020

LINGUISTIC CERTIFICATE

I certify that the thesis entitled (**Investigation of use of the Paraffin as a Phase Change Material with Water in Solar Water Heating Systems**) which has been submitted by " **Hayder Sadoon Sachit** " has prepared under my linguistic supervision. Its language has been amended to meet the English style.

Signature:



Name: Dr. Hayder Jabbar Kurji

(Linguistic advisor)

College of Engineering

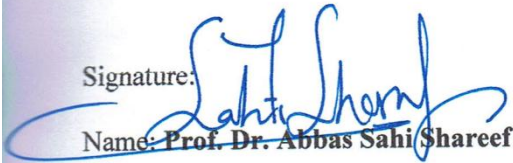
University of Kerbala

Date: / / 2020

EXAMINATION COMMITTEE CERTIFICATION

We certify that we have read this thesis entitled (**Investigation of use of the Paraffin as a Phase Change Material with Water in Solar Water Heating Systems**) and as an examining committee, examined the student (**Hayder Sadoon Sachit**), in its content and in what is connected with it, and that in our opinion it meets the standard of a thesis for the degree of Master of Science in Mechanical Engineering.

Signature:



Name: **Prof. Dr. Abbas Sahi Shareef**
(Supervisor)

Date: / / 2020

Signature:



Name: **Dr. Fadhel Noraldeen Abed Al-Mousawi**
(Supervisor)

Date: 25 / 10 / 2020

Signature:



Name: **Dr. Farhan Lafta Rashid**
(Member)

Date: 21 / 10 / 2020

Signature:



Name: **Assist. Prof. Dr. Hussam Ali Khalaf**
(Member)

Date: / / 2020

Signature:



Name: **Prof. Dr. Ahmed Kadhim Hussein**
(Chairman)

Date: / / 2020

Approval of Mechanical Engineering
Department

Signature:



Name: **Dr. Hayder Noori Mohammed**

(Head of Mechanical Engineering Dept.)

Date: 26 / 10 / 2020

Approval of Deanery of the College of
Engineering / University of Kerbala

Signature:



Name: **Assist. Prof. Dr. Laith S. Rasheed**

(Dean of Engineering College)

Date: / / 2020

بِسْمِ اللَّهِ الرَّحْمَنِ الرَّحِيمِ

وَأَمَّا بِنِعْمَةِ اللَّهِ فَكَلِمَةً نَبِيًّا

وَاللَّهُ أَعْلَمُ بِمَا تُشِيرُونَ
سورة هود ٨٨

صَدَقَ اللَّهُ الْعَالَمِينَ

Dedication

Thanks to God first for all his gifts.

To the one who was supportive of me in this world and did not give him much time, to the soul of (my brother martyr Alaa).

To those who are the reason for my existence in life (my dear father and my dear mother).

To those who lighted the way for me and support me and give up their rights, and who walked with me step by step (my wife) and to my hope in life and the future (my children).

To the candles that burn to light up to others to everyone who taught me a letter (my teachers).

To everyone who helped and encouraged me, my colleagues, and friends.

I dedicate this humble research, hoping the Almighty to find acceptance and success.

HAYDER SADOON

2020 A.D

Acknowledgments

*First, I would like to express my sincere gratitude and thanks to **ALLAH** (be glorious) for the guidance through this work and for all the blessings bestowed upon me.*

*I would like to gratefully and sincerely thank my supervisors **Prof. Dr. Abbas Sahi Shareef, and Dr. Fadhel Noraldeem Abed Al-Mousawi** for their invaluable help, advice, guidance, understanding, and encouragement during this work.*

I sincerely thank all the staff of the Mechanical Engineering Department of the University of Kerbela for their support and teaching.

I thank my family for their support which made me as ambitious as I wanted. I hope they always are well and able to get their satisfaction.

Finally, and most importantly, I would like to thank all my friends. Their continuous help, support, and encouragement enabled me to complete this thesis.

Hayder Sadoon

2020 A.D

Abstract

Solar energy is one of the most important sources of renewable energy used to reduce the effects of pollution and global warming as a result of burning fossil fuels; however, this energy is intermittent and available during daytime only. This research aims to experimentally and numerically study the possibility of improving the heat storage capacity of a solar water heating system by using phase change materials (PCMs). A PCM solar water heating system was designed and manufactured at the University of Kerbala under the climatic conditions of the City of Karbala in Iraq, and the system was experimentally tested for the period between 20 March to 20 April in 2019. Two main heat sources are used in this work; the first one is a flat plate solar collector connected directly to a water tank, and the second heat source was an electric heater element.

For flat plate solar collector configuration, the cases without PCM (the tank contains water only) and with 31% PCM (PCM containers were incorporated within the water tank) was experimentally tested under variable flow rates (1, 3, 5) L/min. The second heat source (an electric heater element) is used to avoid the effect of fluctuating in solar intensity on the PCM behaviour, and a similar scenario was repeated for the cases of without and with PCM. Paraffin wax which dissolves in range of (52 ± 2) °C was used as a PCM material and packed in cylindrical aluminium containers which immersed inside the water tank. Furthermore, numerical modelling using ANSYS Fluent was carried out (including the processes of melting and solidification of paraffin wax) to highlight the behaviour of the PCM material during the charging/discharging heat processes.

Results showed that integrating PCM materials with solar water heating systems is practical and useful as PCM materials can store an extra amount of

heat to be provided at night. Experimental results showed that the proposed PCM solar heating system could achieve a water temperature of about 9.3 °C higher than that of without using PCM and the improvement in hot water temperature due to the use of PCM reached up to 23 %. In contrast, the maximum improvement in heat storage due to the use of PCM is about 14 %. Also, results showed that adding copper mesh reduces the melting time by up to 12.5%; however, it affects the amount of heat storage negatively as a result of reducing the amount of paraffin wax. Finally, experimental and numerical data were validated, and a good agreements are achieved with an average deviation of about 5.17%.

Table of Contents

Abstract	I
Table of Contents	III
Nomenclature	VI
Chapter One – Introduction	1
1. General	2
1.1 Solar energy	2
1.2 Solar Water Heater Systems (SWHS)	4
1.2.1 Solar collector	4
1.2.1.1. Flat plate collector (FPC)	5
1.2.1.2. Evacuated tube collectors) ETC	6
1.2.1.3. Concentrating Collectors .	7
1.3 Solar energy storage	7
1.3.1. Sensible heat storage	8
1.3.2. Latent heat storage	8
1.4 Phase Chang materials PCM, and their characteristics	10
1.4.1. Phase-changing materials Categories	12
1.4.1.1. Organic PCMs.	12
1.5 Heat transfer enhancement	14
1.5.1 Macro encapsulation	14
1.5.2 Microencapsulation	15
1.5.3 Using extended surface	15
1.5.4 Adding particles to highly conductive materials	15
1.6 The aim of the Research	16
Chapter, Two - Literature Review	17
2.1 Experimental research	18
2.1.1. Incorporation PCM into thermal storage systems	18
2.1.2. Improved heat transfer and PCM geometry	22
2.2. Numerical and theoretically Research	26
2.2.1. PCM performance in the thermal storage system	26
2.2.2. Improving heat transfer coefficient and PCM geometry	27
2.3 The Scope of work	29
Chapter Three - MATHEMATICAL MODEL & NUMERICAL ANALYSIS	34
3.1. Assumptions.	35
3.2. Governing equations	36
3.3. Design modeler	37
3.4. Connection contacts	38
3.5. Mesh generation	43
3.6. Numerical solution setup	46
3.7. Boundary condition	47

3.8.The Numerical solution procedure	48
3.9. Flow Chart of numerical analysis	49
Chapter Four- Experimental Study	52
4.1.Place, and date of practical testing	53
4.2. Solar water heater system	53
4.2.1. Flat Plate Solar collector	53
4.2.2. Storage tank water	58
4.2.3. The electric pump	59
4.3. PCMs material	60
4.3.1. PCM module geometry and heat transfer enhancement.	61
4.4. Measurement devices	63
4.4.1. Temperature meter	63
4.4.2. Thermocouples.	63
4.4.3. Solar power meter	65
4.4.4. Flow meter	66
4.5. Experimental procedure.	66
4.6. Governing equations.	68
4.7. Repeatability Check	73
Chapter Five - Results And Discussion	74
5.1. Experimental Results	75
5.1.1. The solar collector, as heat source	75
5.1.1.1. Case 1 (without PCM)	77
5.1.1.2. Case 2 (with PCM)	82
5.1.1.3. Comparison between case 1(without PCM) and case 2 (with PCM	87
5.1.2. Electric driven heat storage system (using 1 kW heater element).	90
5.1.2.1. Case 4: Improving the thermal conductivity of the paraffin wax by adding copper mesh	95
5.2. The numerical results	98
5.2.1 Heat transfer in the tank water	98
5.2.2. Temperature distribution and Thermal energy storage	101
5.3. Validation numerical results with the experimental work	110
5.4. Validation with similar work	113
Chapter Six- Conclusions and Recommendation	115
6.1 Conclusions	116
6.2.Recommendations	117
Reference	118
Appendix .A	126
A.1Calculations of the Rayleigh number (Ra)	127
A.2 Calculation of the top loss coefficient of solar collector	128

A.3 The declination angles	129
A.4 Solar angles for horizontal, inclined and vertical surfaces	130
Appendix B	131
B.1. The temperature meter and thermocouple and Solar power meter	132
B.2. The Phase Change Material Specifications	135
B.3. Calibration of flowmeter	136
Appendix C	137
(C.1). Thermophysical properties of pure water	138
(C.2). Thermophysical properties of air at atmospheric	139

Nomenclature

Roman Symbols

Symbol	Description	Units
A_c	The area of solar collector	m^2
A_{pc}	Collector absorber area	m^2
C_p	Materials specified heat	$kJ/ kg.^{\circ}C$
D_i	Inlet Diameter of pipe	m
E	heat storage	kJ
F_R	The Heat removal factor	-
f	Friction factor	---
G_T	Global radiation	W/ m^2
g	Gravitational acceleration (9.81)	m/s^2
H	Enthalpy	J/kg
\bar{h}	Height of cylindrical container	mm
h_s	convective heat transfer coefficient	$W/m^2 K$
h_w	The wind loss coefficient	$W/ m^2 k$
I	Average insolation	W/ m^2
I_T	Total solar radiation	W/ m^2
K	Thermal conductivity	$W/m K$

L	Length	m
E	The latent heat to phase change	kJ/kg
m	mass	kg
\dot{m}	mass flow rate	kg/s
n	Refraction indices	–
n	Number of days	---
N_g	the number of glass	---
Q_i	collector energy absorbed	W
Q_u	useful energy gain	W
Q_{ui}	instantaneous useful energy	W
T	time	s
T	thickness	mm
T	temperature	°C
U_L	Overall heat loss coefficient	W/m ² °C
U_t	The top loss coefficient of solar collector	W/m ² °C
U_b	The back loss coefficient of solar collector	W/m ² °C
U_e	The edge loss coefficient of solar collector	W/m ² °C
V	Velocity of the wind	m/s

V	The volume of water	liter
W	width	mm
Nu	Nusselt number	-
Pr	Prandtl number	-
Re	Reynolds number	-
Ra	Rayleigh number	-

Subscripts	Description
L	PCM in liquid state
S	PCM in solid state
$Laten$	latent heat storage
$sensible$	sensible heat storage
pcm	phase change material
$loss$	surroundings heat loss
A	ambient air
F	final
P	absorber plate
I	initial
max	maximum
$melt$	melt temperature
min	average water temperature

mesh

mass of mesh

Greek Symbols

Symbol	Description	Units
$(\tau\alpha)_{av}$	Average transmittance- absorptance product	--
T	Glazing transition coefficient	--
τ_r	Transmittance with only reflection losses	—
τ_α	Transmittance with only absorption losses	—
α	plate absorption coefficient	—
A	thermal diffusivity	m ² /s
r	Reflection	---
β	Tilted angle of flat-plate collector	degrees
B	Thermal expansion coefficient	1/K
δ	The declination angle	degrees
ω	solar hour angle	degrees
θ_z	Zenith angle	Degree
φ	latitude angle	degrees
ε_p	The emissivity of plate	--
ε_g	The emissivity of glass	--

M	Dynamic viscosity	kg/m.s
N	Kinematic viscosity	m ² /s
ρ	Density	kg/m ³
H	Efficiency	--
η_{th}	thermal efficiency of a solar collector	--
η_i	instantaneous efficiency of the collector	--
η_o	overall efficiency of the solar heat system	--
Δ	Different between two value	---
∇	Nabla symbol	----
∂	Partial differential operator	---

Abbreviation

Symbol	Description
ANSYS	Analysis System
CFD	Computational Fluid Dynamics
HTF	Heat transfer fluid
FLUENT	Fluid and Heat Transfer Code
FPC	Flat Plate Collector
FVM	Finite Volume Method
l.ph	Liquid phase
PCM	Phase change material
s.ph	Solid phase
SWHS	Solar water heating system
SHS	Sensible heat
SIMPLE	Simi-Implicit Method for Pressure Linked Equation

**C
H
A
P
T
E
R**

1

INTRODUCTION

Chapter one

Introduction

1.General

In recent years, worldwide there is an increasing interest in renewable energy especially in developed countries to be used as alternative energy because of the high oil prices, and the environmental impact of air pollution due to CO₂ emissions. The global warming issue and the lack of rain have led to desertification in many areas around the world which has a significant impact on the Earth's climate and the life of living organisms, On the other hand, renewable energy, especially solar energy, is widely available, and feasible [1].

In the Middle East, oil-producing Arab countries in general and Iraq in particular, have not relied on solar energy because of the abundance of fossil fuels at present, which leads to not thinking seriously about the renewable energy. Moreover, in such countries, the environmental issue has not been in high priority yet. In contrast, in Western countries, solar energy has received considerable attention as a result of its easy collection and high potential in the production of heat and electricity, which reduce the reliance on fossil fuels. The exploitation of solar energy as a form of renewable energy in many applications such as solar water heating systems, it is necessary to know this energy and to clarify some information about it and how to collect it.

1.1 Solar energy

The sun is the main source of solar energy and the most important sources of renewable energy. The sun is a ball of burning gases with a diameter of about 1.4 million kilometres. The total amount of solar radiation energy reaching earth per year is about 5.46×10^{24} J. About 30% of this energy is reflected in

space, and clouds and particles in the air absorbs 20%. However, only 0.1% of the 10% of solar radiation that reaches the earth can provide the world with the energy it needs[1].

The Arab Gulf countries, including Iraq, are rich oil countries. However, these countries have a distinct geographical location through which they can exploit renewable energy sources like solar and wind energies. For example, Iraq has sunshine hours of about 3,000 hours per year with a solar radiation rate of about 4116 W/m² in January and 8,300 W/m² in June[2].

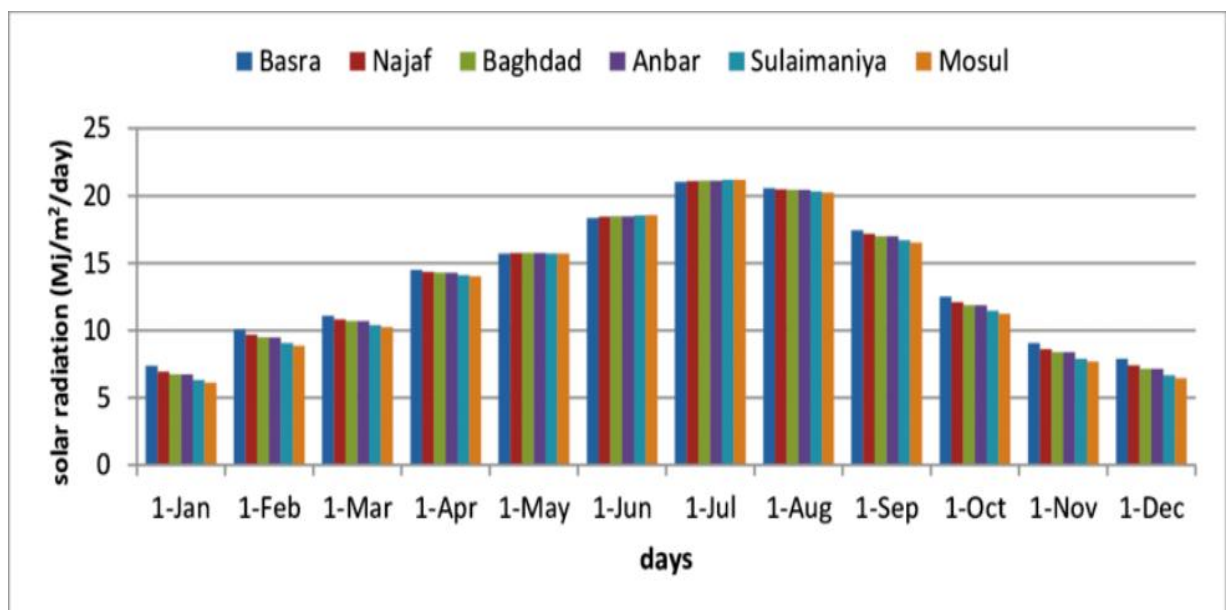


Figure 1-1. Solar radiation rate on flat surfaces[3]

Central regions and desert are the most exposed to solar radiation in Iraq and have a clear sky most of the year. However, this abundant amount of solar energy is not exploited to solve the problem of electricity in Iraq, which has begun since 1991[4]. Since ancient times, the human being has known the utility of solar energy and how to exploit it. Nowadays, solar energy can be used in different fields of domestic and industrial purposes, like heating buildings, drying crops, desalination of saline water or generating electricity [5]. In this work, a hot water solar system will be addressed.

1.2 Solar water heater systems (SWHS)

The system may include a pump to force the working fluid (water) to be effectively circulated through it, and in this case, it is called an active system. When the circulation is a natural process without using a pump, it is called a passive system, as shown in Figure 1-2. If the water is heated directly in the solar collector, the system is called an open-loop system. While, when using a secondary working fluid in the solar collector which passes through a heat exchanger situated in the water tank, the system in the case is called a closed-loop system [5, 6].

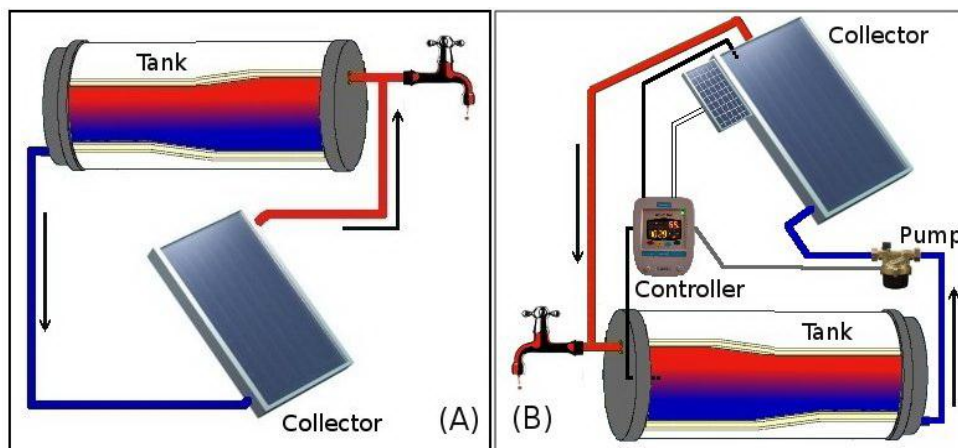


Figure 1-2. (A) passive system (B) active system [5]

1.2.1. Solar collector

The solar collector is one of the most important elements of the solar water heating system. Although there are different types of solar collectors, the concept of working is similar. The solar radiation energy is collected and converted into thermal energy which transferred to the working fluid (water). There are many types of solar collectors; however, the most famous ones can be classified as:

- ❖ No concentration collector (flat-plate, evacuated).

- ❖ Medium concentration collector (parabolic cylinder).
- ❖ High concentration collector (paraboloid).

Solar collectors are often placed on the roofs of houses facing the south orientation with an appropriate angle with the horizon line. Also, solar collectors can be designed to be stationary or moving collectors[7, 6].

1.2.1.1. Flat plate collector (FPC)

This kind is the most widely used, it is used to heat water or air for domestic use or to warm buildings or applications that do not require high temperatures ($<100\text{ }^{\circ}\text{C}$) and their efficiency ranges between 40% to 70%. Figure 1-3 shows the flat plate solar collector.

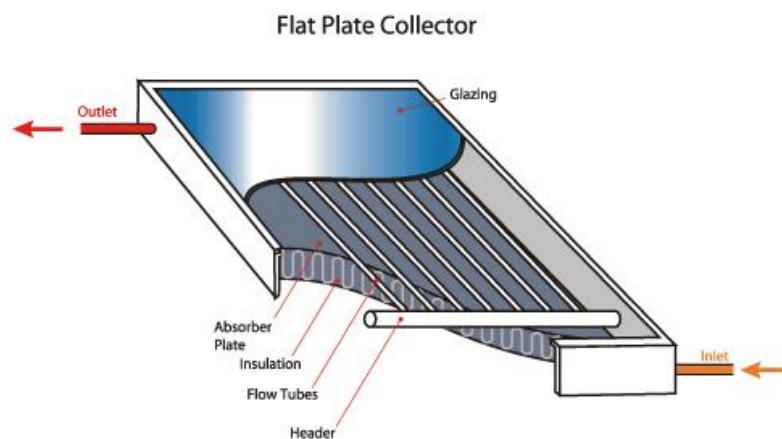


Figure 1-3. Flat plate collector[7]

It contains a thin absorbent layer with high thermal conductivity metal such as copper. The absorbent plate is coated with a black color to increase the energy absorbed from the sun. A set of copper tube is tightly fixed on the absorbent plate. The components are placed inside a wooden or plastic box and covered with a transparent glass to keep the collected heat inside the box and then save the energy. An insulation layer is placed in all the sides and the bottom of the box to reduce heat losses and often have glass wool.[6, 8].

1.2.1.2. Evacuated tube collectors (ETC)

Flat plate and evacuated tube solar collectors are the most widely used types of water heating systems, and they vary in cost and performance. It is important to choose the appropriate solar collector to reduce the cost and get hot water at an appropriate temperature. Therefore, the evacuated tube is used in applications where the required temperature reaches 170 °C [9]. Figure 1-4 shows the evacuated tube collectors.



Figure 1-4 . Evacuated tube collectors [9]

This type of solar collectors consists of a set of vacuum tubes to capture the solar energy that used to heat the water where the heat losses to the surroundings are very small because of the vacuum tubes. The only remaining loss is radiation loss. There are several types of these collectors, such as heat pipe collectors or direct flow collectors, and they can be with or without concentrator [10].

1.2.1.3. Concentrating collectors

This type is used in applications requiring high temperatures and are thus generally used to generate steam for Solar thermal power plants and are not

used in residential applications. The principle of its work depends on the use of a reflective surface to reflect solar radiation to the surface of absorption and then focus this energy to a focal point or focal line, it can be stationary or moveable to keep track of sunlight for high efficiency [11].

1.3 Solar energy storage

One of the biggest problems in the field of solar energy that it is variable and intermittent, therefore this energy must be stored. Solar energy can be stored in different ways, as shown in Figure 1-5, and it is essential to choose the right method for the required application [12].

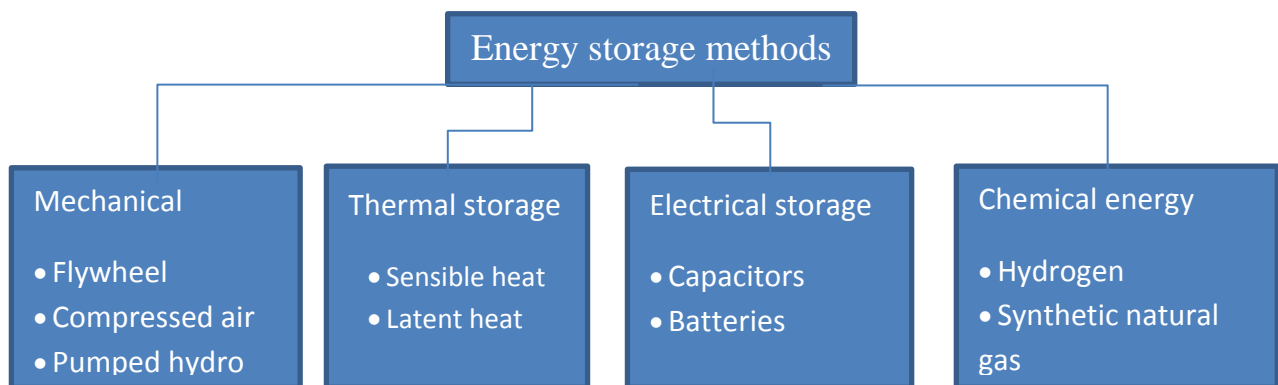


Figure 1-5. Energy storage methods [12]

Thermal energy storage systems can be classified mainly into two categories:

1.3.1. Sensible heat storage

In this type, the thermal energy accumulates and is stored with the high temperature of the solid or liquid stored material, provided that no change occurs in the phase of the material. The amount of heat stored in this system is depended on the material specified heat, change in temperature, and the mass of the storage materials, as in equation (1.1).

$$E_{sensible} = m C_p (T_f - T_i) \quad (1.1)$$

The most important feature of this type is to store the heat in the material and restore it several times without any problems, however, requiring a large volume of storage media can be considered as a disadvantage of this system.

Water is the best medium for storage at low temperatures, due to its large thermal capacity relative to other materials, inexpensive, and available, so solar water heaters that use water as heat transfer fluids are the best example of this type of storage [13, 14].

1.3.2. Latent heat storage

It is the amount of heat needed to convert a substance from one state to another (from solid to liquid or from liquid to gaseous). During the phase change process, the material can store the thermal energy without a change in the temperature. High storage capacity is what distinguishes this kind of heat storage if we compare it with sensible thermal storage, materials used in this type are called phase-changing materials PCMs. The amount of heat stored in these substances can be expressed in equation (1.2) [12, 15].

$$E_{Latent} = \int_{T_i}^{T_m} m_{pcm} \cdot C_{p_s} \cdot dt + m_{pcm} \cdot \Delta E + \int_{T_m}^{T_f} m_{pcm} \cdot C_{p_l} \cdot dt \dots (1.2)$$

The phase change material can be classified as three categories:

1. Liquid to gas phase change: this type of change can generate a large amount of heat because of the high temperature needed. This case is difficult to apply in real applications, where a large storage container is required as a result of the large volume of the generated gas.
2. Solid to liquid phase change: the materials of this case have medium latent energy and temperature of the phase change. Also, they do not produce a large change in volume which makes them suitable for many applications.
3. Solid to solid phase change: the materials of this case usually have a small latent thermal capacity compared to the other types. Also, the behavior of these materials is similar to the solid to liquid phase change materials, but the applications of this type are limited [5].

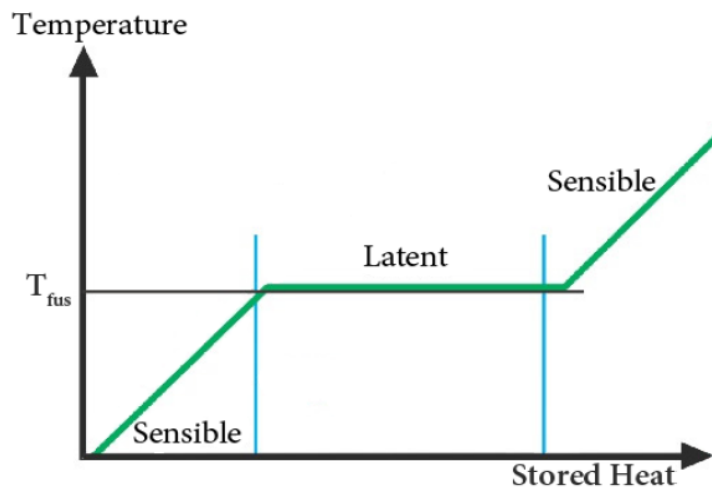


Figure 1-6. A curve showing the different steps during storage of (solid / liquid) [5]

Figure 1-6 shows that the latent heat is much higher than that of the sensible heat, and the temperature of the PCM material at the fusion point is constant (in case the material is pure depending on the materials used). If the material is not purified, the curve changes to be as shown in Figure 1-7.

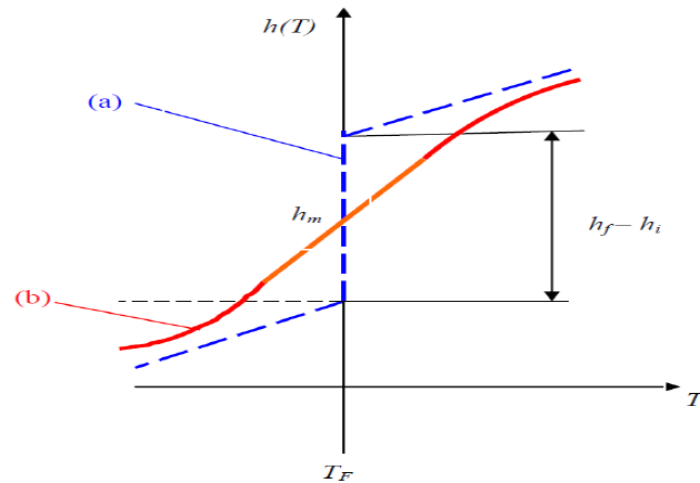


Figure 1-7. The difference in latent heat is based on temperature. (a) to a pure substance (b) to the mixture [5]

1.4 Phase Chang Materials PCM, and their characteristics

Thermal energy storage is used to improve the performance of renewable energy systems, where, high-efficiency materials are used to store sensible and latent heat energy. During the phase change process, these materials can change their physical condition in a narrow temperature field and are called Phase Change Materials (PCMs) [16].

These materials have different physical, chemical and thermal attributes. The most important of these characteristics are the latent heat of the fusion and the temperature of phase change in addition to the density, thermal conductivity, and the viscosity are less important characteristics but should be taken into consideration [17].

There are many types of phase change materials, some of them were found naturally and others were manufactured. However generally they can be classified the solid to liquid phase change into three categories as organic (O), inorganic (IO) and eutectic (E) materials. These materials can be classified in more detail in figure 1-8 [18].

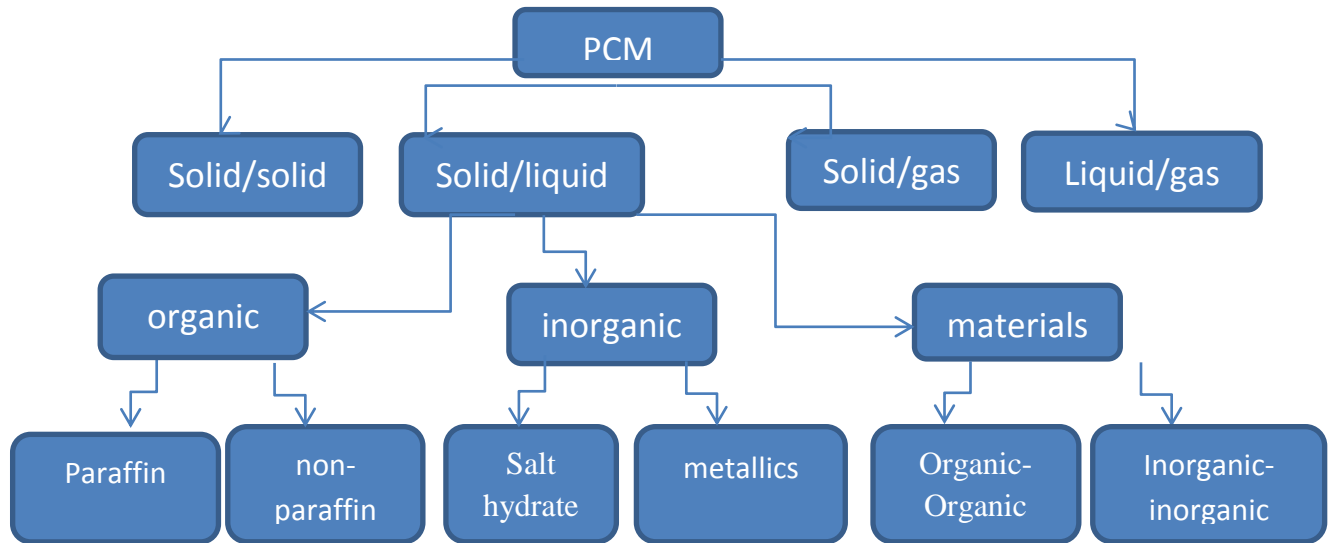


Figure 1-8. Phase-changing materials Categories [18]

Table 1-1 shows the most important characteristics of phase change materials PCM [19, 20], which helps to choose the suitable PCM materials depending on the type of application.

Table 1-1: PCM important features favorites [19]

Thermal properties	<ul style="list-style-type: none"> • The melting point of the material should be suitable for the application used (within the temperature range). • The latent heat of the material fusion must be high. • For faster heat transfer and reduced charging and discharging time, the material must have a high thermal conductivity. • It must have high-quality heat to store a larger amount of additional reasonable heat.
Physical properties	<ul style="list-style-type: none"> • The process of phase change is homogeneous, especially if it is not pure or is composed of several materials. • The material must be of high density as it affects the size of the container. • The material must have a small volume change during the phase change phase. • The material should be of low vapor pressure to reduce the storage size and cost.
Kinetic properties	<ul style="list-style-type: none"> • Low or no subcooling effect in the discharge phase because it reduces the thermal efficiency of the storage units (changes the

	<p>phase temperature change and becomes incompatible with the application).</p> <ul style="list-style-type: none"> • The dissolved material must be crystallized at the freezing point.
Chemical properties	<ul style="list-style-type: none"> • It must be chemically stable for a long period and not chemically degraded, especially after several stages of cycle change. • Do not react with the container causing corrosion. • Non-toxic, non-flammable, non-polluting and non-explosive.
Economic criteria	<ul style="list-style-type: none"> • Available in the market and not expensive

Since there is no material with all the ideal advantages required in thermal storage media, available materials are used and try to remedy defects using an appropriate system design [21].

1.4.1. Phase-changing materials Categories:

1.4.1.1. Organic PCMs.

Organic compounds, characterized by the presence of carbon atoms in their structure, there are a large number of this type of material with different melting temperatures ranging from 0 to 200 °C, but they are unstable at high temperatures. Organic PCM compounds usually have desirable properties such as melting congruence, meaning frequent thawing and freezing without phase separation, self-enlightenment and non-corrosion, and it has a high latent heat of fusion. But the thermal conduction coefficient of these compounds is very low. Therefore, they require mechanisms to promote heat transfer at reasonable rates. Organic PCMs are divided into paraffin and non-paraffin [22, 17].

Paraffin is one of the most highly variable phase change materials that have been studied extensively by researchers in recent years, for its many

advantages. They are a mixture of pure alkanes and their chemical formula C_nH_{2n+2} , the fusion temperature of the material increases as the number of C atoms increases, paraffin is liquid at room temperature when the value of n is between 5 and 15 and is solid if the value of n increases. The melting temperature of these materials ranges from 5 to 130 °C, but the materials used for thermal storage, especially solar, have a melting temperature of between 42 and 60 °C. Its advantages are that its latent fusion temperature is high, its temperature range is wide (the range of its applications is wide) and the rate of volumetric change is low of about 10%. It is not soluble in water, non-toxic and does not react with metal storage containers. The lack of phenomenon of supercooling, and phase separation.it can be used for long periods in thermal cycles without a change in chemical properties (chemically stable), low cost and available in the market. However, it has extremely low thermal conductivity, flammable and plastic containers cannot be used for storage due to their softening effect [23, 5, 24]. Figure 1-9, shows the chemical composition of paraffin.

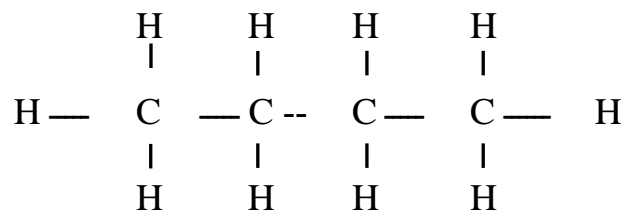


Figure 1-9. Chemical composition of paraffin [24]

Table 1-2: A group of paraffins used in solar thermal storage [25]

Name	Chemical Formula	Melting Point (°C)	Latent Heat (kJ/kg)

n-Eicosane	$C_{20}H_{42}$	37	247
n - Heneicosane	$C_{21}H_{44}$	41	215
n-Docosane	$C_{22}H_{46}$	44	249
n - Tricosane	$C_{23}H_{48}$	47	234
n-Tetracosane	$C_{24}H_{50}$	51	255
n - Pentacosane	$C_{25}H_{52}$	54	238
n-Hexacosane	$C_{26}H_{54}$	56	257
n - Heptacosane	$C_{27}H_{56}$	59	236
n-Octacosane	$C_{28}H_{58}$	61	255
n - Nonacosane	$C_{29}H_{60}$	64	240
n-Triacontane	$C_{30}H_{62}$	65	252

1.5 Heat transfer enhancement

One of our biggest problems in the use of PCMs in thermal storage is the low thermal conductivity of these materials. This makes the thermal diffusion of PCM very low, and the fusion process is slow. Hence, the process of storing heat takes a lot of time, and the same happens in the sclerosis process. To solve this problem, two methods can be used, the first is to improve the PCM thermal convection in the liquid phase by increasing the heat transfer area by properly encapsulating it, or use fins, tubes or metal rings to enhance heat transfer, and the second is to add high conductivity materials such as graphite, aluminium, and butadiene to improve thermal conductivity. Other researchers include designing a heat storage tank and creating new PCM materials to increase thermal diffusion[22, 26].

1.5.1 Macro encapsulation

It is the process of placing PCM in cylindrical, spherical, pipes, or bags containers stacked inside the storage tank, to ensure excellent heat transfer between the heat transfer fluid that surrounds the PCM material. The ratio between the surface area to the volume of the packaging should be high,

(Low thermal resistance), so smaller containers are better, and here shows the problem of cost [28].

1.5.2 Microencapsulation

This type uses very small capsules that measured in micro and stacked in the form of matrices inside the heat storage tank. The process of heat transfer is faster than macro encapsulation, so less time to charge and discharge heat is needed [19].

1.5.3 Using extended surface

It is the process of increasing the surface area through the use of metal structures or fins to increase the amount of heat transfer between the fluid and the PCM material. These fins have the basic factors that affect the performance of the system [15].

1.5.4 Adding particles to highly conductive materials

It is the process of adding nanoparticles such as copper, aluminum, iron, graphite or metal foam with a good conductivity factor to PCM to improve heat transfer and reduce melting or solidification time[13].

1.6.The aim of the Research

This research aims to study the effect of using phase change material on the performance of a solar water heating system that has been designed and manufactured according to engineering specifications. Moreover, it highlights the study of a range of parameters of parameters:

1. Study the effect of using variable flow rates on the thermal performance of this system in terms of heat storage, thermal efficiency, PCM behaviour during energy charging and discharging operations, final water temperature, and its comparison with the state in which PCM is absent.
2. Study the possibility of improving the coefficient of poor thermal conductivity of paraffin wax materials by adding a substance with high thermal conductivity.

**C
H
A
P
T
E
R**

2

Literature Review

Chapter Two

Literature Review

Due to the great importance of thermal storage and energy-saving, many researchers around the world have paid great attention to the Phase Change Materials PCMs. Their applications, their physical properties, and the methods used to improve their performance have been studied briefly in the literature. For best performance, it is crucial to choose suitable properties of PCMs for a specific application. This chapter reviews the experimental and numerical literature that utilized PCM materials in various applications, especially in solar water heating systems.

2.1. Experimental researches

2.1.1. Incorporation PCM into thermal storage systems

Many researchers have proven that the process of incorporating PCM materials into thermal storage systems increases the efficiency of these systems due to the advantage of the high heat storage capacity of PCM materials during the phase change process compared to other materials.

E. Mettawee and G. Assassa[29], 2006 presented an experimental study of a water heating system, the compound consisted of a solar absorber and PCM storage plate. Paraffin wax (dissolves at 53.3 °C) was used. The PCM is heated by solar energy. Results showed that the rise in the PCM temperature increased gradually with the increase of solar radiation, and the amount of heat increased as the flow rate increased. Also, results showed that the temperature of the PCM outer layer reaches the melting point before the rest.

H. Benli, and A. Durmus[30], 2009 studied experimentally a PCM heating and charging system using ten solar air collectors. $\text{CaCl}_2 \cdot 6\text{H}_2\text{O}$ was used as a PCM with a melting temperature of 29 °C. The study proved that the use of PCM material increases the stored thermal energy for heating purposes by about 18-23% compared to the regular heating device (without PCM).

Al-Hinti et al. [31], 2010 studied the effect of PCM material integrated with a solar water heating system. A cylindrical water tank with 38 aluminium containers filled with paraffin wax with a melting temperature of 52 °C is used. Also, a heater element was used as a secondary energy source. Results revealed that the main benefit of using PCM is to keep the water temperature hot for a longer time and keep the temperature difference by up to 14 °C. The forced flow showed an apparent effect on the water temperature of the tank, and the time required to heat the water.

Fazilati, and Alemrajabi, [32] 2013 tested the effect of using paraffin wax with a melting temperature of 55 °C filled in 180 spherical capsules with a diameter of 38 mm utilizing solar energy. Copper wires were added inside the capsules to improve the heat transfer coefficient. Three different temperatures of 40, 60, and 80 °C were used with 0.2, 0.3 and 0.4 L/min water mass flow rate. Results showed that the energy storage efficiency improved after using paraffin wax, and the highest rate was 39% at 80 °C due to the melting of all wax at this temperature. Also, the time of supply hot water was increased by up to 25%.

Chaichan et al., [33] 2014 examined the solar water heaters and enhancing their energy storage by using two types of PCMs pebbles for storing sensible heat, and paraffin wax with a melting point of 45 °C for latent heat. The PCMs were inserted into ten copper tubes placed inside the water tank, and three cases were studied, namely water only, water with pebbles, and water with paraffin wax. Results showed the hot water can remain at a temperature of 15-20 °C higher the temperature of feed water throughout the day and at night, and the fluctuations in water temperature are reduced. Also, results showed that the amount of energy stored was higher with paraffin, compared to that of pebbles.

Kavitha and S.Arumugam, [34] 2015 studied the efficiency of a thermal solar energy storage system, where 40 iron pipes filled with paraffin wax with a melting temperature of 44 °C were arranged crisscross inside a square water tank on four layers. Results showed that using empty pipes improved the efficiency of the storage system. Also, increasing the number of pipes increased the energy stored, and enhanced the system efficiency. When using 4 litres of water without PCM, the storage system efficiency was 10%. When adding one pipes layer, the efficiency increased to 16%. Also, using 12 litres of water with 40 empty tubes show an efficiency of 38%. Finally, using four pipes layers filled with PCM increased the efficiency by up to 43%.

Mongibello et al., [35] 2017 studied a storage system designed to heat water which reinforced with PCM. The system consist of a cylinder tank with a capacity of 420 litres, a copper heat exchanger, and 14 aluminium cylinders with a capacity of 3 litres. Each bottle contain 1.7 kg of paraffin wax, which melts at 58 °C. Several tests were performed at a constant water mass flow rate (0.2 kg/s) using two cases; the first case had water only while the second

had water and PCM. The results indicated the effects of the presence of PCM, not all PCMs were subjected to thawing, and it needed to add materials with high conductivity to enhance the thermal conductivity.

Senthil and Cheralathan, [36] 2017 studied a system generating a water vapour for cooking or electricity generation utilizing a solar collector contained a set of mirrors. The receiver contained $\text{MgCl}_2 \cdot 6\text{H}_2\text{O}$ that dissolved at 117°C as a PCM material while fins were added to increase the heat transfer area. The results showed that the efficiency of the system increased by 5.6%, and the time required to boil water decreased by 20%. Also, increasing the water flow rate lead to an increase in the efficiency of the system.

Olubunmi and Ajayi, I. S, [50] 2017 studied the performance of a solar heater which was enhanced by adding copper tubes containing paraffin wax with a melting point of 45°C . Water was used as a heat transfer fluid that flowed in the siphon method. Results showed that the hot water supply was larger compared to the case of water-only. The water temperatures on the next day of the test were 57.6°C and 46.5°C using PCM and water only respectively. Maximum temperatures at the end of the charging process were 65°C and 54.5°C for the cases of PCM and water only, respectively.

Nasir et al., [37] 2018 studied a solar water heater system consisting of an 80-litre water tank and a vacuum collector of vacuum tubes to study the melting process of 12 kg of black Iraqi paraffin wax melting at 45°C , placed inside a heat exchanger. Variable forced water flow rates of 200, 300 and 500 litres/hour with different operating conditions were utilized. Results showed that the time required to melt all the wax is 3 to 4 hours in summer, while it needed 14 to 16 hours in winter. The proportion between the

intensity of the solar radiation and the stored energy was direct, while the proportion between the rate of water flow rate and the melting time was inverse.

Gupta and Ramachandran, [38] 2018 added PCM to a cold storage system to keep the storage box cool as long as possible. Water was added to ethylene glycol in different proportions, namely 0%, 25%, 50%, and 75%. The results indicated that adding water to the phase change material increased the cooling retention and best results when the compound was composed of 50% ethylene glycol and 50% water.

2.1.2. Improved heat transfers and PCM geometry

As mentioned in Chapter 1, one of the most significant drawbacks of PCM is the low thermal conductivity. Researchers have used several techniques to improve heat transfer in PCMs. The same thing is applied to the PCM container geometry, which should be designed carefully to ensure adequate heat transfer rates between heat transfer fluid and PCM and through the PCM itself.

Weinstein, et al., [43] 2012 investigated the thermal properties of PCM with the addition of 5.5% and 11% graphite nanofibers, compared with pure. Organic PCM paraffin was used with a solubility degree of 54.4 °C. Two models of containers were designed to place the material inside, cubic and rectangular. Significant improvement in thermal diffusion and a 60% reduction in melting time was observed when 5.5% of graphite nanofibers were added. When using 11%, it was found that the solubility was more balanced, and the design of the container affected thermal performance and that the rectangular models were better at heat transfer.

Saw, et al, [44] 2013 studied the efficiency of a solar heater system consisting of a flat plate solar collector and paraffin wax with a melting point of 60 °C. The PCM was placed under the absorbent plate while 37 fins were used to increase the heat transfer area. 1% of copper nanoparticles were added to improve the physical properties of PCM material. Tests were carried out in the case of without PCM, with PCM, and with nanoparticles and PCM. Results showed that the hot water temperatures the next day were 40.2, 42.2, 35.2 °C for the cases of with PCM, with nanoparticles and PCM, without PCM, respectively. System efficiency improved by 6.9% and 8.4% for the cases of PCM, and nanoparticles and PCM respectively.

Kenfack and Bauer, 2014[45] investigated and developed a new phase-change material mainly contains salt hydrate. To overcome the phase separation phenomenon, materials like aluminium sulfate hydroxide $\text{Al}_2(\text{SO}_4)_3 \cdot 18 \text{H}_2\text{O}$ was added. Many heating and cooling cycles of various PCM materials have studied. Graphite has also been added to the developed salt hydrate, to improve the thermal conductivity. Results indicated that the newly developed salt hydrate had a stable thermal behaviour and high storage capacity compared to the other materials tested. Also, the addition of 5% of graphite to developed salt hydrate, improved thermal conductivity by up to 40%.

B. Kadim, et al, [46] 2015 studied the effect of adding a copper brush at different fractions of 97%, 94% and 90% to improve the thermal conductivity of paraffin wax with a melting point of 60 °C. An electric heater was used to heat the system, and the cooling was achieved by passing air at different flow rates (1, 2, 2.5 and 3 m/s). Results indicated that as flow rate increased, the amount of heat transferred increased which reduced the solidification time, especially with the addition of a copper brush. The

lowest melting time occurred at 90% fraction with the case of the maximum airflow rate, which was 4.46 times less compared to the absence of a copper brush.

B. Hammendy, et al., [47] 2015 improved the thermal conductivity of paraffin wax with melting temperature 63.7 °C, by adding copper rings with different diameters (0.5, 1) cm in proportions (3%, 6%, and 10%). The electric heater was used for the heating process, and the air was used as a heat transfer fluid, with different flow rates (1, 2, 2.5 and 3) m/s. Results showed that the soluble time was less when a more significant proportion of copper rings are used, and the amount of heat transferred was higher compared to paraffin without copper rings. However, their impact was limited during the solidification process, and the range with diameter 0.5 cm showed better results than 0.6 cm.

N. Beemkumar, et al. [48] 2017 studied the amount of energy stored in paraffin wax at a melting point of 50 to 60 °C with a spherical container made of different materials namely copper, aluminium and brass and placed in a cylindrical tank. Two heat transfer fluids, namely water and Therminol-66, were used. It was observed that the copper spherical containers were the best in terms of storing heat followed by aluminium and brass due to the high thermal conductivity coefficient of copper. Also, the amount of heat stored in the water was higher than that of Therminol-66.

Abdulmunem, [49] 2017 cooled PV panels and regulated their temperature by using a PCM material with a melting point of 42 °C, placed in an aluminium container to absorbing heat from them and thus improved the electricity generation efficiency. An aluminium matrix was added to enhance the thermal conductivity of paraffin wax. The process resulted in decreasing

the temperature of the photovoltaic panel from 61.39 °C to 46.2 °C when the PCM was used. Also, adding an aluminium matrix reduced the temperature of the PV panel to 39.58 °C. The efficiency of the photovoltaic generation improved from 10.19% to 12.73% by using PCM only, and to 13% by adding an aluminium matrix.

Ridha, et al., [51] 2018 improved the properties of paraffin wax, which dissolves at 62 °C, by adding metal copper, aluminium, and iron Swarf to the PCM at different weight ratios to improve the thermal conductivity coefficient. The results indicated that the addition of metal Swarf by 7.5% to 17.5%, improved the heat transfer during the charging process by 5.5% to 22.1%, respectively. And adding 17.5% of aluminium Swarf improves thermal conductivity up to 53 times. In the process of discharging heat, the addition of metal Swarf reduces heat release time by (27% to 77%) when adding (7.5-17.5%). Aluminum Swarf recorded the best results during the tests.

2.2.Numerical and theoretical Researches

2.2.1. PCM performance in the thermal storage system

Many researchers have used theoretical solutions and numerical programs to highlight the advantages of using PCM as a potential heat storage material.

Eames et al., [39] 2006 used a finite volume model to predict the amount of heat stored in a rectangular cross-section solar storage system filled with water and paraffin wax PCM with a melting point of 65 °C with different concentrations (10, 15, 20, 25 and 30% PCM). Results showed, that the benefit of using PCM in solar energy systems as heat storage materials. It provided additional stored heat energy that can be used on request.

Milisic [12] 2013 calculated the stored thermal energy of a variety of PCMs salts namely NaS₂O₃ with a melting point of 48 °C, CaCl₂ with a melting point of 28 °C and organic matter RT42 Paraffin with a melting point of 60 °C. The mathematical analysis was in one-dimensional, for the process of charging and discharging for two concentric tubes. The interior contained PCM material, and the outer contained the heat transfer fluid (water). The theoretical results indicated that all types used were better in thermal storage capacity than PCM-free water, except RT42 because the latent heat energy of the material was low. The storage capacity of the salt hydrate was better than that of organic matter (RT42, Paraffin) because the latent heat of fusion was higher.

Sarafraz, [40] 2013 applied a CFD modelling using ANSYS CFX program to study a solar water heating system integrated with a PCM material. The system consisted of four cylindrical tanks, and each tank had a different ratio

of Lauric Acid with a melting point of 44 °C coated in flat sheets. The stored energy can reach 2 to 5 times higher than that obtained from the heat stored by water only. Results showed that increasing the percentage of PCM in the tank from 2.5% to 15%, led to an increase in the charging time to 2.8 times and increased the amount of energy stored.

Kumar, et al., [41] 2016 applied ANSYS software to analyze the performance of a solar water heating system. The system was designed depending on experimental research, and it consisted of two boxes, one with a capacity of 8 litres, containing water and the other with a capacity of 6 litres, including coconut oil which used as PCM material. The melting point of coconut oil is 28 °C while water was used as the heat transfer fluid. Solar energy is used by reflective plates to heat the water flowing in the system. Results showed that the PCM material used can improve energy storage during the night by up to 16%.

2.2.2. Improving heat transfer coefficient and PCM geometry

Many experimental and numerical techniques were carried out to improve the heat transfer coefficient in the thermal storage systems and PCM containers to enhance the overall performance of such systems.

Mahmud, et al., [52] 2009 investigated the thermal and physical properties of paraffin wax melting point of 50 °C using the MATLAB program. The PCM material was put in 36 black aluminium cylinders to increase the absorption of solar energy. 5% of aluminium powder was added to enhance the thermal conductivity of paraffin wax. A solar simulator heated PCM while a forced airflow achieved cooling. It was observed in the energy discharge process, that the increase in the rate of airflow caused a decrease

in the solidification time of the PCM, as it took (8 hours) at a flow rate of 0.05 kg/s and about (3.5 hours) at a flow rate of 0.19 kg/s.

Joudi and Taha, [53] 2012 simulated some stored energy released during the melting and hardening of four types of paraffin with melting point 28, 48, 64, and 84 ° C, respectively, which are placed in containers of different shapes. It was found that the melting time and solidification time in cylindrical containers are less than those of the square containers. Increasing the volume of the container increased the melting time and solidification time. Paraffin wax 48 °C had a better latent heat than other types, but the time of solubility and solidification was higher than others due to its low thermal conductivity. Paraffin wax melting point of 84 °C had the lowest latent heat but high thermal conductivity.

Hosseinzadeh, et al., [54] 2012 studied the behaviour of Rubitherm (RT27) with fusion temperature 28-30 °C, which was used as PCM material. Copper nanoparticles were added in different concentrations, namely 0, 0.02 and 0.04 % to improve the thermal conductivity coefficient of the PCM. The compound was placed in a spherical-shaped plexiglass container. Results showed that the thermal conductivity had increased due to the use of nanoparticles, and the fusion time is reduced to 2,3- and 5-minutes relative to the three concentrations used.

Mat, et al., [55] 2013 carried out a numerical investigation using ANSYS Fluent 6.3.26 software to study RT 82 PCM material which dissolves at 77 °C. The material was placed in a copper-tube heat exchanger with a variety of diagonally placed internal and external fins to improve thermal conductivity and reduce melting time. The location of the heat source was

also changed during the study. Results showed that the heat transfer and melting time decreased by 43.3% when fins were used.

Reddy, et al., [56] 2014 studied $\text{Na}_2\text{S}_2\text{O}_3 \cdot 5\text{H}_2\text{O}$ with a solubility of 48°C to be used as PCM material placed in capsules with of various forms including cylindrical, spherical and square. Results showed that, as water flow rate increases, the time of charging heat decreases due to the low thermal resistance of the cylindrical shape compared to other shapes. The cylindrical shape shows better results as a result of the better charging process in the system.

Solano, et al., [57] 2018 analyzed a closed type of solar water heating system. An aluminum tube with eight rectangular fins pass through a shell and tube heat exchanger and filled with paraffin wax meting point of 55°C was used. The system was connected to a flat plate solar collector with a capacity of solar radiation of 500 W/m^2 in the winter and of 1000 W/m^2 in summer. Results showed that the storage of thermal energy increased up to 2.2 times compared to winter. Also results showed that adding fins led to reduce the melting time and increase storage of thermal energy.

2.3 The Scope of work

In this study, an experimental and numerical test is performed on the performance of the active type solar water heating system, which operates with different flow rates. This system is experimentally tested under the climatic conditions of the city of Karbala in Iraq from March 20 to 20 April 2019. Also, a numerical model of the proposed solar water heating system was carried out using ANSYS Fluent. Paraffin wax was added as a PCM material. A set of parameters will be studied:

1. Highlight the effect of using phase change materials on the performance of a solar water heating system, in terms of heat storage, thermal efficiency, PCM behaviour during charge and discharge operations, final water temperature and comparison with PCM absence.
2. An electric heater is used as a constant heat source in addition to a flat plate solar collector to avoid the effect of variable solar radiation intensity during the test period. In the experimental test, different volumetric percentages (22% and 31%) of paraffin wax are used, to increase the reliability of the results obtained. Also, a copper mesh is added to improve the weak thermal conductivity of the paraffin wax material and study the effect of this on the thermal behaviour of the paraffin wax material and the thermal storage of the system.

Table: 2.1. Summary of experimental research

NO	Reference	Type of PCM	Results and remarks
1	Mettawee and Assassa. [29] 2006	paraffin wax, $T_m = 53.3 \text{ }^\circ\text{C}$	The increase in the intensity of solar radiation and the flow rate of HTF has a significant impact on the amount of heat acquired. The weak thermal conductivity of the PCM affected the heat transfer through the PCM layers.
2	H. Benli and A. Durmuş [30] 2009	CaCl ₂ ·6H ₂ O $T_m = 29 \text{ }^\circ\text{C}$	The use of PCM material increased the stored thermal energy for heating purposes by about 18-23% compared to the regular heating device (without PCM).
3	Al-Hinti et al., [31] 2010	paraffin wax $T_m = 52 \text{ }^\circ\text{C}$	the main benefit of using PCM is to keep the water temperature hot for a longer time and keep the temperature difference by up to 14 °C. The forced flow shows an apparent effect on the water temperature of the tank, and the time required to heat the water.
4	Weinstein and Fleischer [43] 2012	paraffin wax $T_m = 54 \text{ }^\circ\text{C}$	significant improvement in thermal diffusion and a 60% reduction in melting time was observed when 5.5% of Graphite nanofibers were added. When using 11%, it was found that the solubility is more balanced, and the rectangular models were better at heat transfer.
5	Fazilati, and Alemrajabi, [32] 2013	paraffin wax $T_m = 55 \text{ }^\circ\text{C}$	That the energy storage efficiency improved after the use of paraffin wax in the three levels of degrees, and the highest rate was 39% at 80 degrees, and the time of supply hot water increased by 25%.

6	Saw et al. [44] 2013	paraffin wax $T_m = 60\text{ }^\circ\text{C}$	that the temperature of hot water the following day was 40.2, 42.2, 35.2 $^\circ\text{C}$, when, with PCM, with Nano-PCM, without PCM, respectively. System efficiency improved by 6.9% and 8.4% when with, PCM, and Nano-PCM, respectively.
7	Kenfack and Bauer, [45] 2014	Hydrate salt+Al ₂ (SO ₄) ₃ .18 H ₂ O	that the newly developed salt hydrate has a stable thermal behaviour and high storage capacity compared to the other materials tested. The addition of 5% of graphite to developed salt hydrate, has improved thermal conductivity of about 40%.
8	Chaichan. et al. [33] 2014	paraffin wax $T_m = 45\text{ }^\circ\text{C}$ + pebbles	a significant improvement in the storage efficiency of the system when using pebbles, paraffin wax, and the water stays hot, at 35 $^\circ\text{C}$, until 10 pm, 7 pm, when using paraffin wax, pebbles. The amount of energy stored was greater when used paraffin, compared with pebbles.
9	Kadim, et al, [46] 2015	paraffin wax $T_m = 60\text{ }^\circ\text{C}$	The lowest melting time occurs at 90% void fraction and highest airflow velocity, which was 4.46 times compared to the absence of a copper brush.
10	Hammendy, et al., [47] 2015	paraffin wax $T_m = 63.7\text{ }^\circ\text{C}$	the amount of heat transferred was higher compared to paraffin without copper rings, and the use of rings of 0.5 cm diameter better than 0.6 cm.
11	Kavitha, et al. [34] 2015	paraffin wax $T_m = 45\text{ }^\circ\text{C}$	when adding one layer of copper tubes filled with PCM, the efficiency increased to 16%. When using 40 empty tubes, the efficiency was 38%, and when using four layers of tubes, the efficiency increased to 43%.
12	Mongibello, et al. [35] 2017	paraffin wax $T_m = 58\text{ }^\circ\text{C}$	the importance of using PCM in thermal storage, also, the weak thermal conductivity of PCM and the need to use materials with high conductivity to enhance thermal conductivity.
13	Beemkumar, et al. [48] 2017	paraffin wax $T_m = 50\text{-}60\text{ }^\circ\text{C}$ and Therminol-66	It was observed that the copper spherical containers were the best in terms of storing heat followed by aluminium and brass due to the high thermal conductivity coefficient of copper. Also, the amount of heat stored in the water was higher than that of Therminol-66.
14	Abdulmunem, [49] 2017	paraffin wax $T_m = 42\text{ }^\circ\text{C}$	decrease the temperature of the photovoltaic panel from 61.39 $^\circ\text{C}$ to 46.2 $^\circ\text{C}$ when using the PCM only, but when adding matrix aluminium foam, the temperature decreased to 39.58 $^\circ\text{C}$. The efficiency of the photovoltaic generation improved (10.19% to 12.73%) by using PCM only, and (13%) when adding matrix.
15	Senthil and Cheralathan . [36] 2017	MgCl ₂ .6H ₂ O) $T_m = 117\text{ }^\circ\text{C}$	the results showed that the efficiency of the system increased by 5.6%, and the time required to boil water decreased by 20%. Also, increasing the water flow rate

			leads to an increase in the efficiency of the system.
16	Olubunmi et al. [50] 2017	paraffin wax $T_m=45\text{ }^\circ\text{C}$	the hot water supply period was higher, compared with the water-only system, and the water temperature on the second day of the test was $57.6\text{ }^\circ\text{C}$, $46.5\text{ }^\circ\text{C}$, when using PCM, only water, respectively.
17	Nasir, et al. [37] 2018	Iraqi paraffin wax $T_m=45\text{ }^\circ\text{C}$	The time needed to melt the wax is 3 to 4 hours in the summer, while it needs 14 to 16 hours in the winter. The intensity of the solar radiation and the energy stored are directly proportional, while the rate of water flow and melting time is inversely proportional.
18	Ridha, et al., [51] 2018	paraffin wax, $T_m=62\text{ }^\circ\text{C}$	the addition of metal Swarf by 7.5% to 17.5%, improved the heat transfer during charging by 5.5% to 22.1%, respectively. And adding 17.5% of aluminium Swarf improves thermal conductivity up to 53 times. In the process of discharging heat, the addition of metal Swarf reduces heat release time by (27% to 77%) when adding (7.5-17.5%).
19	Gupta and Ramachandran. [38] 2018	Water + ethylene glycol	when using pure ethylene glycol, the effect of its use was minimal compared to the absence of PCM. The best result was when the compound was composed of 50% ethylene glycol and 50% water.

Table 2.2. Summary of numerical Research

NO	Reference	Type of PCM	Results and remarks
1	Eames, et al. [39] 2006	paraffin wax $T_m= 65\text{ }^\circ\text{C}$	the benefit of using PCM in solar energy systems as heat storage materials. It provided additional stored heat energy that can be used on request.
2	Mahmud et al., [52] 2009	paraffin wax $T_m= 50\text{ }^\circ\text{C}$	the high airflow rate, causing a decrease in freezing time of PCM
3	Joudi and Taha, [53] 2012	paraffin used were fusions of 28, 48, 64 and $84\text{ }^\circ\text{C}$	the melting, solidification time in cylindrical containers is less than square containers. Increasing the volume of the container will increase the melting and solidification time. Paraffin wax $48\text{ }^\circ\text{C}$ has a better latent heat than other types.
4	Hosseinizadeh et al. [54] 2012	PCM fusion temperature $28/30\text{ }^\circ\text{C}$	the thermal conductivity has increased due to the use of nanoparticles, and the fusion time has been reduced to 2,3,5 minutes relative to the three nanomaterial concentrations used.

5	Milisic, [12] 2013	NaS ₂ O ₃ T _m =48 °C, CaCl ₂ T _m 28 °C, Rt42, paraffin T _m 60 °C	all types used were better in thermal storage capacity than PCM-free water, except RT42 because the latent heat energy of the material was low.
6	Mat, et al. [55] 2013	Rt 82	The results indicated that the heat transfer and melting time decreased by 43.3% when fins were used.
7	Sarafraz, [42] 2013	fluoric acid, with T _m = 44 °C	the increasing percentage of PCM in the tank from 2.5% to 15%, led to an increase the charging time to 2.8 times and increased the amount of energy stored.
8	Kumar et al. [41] 2016	coconut oil is T _m =28 °C	The results showed the benefit of using PCM to improve energy storage and use during the night by 16%.
9	Reddy, et al. [56] 2014	Na ₂ S ₂ O ₃ .5H ₂ O T _m =48 °C	the discharge time of the cylindrical capsules was longer than the square capsules; the cylindrical shape is better because of the importance of the charging process in the system.
10	Solano et al., [57] 2018	paraffin wax, T _m =55 °C	the storage of thermal energy increased to 2.2 times compared to winter and that the addition of fins led to reduced melting time and increased storage of thermal energy.

**C
H
A
P
T
E
R**

3

**Mathematical Model & Numerical
Analysis**

Chapter Three

Mathematical Model & Numerical Analysis

In this chapter, the process of heat storage and its associated phenomena are analyzed. A two-dimensional ANSYS Workbench v17.2 model was used to simulate the water tank with PCM bottles similar to that used in the experimental facility. Two cases of modelling were carried out with PCM and without PCM to highlight the advantages of using PCMs in the storage system.

3.1. Assumptions.

1. The PCM material is homogenous and incompressible, during the melting or solidification process. Also, the melt flow is considered laminar.
2. The PCM container is filled completely with Paraffin wax.
3. Neglecting the volume change of PCM during phase change.
4. Hourly steady state, Newtonian fluid flow, a single-phase fluid for water.
5. The heat flux generated by the heater element is constant throughout the charging process.
6. Natural heat transfer convection between the heater element and water, as well as between the water and the container of PCM, since there is no water moving force inside the tank, the low water speed will be a proof of this [50].
7. The heat convection currents of the water are of a laminar type, as the heater is a horizontal cylindrical object immersed in the water. Rayleigh number $(Ra) = 3.27 \times 10^8$ [50].

The calculation of the Rayleigh number (Ra) attached in Appendix A.1.

8. The system is thermally insulated.

3.2. Governing equations

The differential and algebraic equations list for 2D- model, can be written as in equations [59,60,61]:

$$\text{❖ Continuity Equation:} \quad \frac{\partial \rho}{\partial t} + \frac{\partial(\rho u)}{\partial x} + \frac{\partial(\rho v)}{\partial y} = 0 \quad (3.1)$$

❖ Momentum equation :

$$\text{X-direction} = \frac{\partial(\rho u)}{\partial t} + \frac{\partial(\rho uu)}{\partial x} + \frac{\partial(\rho uv)}{\partial y} = -\frac{\partial p}{\partial x} + \frac{\partial}{\partial x} \left[\frac{\partial \mu u}{\partial x} \right] + \frac{\partial}{\partial y} \left[\frac{\partial \mu u}{\partial y} \right] + F_X \quad (3.2)$$

$$\text{Y-direction} = \frac{\partial(\rho v)}{\partial t} + \frac{\partial(\rho uv)}{\partial x} + \frac{\partial(\rho vv)}{\partial y} = -\frac{\partial p}{\partial y} + \frac{\partial}{\partial x} \left[\frac{\partial \mu v}{\partial x} \right] + \frac{\partial}{\partial y} \left[\frac{\partial \mu v}{\partial y} \right] + F_Y \quad (3.3)$$

F_x, F_y indicate the external forces, such as buoyancy, In the natural convection.

$$F = \rho g \quad (3.4)$$

$$\text{The buoyancy force:} \quad F = \rho g \beta (T - T_{ref}) \quad (3.5)$$

❖ Energy equation :

$$\text{Enthalpy formulation} \quad \frac{\partial(H)}{\partial t} = \frac{\partial(Hu)}{\partial x} + \frac{\partial(Hv)}{\partial y} = \frac{\partial}{\partial x} \left[\frac{\partial(KT)}{\partial x} \right] + \frac{\partial}{\partial y} \left[\frac{\partial(KT)}{\partial y} \right] \quad (3.6)$$

$$\frac{\partial(h)}{\partial T} = \rho C_p \quad (3.7)$$

$$h = \begin{cases} C_{p_s} T & T < T_m \\ C_{p_l} T + (C_{p_s} - C_{p_l}) T_m + L & T \geq T_m \end{cases} \quad (3.8)$$

The total enthalpy H represents the summation of the sensible enthalpy h and latent enthalpy ΔH and can be described by equation [61]:

$$H = h + \Delta H \quad (3.9)$$

Where,

$$h = h_{ref} + \int_{T_{ref}}^T C_p dT \quad (3.10)$$

$$\Delta H = fL \quad (3.11)$$

The liquid fraction f which is defined as [61]:

$$f = \begin{cases} 0 & \text{if } T \leq T_s \\ \frac{T-T_s}{T_l-T_s} & \text{if } T_s \leq T \leq T_l \\ 1 & \text{if } T \geq T_l \end{cases} \quad (3.12)$$

where, T_s and T_l refer to solids and liquids temperatures of PCM, respectively. The local temperature is denoted by T .

3.3.Design modeler

A two-dimensional physical model is used to simulate the water heating system presented in this study. In the first case (without PCM), a model consisting of five bodies, a container water, water, air and glass wall insulating tank. In the second case, 10 bottles of aluminum are filled with PCM divided into two rows, each row contains 5 bottles. The volume ratio of PCM to the water to be heated is 31%. The geometry of the PCM container is designed by Space claim program, to ensure having the required accuracy. Figure 3-1 shows the schematic diagram of the proposed model while Table 3-1 shows the specifications and measurements for each component of the model.

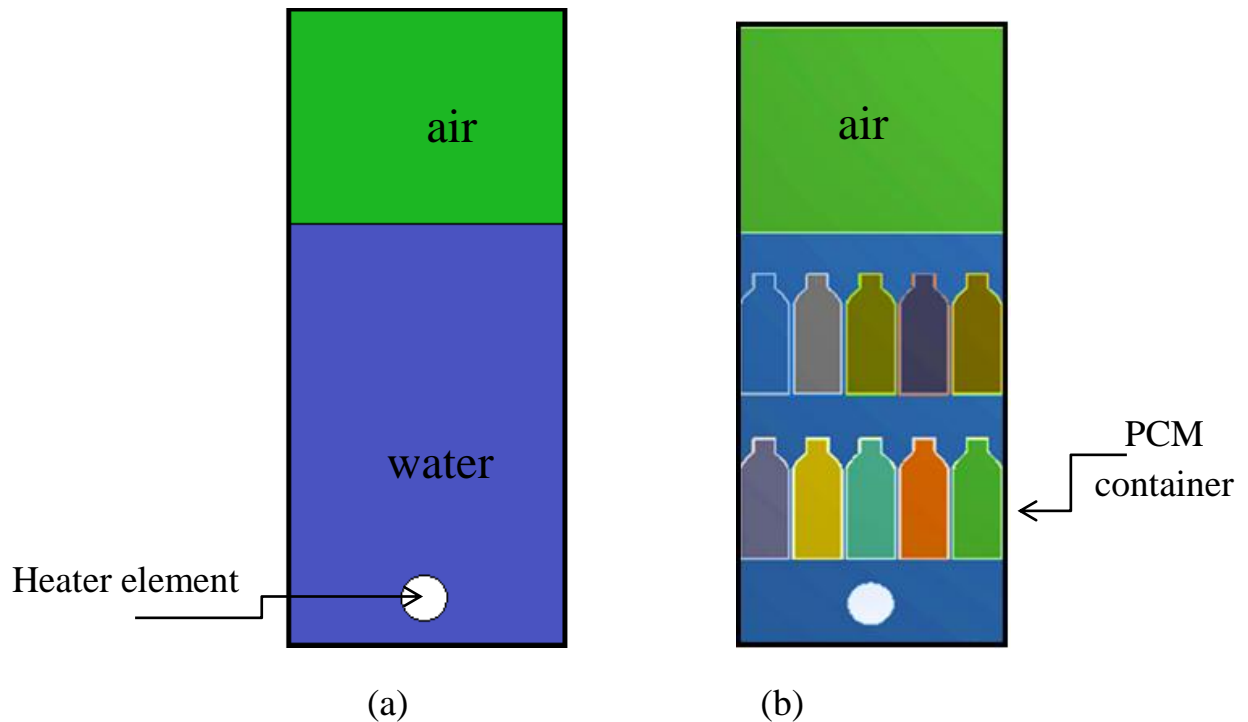


Figure 3-1. 2-D model of the water tank, (a) without PCM, (b) with PCM container.

Table 3-1: Physical characteristics of the proposed model

Component	Diminutions (mm)	Marital
water tank	$L=750, W =285, t =2$	steel
water domain	$L=500, W =285$	water
air domain	$L=250, W =285$	air
PCM container	$h=130, D=50$	aluminum
heater element	$D =50$	copper

3.4. Connection contacts

When a model consists of a group of components that contact with each other and have different specifications, characteristics, and behaviour, these bodies must be linked together so that they are as one unit under the influence of the loads imposed on them, such as temperature, pressure, heat flux generated, etc. Figures 3-2, 3-3, and 3-4, show the connection contacts, among the components of the model.

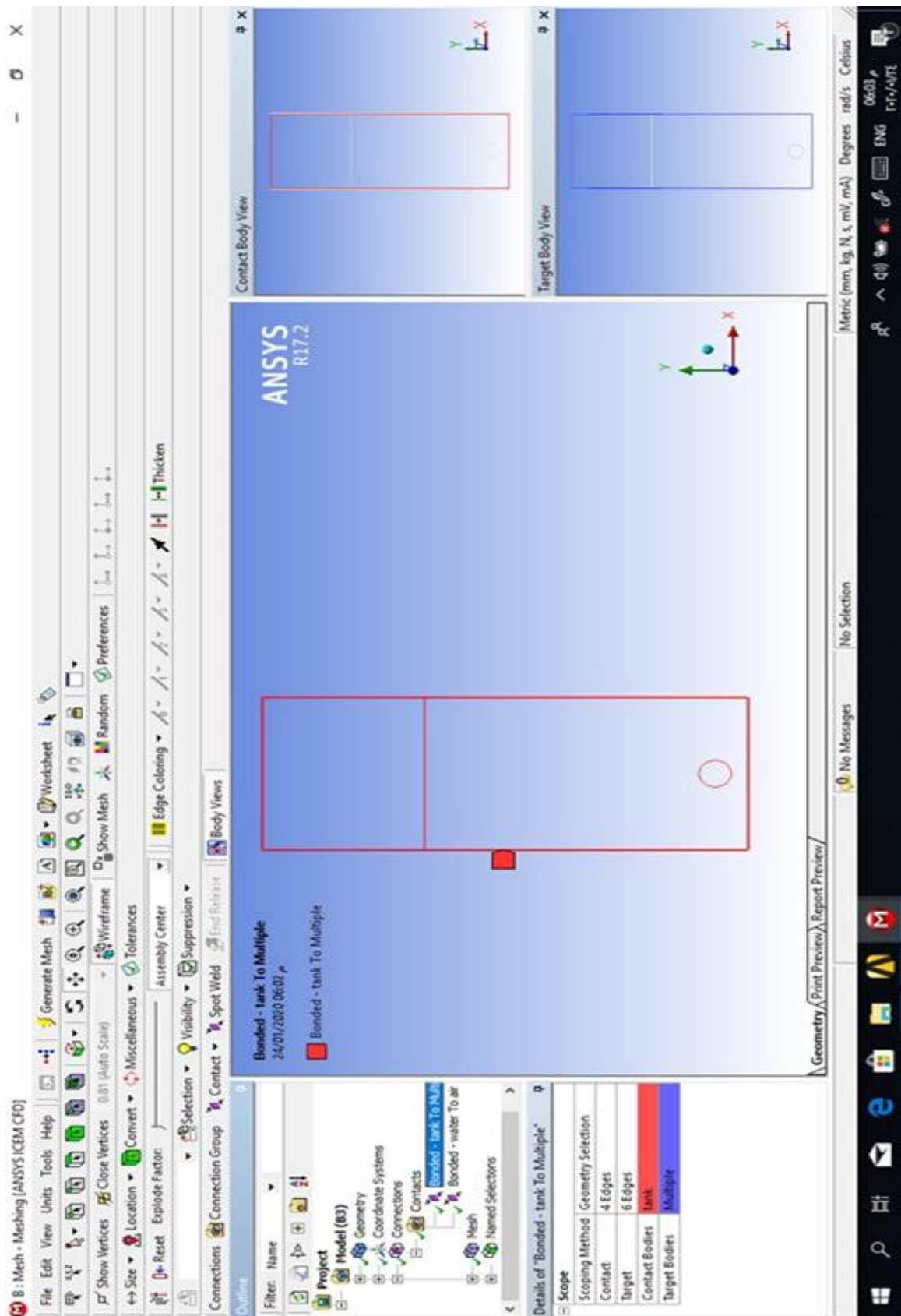


Figure 3-2. Water and air –inner wall container connection contacts

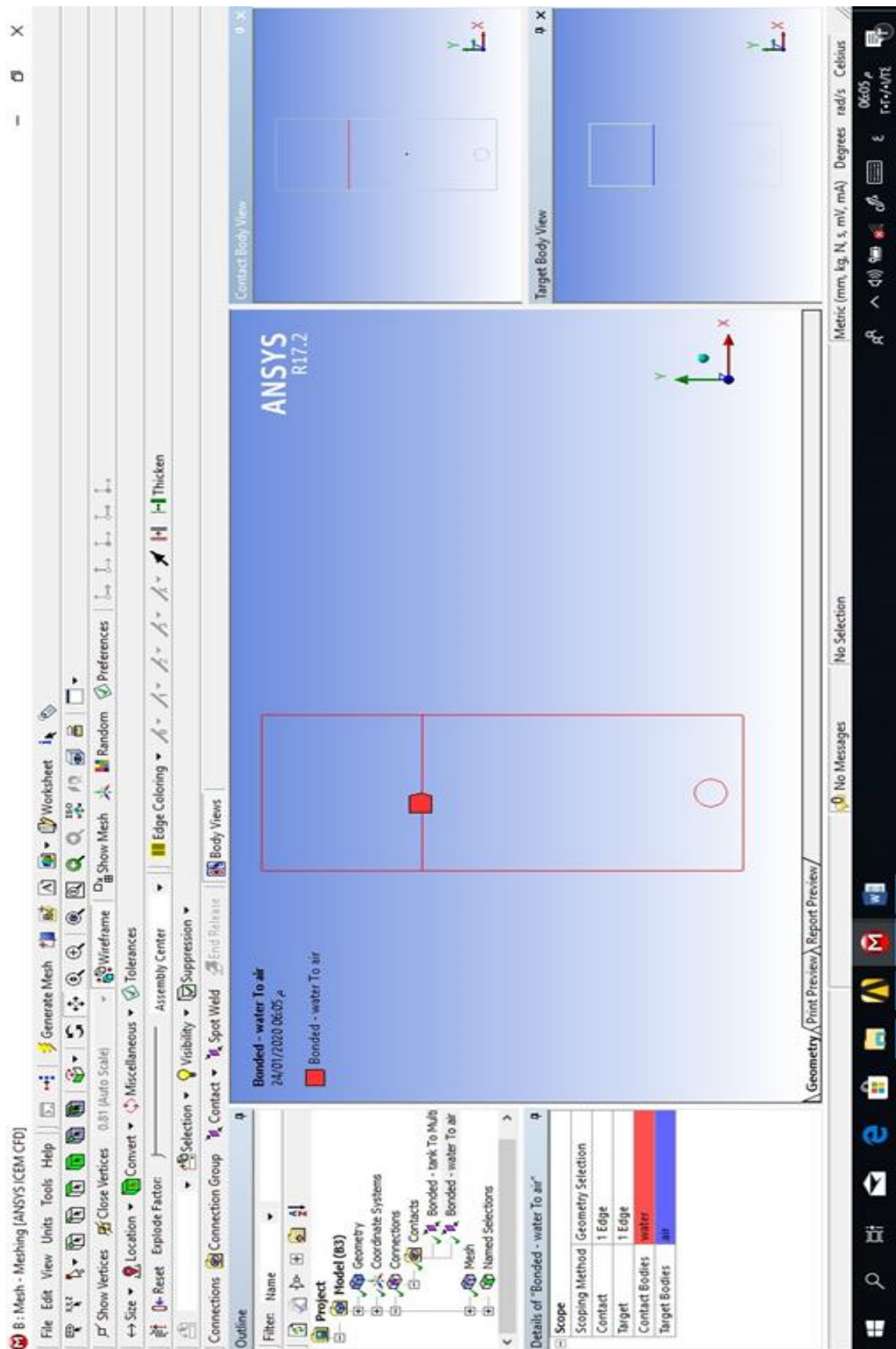


Figure 3-3. Water - air connection contacts

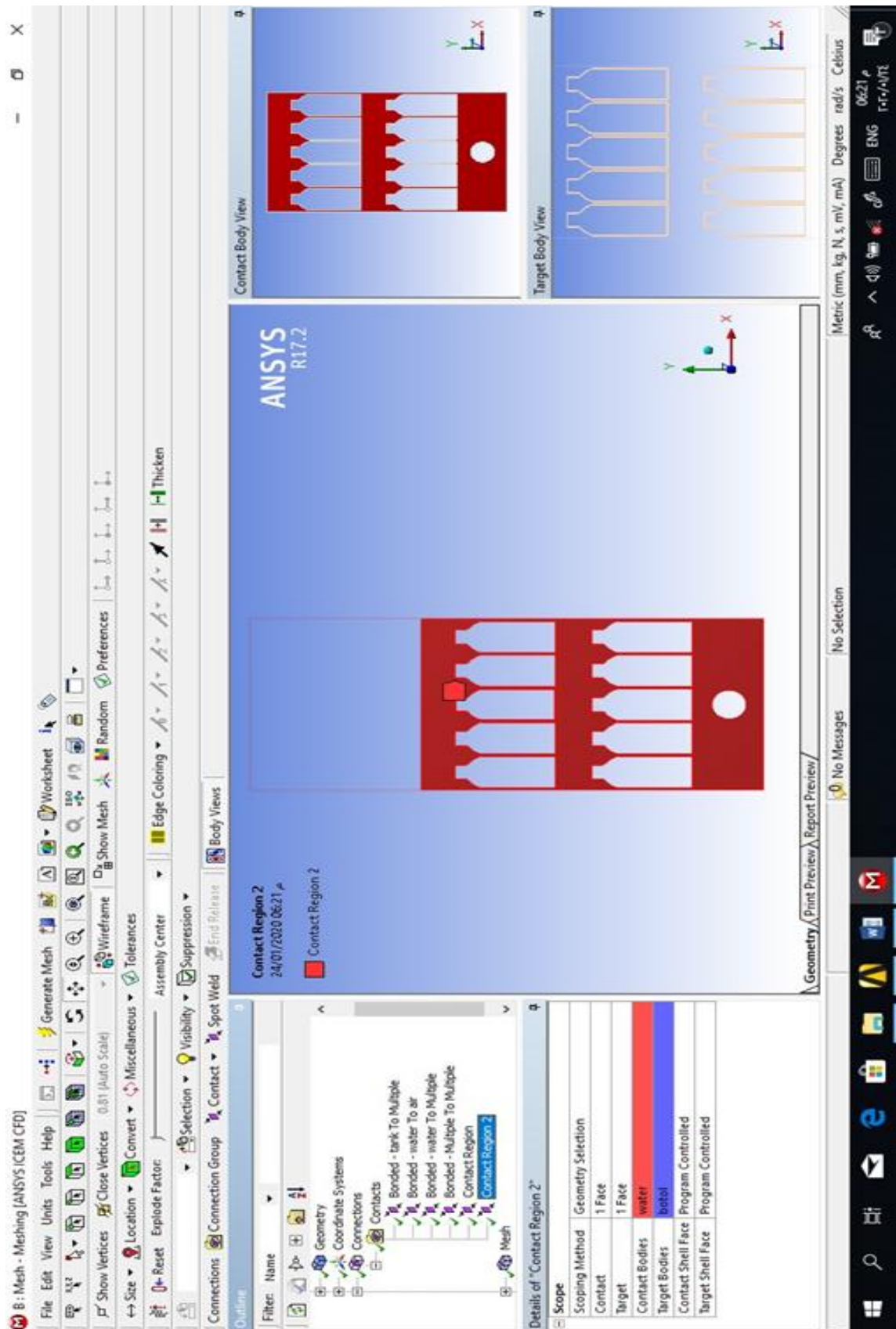


Figure 3-4. Water – PCM container connection contacts

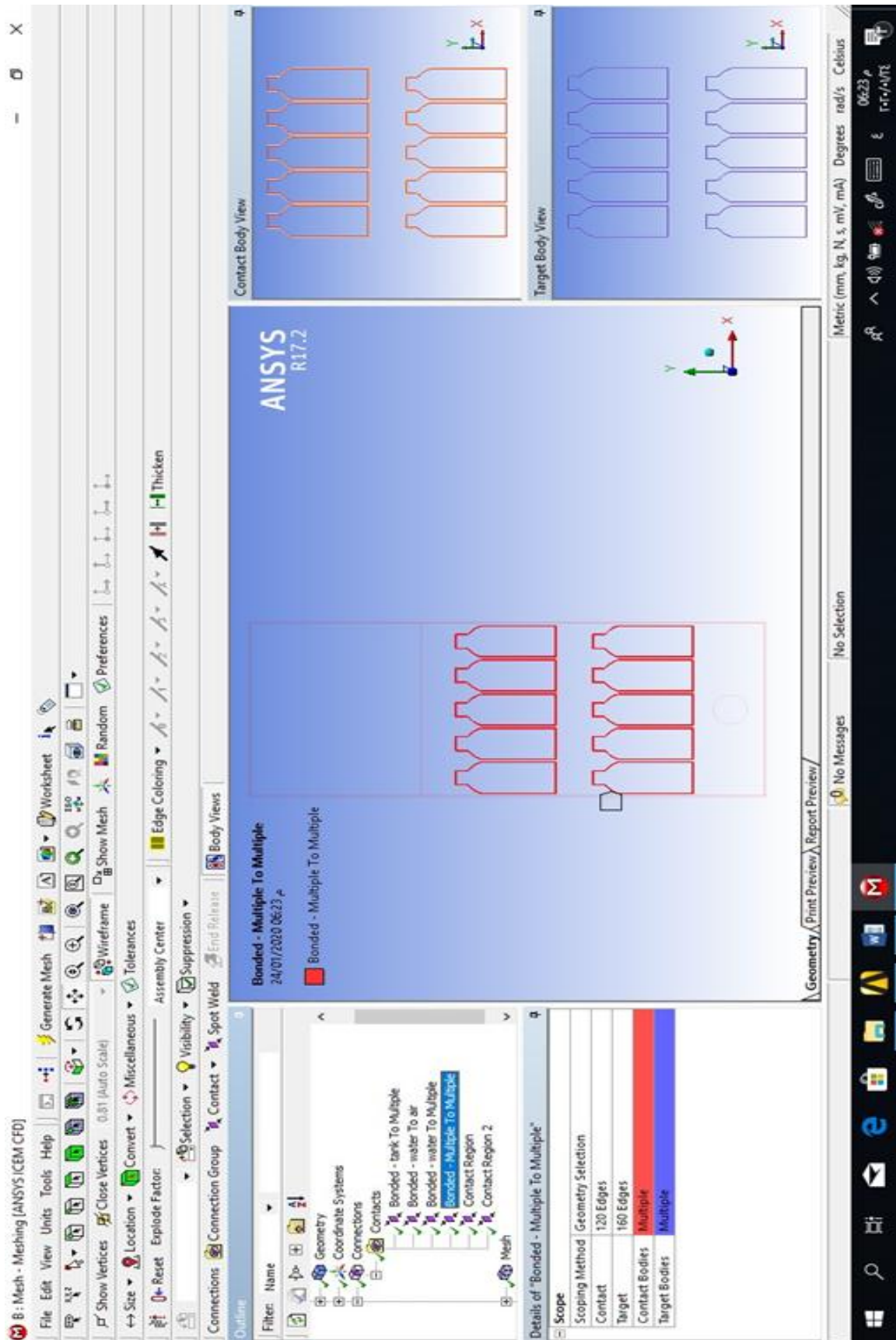


Figure 3-5. PCM – PCM container connection contacts

3.5. Mesh generation

The second stage in the model analysis is the mesh generation and dividing the model into elements. A quadrilateral shaped unstructured mesh element was used to obtain a stable convergence solution [51]. It is possible to control the mesh size that makes up the elements of the model. The smaller the mesh size, leads to greater the number of mesh and greater the accuracy of the solution. The simulation geometry model was tested for the case in which the PCM material is used, to choose the appropriate mesh size for the simulation process and then generalize it to the first case (without using PCM).

Test mesh showed that the sizes of large mesh had a difference results more than 3% compared to the results of the chosen mesh size.

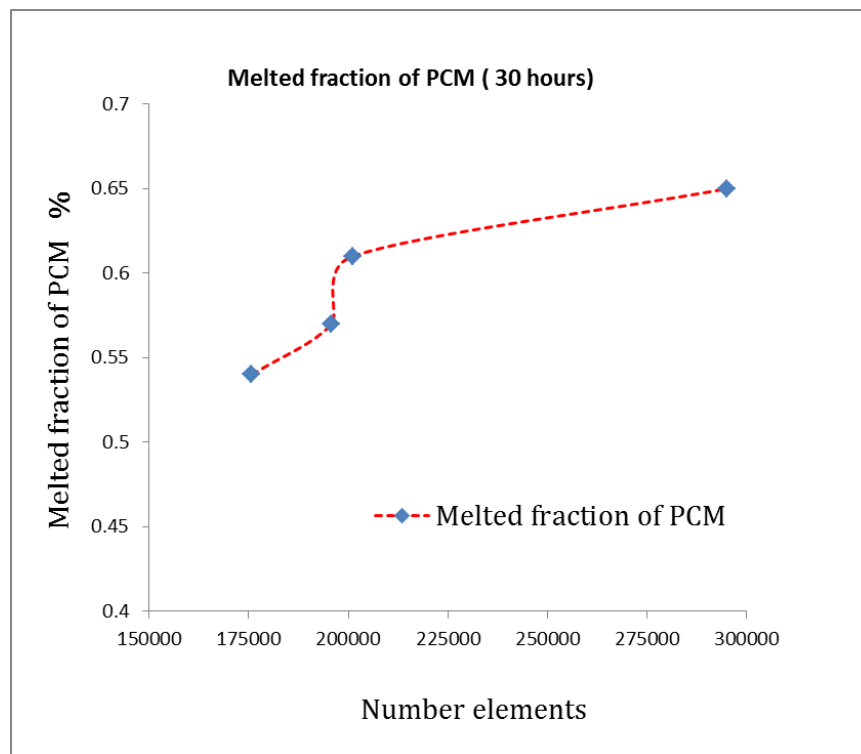


Figure 3.6: Mesh dependency test: number of elements and liquid fraction

With the Inflection option, the number of layers around some elements was increased, from 8 to 10 layers, to show more accuracy and reduce the error. Several numerical tests were carried out to have an accurate solution.

Table 3-2, Figure 3-7 shows the mesh size and the total number of mesh for Case1 (without PCM).

Table 3-2: Mesh generation of Case1 (without PCM)

Component name	Element mesh size	Inflection option	Total number (mesh element, nodes) for model
Container wall	2 mm	8 layers	Nodes = 149740 Mesh elements = 147059
water domain	2mm	-	
air domain	3mm	-	
heater element	2 mm	10 layers	

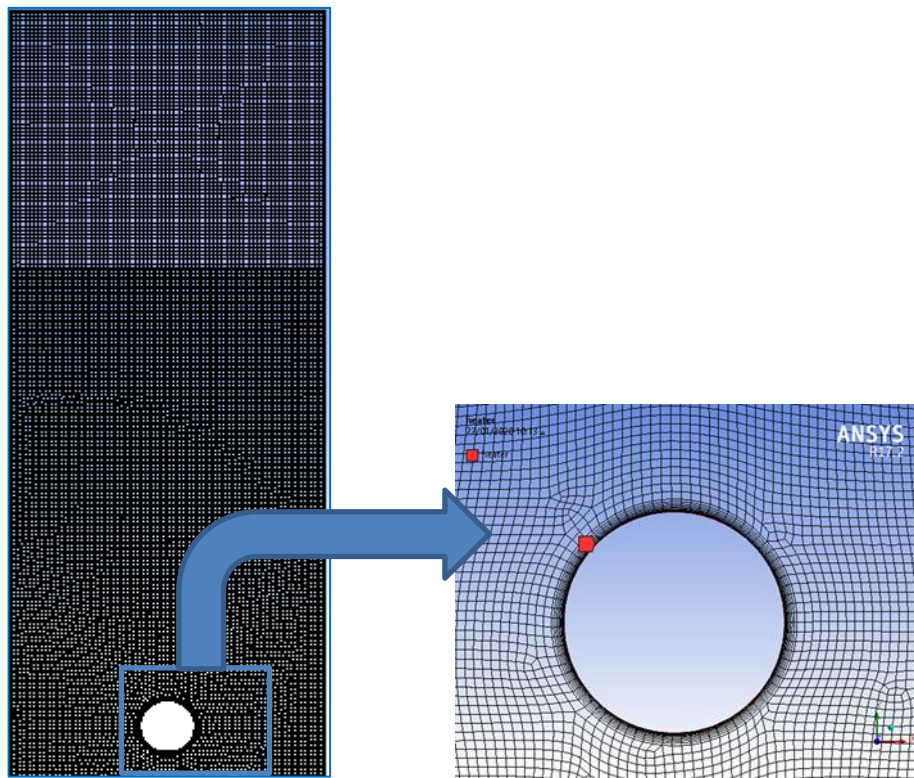


Figure 3-7. Mesh generation for case1 (without PCM)

In case 2 (with PCM) the number of mesh increased to double as more components were used. Also, the number of layers of the external wall, internal wall and PCM container are increased to ensure having accurate results. Table 3-3, Figure 3-8 show the mesh size and the total number of mesh for the case 2 (with PCM).

Table 3-3. Mesh generation of case 2 (with PCM)

Component name	Element mesh size	Inflection option	Total number (mesh element, nodes) for model
container wall	2 mm	8 layers	nodes = 320983 mesh elements = 295043
water domain	2mm	-	
air domain	3mm	-	
heater element	2 mm	10 layers	
PCM bottle	1 mm	8 layers	
PCM	0.6 mm	8 layers	

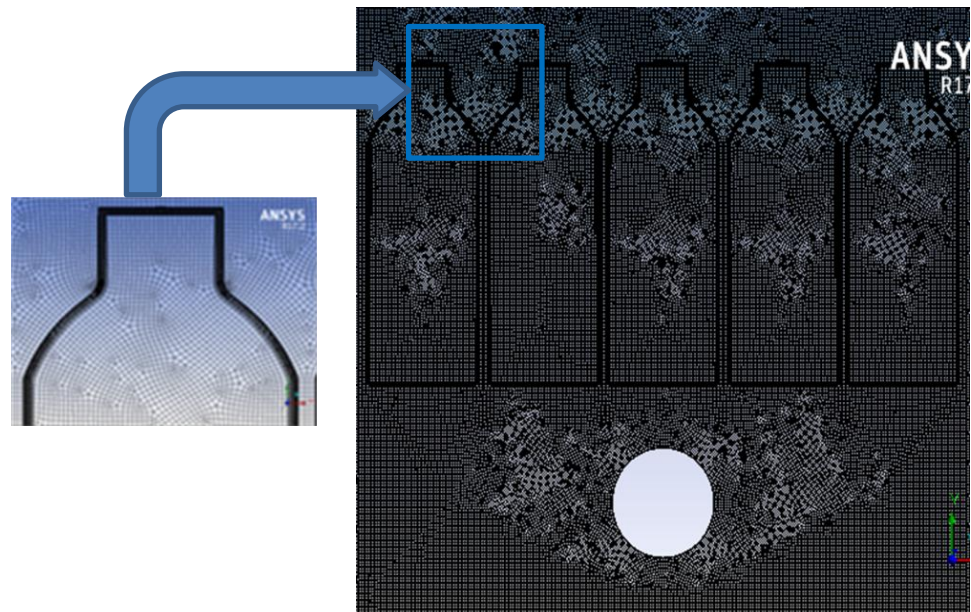


Figure 3-8. Mesh generation for case 2 (with PCM)

3.6. Numerical solution setup

In order to satisfy phase change PCM material condition, energy and solidification and melting are enabled. Table 3-4 shows the generic model solver settings.

Table 3-4: Generic model solver settings.

Model	Settings
Space	2D space, planer
solver, type	pressure based
velocity formulation	relative
Time	transient
gravity	-9.81 m/s ²
energy enable	enable
solidification and melting	enable

The thermo-physical properties of the model components are taken from a fluent database, and listed in Table 3-5.

Table 3-5. Thermo-physical properties of the numerical model

Component name	Material	Physical condition	Thermo-physical properties
water tank	steel	solid	$\rho = 8030 \text{ kg/m}^3$ $C_p = 0.502 \text{ kJ/kg.k}$ $K_{\text{steel}} = 16.27 \text{ w/m.k}$
PCM container	aluminum	solid	$\rho = 2719 \text{ kg/m}^3$ $C_p = 0.871 \text{ kJ/kg.k}$ $K_{\text{aluminum}} = 202.4 \text{ w/m.k}$
heater	copper	solid	$\rho = 8978 \text{ kg/m}^3$ $C_p = 0.381 \text{ kJ/kg.k}$ $K_{\text{copper}} = 387.6 \text{ w/m.k}$
Insulator	glass wall	solid	$\rho = 8978 \text{ kg/m}^3$ $C_p = 0.381 \text{ kJ/kg.k}$ $K_{\text{glass wall}} = 387.6 \text{ w/m.k}$
water	Water-liquid	fluid	Boussinesq approximation density

			(ρ) = 998.2 kg/m ³ C _p = 4.18 kJ/kg.k K _{water} = 0.6 w/m.k μ = 1.03*10 ⁻³ kg/m.s
air	air	fluid	ρ = 1.225 kg/m ³ C _p = 1 kJ/kg.k K _{air} = 0.024 w/m.k μ = 1.789*10 ⁻⁵ kg/m.s
PCM	PCM	2-phase change	It is based on table 4-2 Boussinesq approximation density

3.7. Boundary conditions

The boundary condition for model elements zone is shown in the Table 3-6.

Table 3-6. Boundary conditions for the model elements zone.

Element zone	Adjacent cell zone	Momentum	Thermal
Heater	water	stationary wall no slip	heat flux = 11000 w/m ² , for 2hour (charging process) heat flux = 0 w/m ² , for discharging process
wall-PCM container	PCM domain	stationary wall no slip	heat flux = 0 w/m ² wall thickness = 1 mm
insulation wall	tank- wall	stationary wall no slip	convection stream temperature = 22 °C wall thickness = 50 mm

3.8. Numerical solution procedure

- ❖ All components of the numerical model, are set at an initial temperature, $T_i = 24\text{ }^\circ\text{C}$.
- ❖ Conducting the process of charging the heat (heating), for the first two hours of operation, set heat flux = 11000 W/m^2 .
- ❖ The process of discharging the heat (cooling), for 22 hours of operation, set the heat flux = 0 W/m^2 .
- ❖ The temperature of the insulation wall is constant throughout the all operation process, $T_{\text{insulation}} = 22\text{ }^\circ\text{C}$.
- ❖ The water and PCM material temperatures are set to be auto-saved every (time step size) every 1 second, and time steps every 300 second.
- ❖ Temperature distribution and liquid-fraction contours are recorded at different times.
- ❖ At the end of the simulation, data is transferred to an excel sheet.

3.9. Flow Chart of numerical analysis

Figure 3-9 shows a flowchart of the steps for building a two-dimensional model by utilizing ANSYS FLUENT 17.2 software package to simulate a water tank with PCM bottles similar to that used in the experimental facility to highlight the advantages of using PCMs in a storage system.

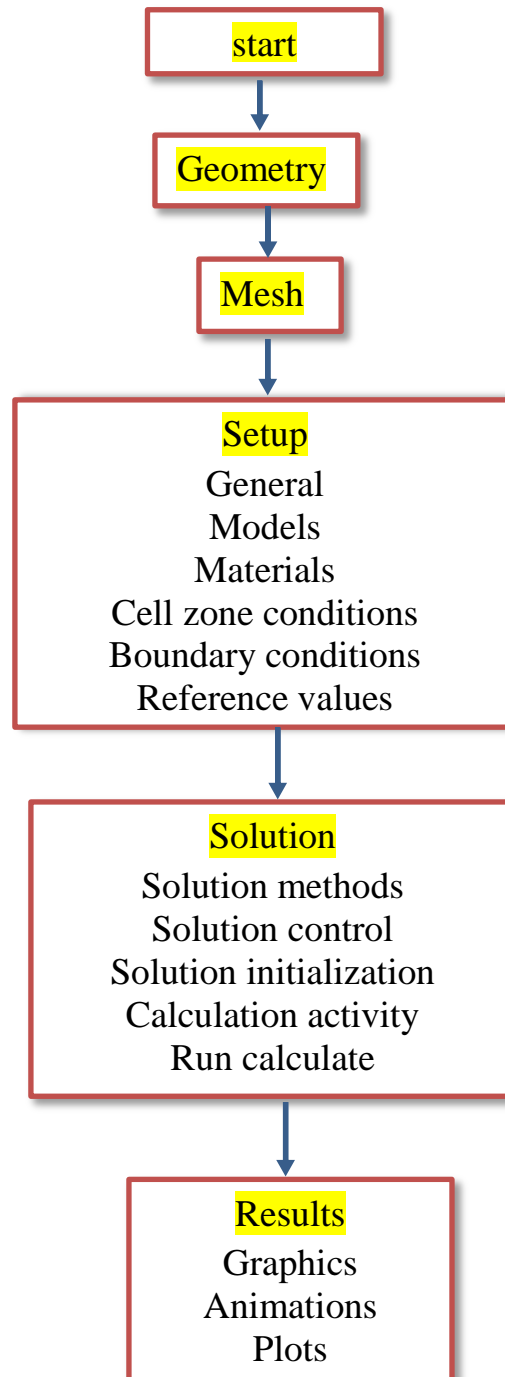


Figure 3-9. The Flow chart of numerical analysis

Figure 3-10, 3-11 shows the temperature distribution and liquid-fraction contours for the cas2 numerical model.

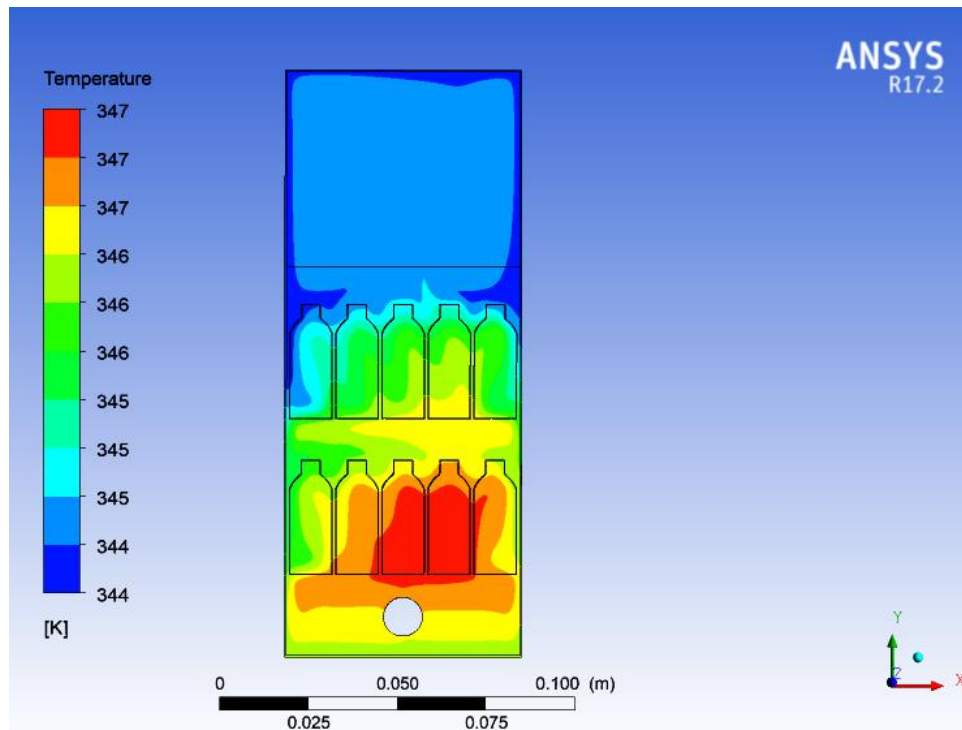


Figure 3-10. Temperature distribution contour for the second case (with PCM).

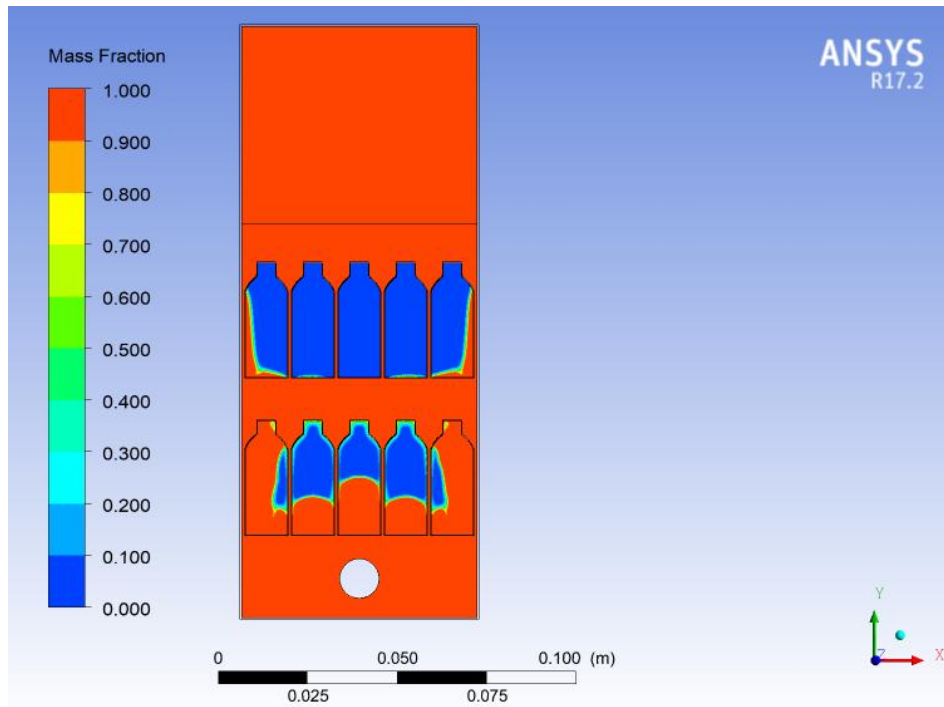


Figure 3-11. Liquid-fraction contour for the second case (with PCM)

**C
H
A
P
T
E
R**

4

EXPERIMENTAL STUDY

Chapter Four

Experimental Study

This chapter shows the main steps of assembling a PCM solar heating system including designing and manufacturing of a flat plate solar collector, a water storage tank, and all the necessary tools and equipment used for measurements. Subsequently, experiments of the solar heating system started with paraffin wax, to improve the system performance in terms of solar heat storage, and provide hot water for a longer time and results compared to those of without paraffin wax.

4.1. Place, and date of practical testing

The experimentally study was conducted in Karbala - Iraq, at latitude of 32.5 ° N, and longitude of 44.3 ° E, for the period from 20 March to 20 April 2019. This period was chosen for practical experiments because it represents the average solar radiation and temperature during the year.

4.2. Solar water heater system

The prototype system is designed and built depending on the engineering principles and the literature review. Similar to traditional solar water heaters, it is designed to provide 32 litres of hot water, with an active open-loop type, where the heat transfer fluid (water) is forced to circulate through the system. It consists of several components:

4.2.1. Flat Plate Solar collector

The flat plate solar collector is chosen because it is easy to manufacture and install with low cost and less maintenance. It can absorb direct and indirect solar radiation so that it can produce a temperature range of 40 to 75 °C, which is suitable for many applications[7].

To know the required area of the desired collector, the following assumptions and equations are applied[54].

- ❖ The volume of water to be heated is $V_w = 32$ L.
- ❖ The average solar heating time during the test is 6 hours.
- ❖ Average insolation (I) is 750 W/m²
- ❖ Ambient temperature, $T_a = 20$ °C
- ❖ Initial water temperature, $T_i = 20$ °C
- ❖ Maximum hot water temperature, $T_{max} = 75$ °C
- ❖ The efficiency of the collector is $\eta = 60$ %
- ❖ Specific heat of water, $C_{p_w} = 4200$ J/kg.°C
- ❖ Water density, $\rho = 1000$ kg /m³

The amount of useful heat gained (Q_U) can be found from equation (4.1) [54]:

$$Q_U = \rho \cdot V_w \cdot C_{p_w} (T_{max} - T_i) \quad \dots\dots\dots (4.1)$$

The collector absorber area (A_{pc}) can be obtained from equation (4.2) [54]:

$$A_{pc} = Q_U / \eta \cdot t \cdot I = \frac{\rho \cdot V_w \cdot C_{p_w} (T_{max} - T_i)}{\eta \cdot t \cdot I} \quad \dots\dots\dots (4.2)$$

$$= 0.815 \text{ m}^2 \sim 0.85 \text{ m}^2$$

- ❖ Copper is chosen to be used as an absorbent plate as it has high thermal conductivity compared to other cheap material. The plate has dimensions of 1 x 0.85 m and a thickness of 1 mm[54].
- ❖ A copper tube with an outer diameter of 10 mm and a thickness of 1 mm is used to make ten tubes risers, with a length of 960 mm. Another copper tube with an outer diameter of 20 mm and a thickness of 1 mm is used to make two headers with a length of 970 mm.

Circular section tubes are used because they are the best in the heat transfer process, thus increasing the efficiency of the collector [55].

- ❖ To form a pipe grid the risers and headers are welded by a silver welding wire. The distance between the risers is 80 mm from the centre to the centre. The smaller distance between the risers leads to an increase in the heat removal factor between the absorbent plate and the heat transfer fluid, which increases the efficiency of the collector [64,65].
- ❖ Then the pipe grid is welded with silver welding wire on the top surface absorption plate, to gives the best efficiency [55].
- ❖ The combination of the absorber plate and pipe grid is coated with 1mm a matte black coating with an absorption coefficient (0.9), emittance plate (ϵ_p) = 0.1, to increase the solar radiation absorbed, and reduce the wavelength radiation losses from the absorbing surface[7,66].
- ❖ A wooden box with dimensions surrounds the combination (1220, 1050, and 200) mm and 20 mm thickens. The box is insulated using of glass wool from the bottom and sides to reduce the conduction losses [56], Fig 4-1 showed the best insulation from the bottom and sides are 80 mm, 60 mm thickness, respectively.

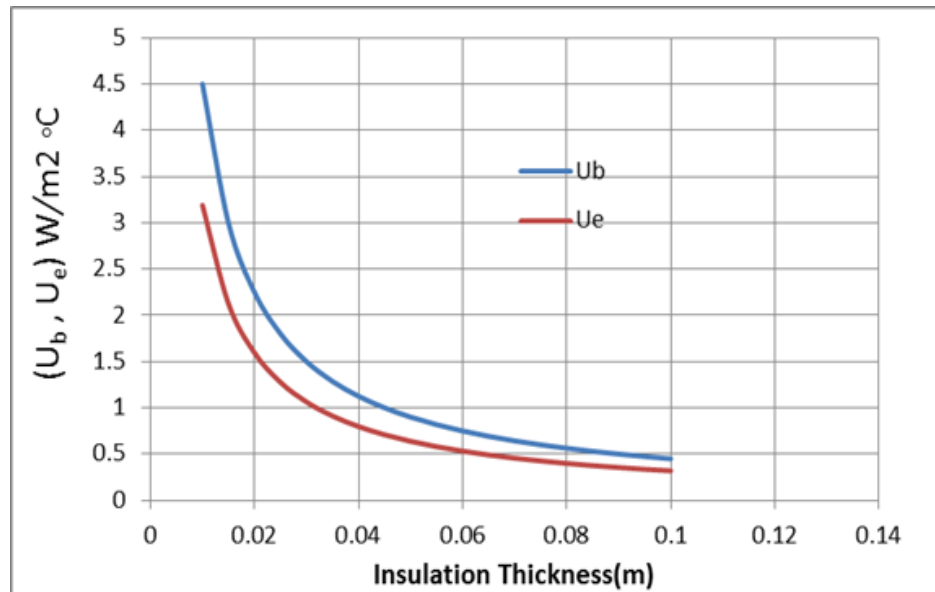


Figure 4-1 Variation of thermal losses from the back side of the solar collector with the insulation thickness

- ❖ Two layers of 4 mm thickness transparent window glass with a transmittance of about 85% and an emittance of $\epsilon_g = 0.88$ are used as a cover of the collector. The distance between the two layers is 3 cm. The gap between the inner glass layer and the copper absorption plate is 4 cm. This technique is used because it has high transmittance to visible light, with very little infrared transmittance and trapping heat energy inside the collector. Thus reducing the amount of heat energy lost to the surrounding environment [64, 67].
- ❖ The solar collector is installed on a steel frame with dimensions (1300, 1100, and 1200) mm, and equipped with wheels for smooth movement. A lever containing a spiral tube is used to make the angle of inclination with the horizon.

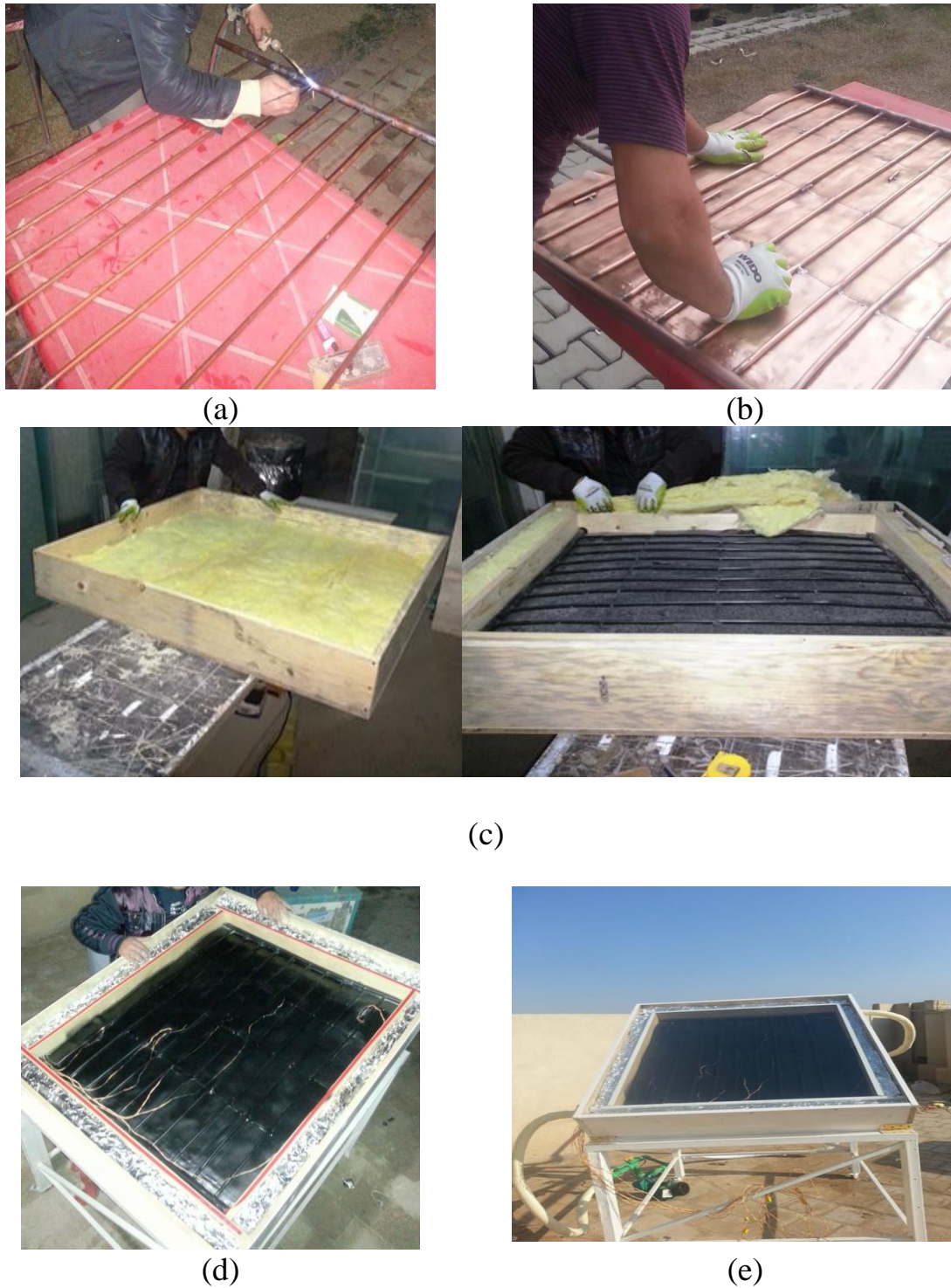


Figure 4-2. Manufacturing the solar collector, (a) the risers and headers are welded to form a pipe grid, (b) the copper pipe grid formed is welded on the absorption plate, (c) insulation with a glass wool from the bottom and sides, (d) two layers of glass to cover the solar collector, (e) the solar collector is mounted on an iron frame.

Table 4-1: The flat plate solar collector components

Components	Dimensions	Material
Collector box	1.22 m x 1.05 m x 0.2 m	wood
Absorber plate	1 m x 0.85 m x 0.001 m	black painted copper $\varepsilon_p = 0.1, \alpha = 0.9$
Transparent cover	4 mm thick	ordinary window glass, Number of glass: 2 $\varepsilon_g = 0.88$
Raiser pipes	inner diameter 8 mm, outer diameter 10 mm, length 96 cm, 8 cm distance spacing centre to centre	copper Number of tubes: 10
Header pipes	inner diameter 18 mm, outer diameter 20 mm, length 100 cm	copper Number of tubes: 2
Bottom insulation	0.08 m thick	fiberglass wool
edges insulation	0.06 m thick	fiberglass wool

4.2.2. Storage tank water

Under normal conditions, a 1 m^2 collector is used to heat an amount of water between 50 to 100 litres per day, with safety factor 1.5 of the volume water to be heated[54]. Therefore, the volume of the water container for 32 litres of water to be heated is 49 litres. A 49-litre cylindrical water tank with 75 cm high, 28.5 cm inner diameter and 1mm thickness is already available in the market. The tank is insulated with 50 mm glass wool, as shown in Figure 4-3.



Figure 4-3. Water tank used in the solar heating system

Perforated metal sheets are placed inside the water tank to carry the PCM containers, at a height 100 and 300 mm, respectively. A 1kW, electric heater, is used at the bottom of the water tank to generate a heat flux under controlled conditions.

4.2.3. The electric pump

An electric pump of 0.37 kW with 30 m head is used to circulate the working fluid through the solar heater system. Manual valves and bypass pipes are used to control the amount of liquid passing through the system. A 3/4 inches, insulated plastic tubes are used to making connections between the solar collector with the water tank.

4.3. PCM material

The first criteria for selecting the appropriate PCM is the melting point which must be within the range of the required application. Also, a latent heat, thermal conductivity and chemical stability are key parameters [33]. Therefore, paraffin wax was used according to its physical and chemical properties, which we mentioned earlier in Chapter 1. The average temperature in the studied system ranges from 20 to 75 °C, often for domestic hot water needs, for bathing and domestic washing at around 45°C, so the melting point of the wax should be between 40 and 55 °C[18]. Therefore, paraffin wax which dissolves in range of (52 ± 2) °C is used in this study. Table 4-2 list the paraffin wax specifications used.

Table: 4-2. Thermo-physical properties of the PCM used in this study [18]

Properties	Value
Melting temperature range	52 ± 2 °C
Latent heat fusion (L)	230 kJ/kg
Density (solid) ρ (s.ph.)	930 kg/m ³
Density (liquid) ρ (l.ph.)	830 kg/m ³
Specific heat (liquid) $C_{p_{pcm}}$	2.4 kJ/kg.k
Specific heat (solid) $C_{p_{pcm}}$	2.1 kJ/kg.k
Thermal conductivity, K_{pcm}	0.25 w/m.k
Viscosity μ	0.031 kg/m.s
Thermal expansion	$11 * 10^{-3}$ 1/k

4.3.1. PCM module geometry and heat transfer enhancement

Due to the low thermal conductivity of paraffin wax, the cylindrical packaging is chosen to improve the heat transfer between the packaging casing and heat transfer media [59]. A 32 thin cylindrical PCM containers made of aluminium are used. The container capacity was 0.31 litres, 1mm thickens, filled with 0.25 kg of paraffin wax. The PCM containers are placed inside the water tank and gathering on two rows, each containing 16 containers.



(a)



(b)

Figure 4-4. (a) PCM cylindrical container, (b) the copper mesh.

To improve the heat transfer coefficient and to ensure a homogeneous phase change, the thermal conductivity of paraffin wax is improved by adding high conductivity metal [13]. In this case, the amount of PCM was reduced to 225 g, and 25 g of copper mesh added, which is equivalent to 11.11% of the weight of paraffin wax in each aluminium bottle. Figure 4-5 shows a schematic diagram of a solar heating system test facility approved in this study. Figure 4-6 shows an experimental test facility for the solar heater system.

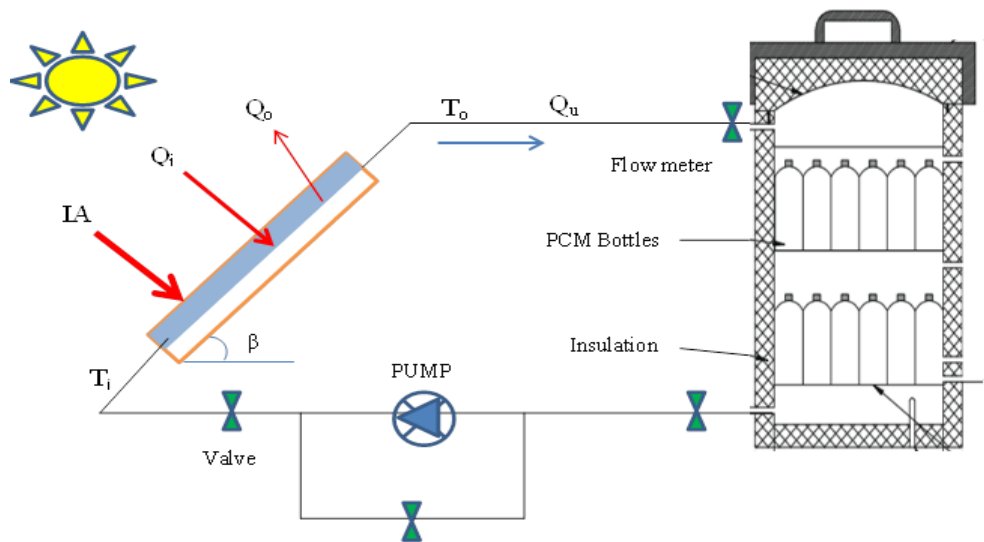


Figure 4-5. Schematic diagram of the test facility of the solar heater system adopted in this study



Figure 4-6. Experimental test facility of the solar heater system

4.4. Measurement devices

Experimentally, a set of instruments have been used, such as temperature meter, thermocouples, solar power meter, and water flow meter.

4.4.1. Temperature meter

The temperature recorder BTM - 4208SD (12 channels) with SD-Ram storage, shown in figure 4-7 is used. The thermocouple reading is stored every 10 minutes and transferred to the calculator and saved in an excel sheet. Calibration was performed at the Ministry of Science and Technology, Renewable Energies Directorate, in Baghdad, Iraq, and listed in Appendix B.1.



Figure 4-7. Temperature meter

4.4.2. Thermocouples.

Temperature recording and measuring system include thirteen thermocouples of type K, which have been pre-calibrated, as shown in Figures 4-8 and 4-9. Two thermocouples are installed on the inlet and outlet tubes of the collector, one thermocouple inserted in one of the PCM containers, one to measure the surrounding air temp, two on the absorbing plate and one thermocouple at air gap between the plate and glass. The calibration of thermocouples is listed in Appendix B.1 The thermocouple is

installed on the absorber plate, and the riser tubes, by welding aluminium, due to, its good heat conduction.

Table 4-3: Thermocouples distribution of the solar collector.

No. of Thermocouple	Location
1,2,3	Top surface of risers tube
4,5	Absorber plate
6	Air gap between the plate and glass
7	Inlet tube
8	Outlet tube
9	Ambient
10,11	Water temperature in the tank
12	The temperature of PCM
13	Glass cover

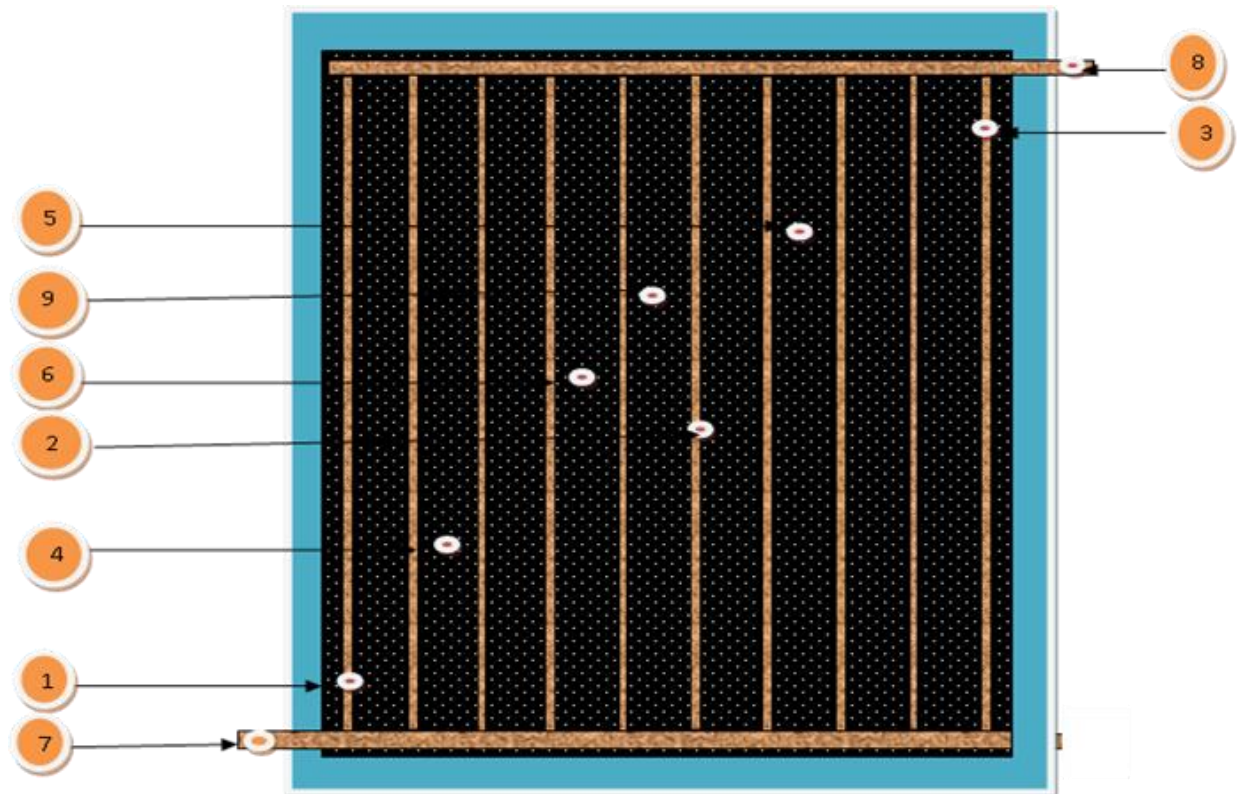


Figure.4-8 Thermocouples distribution in the solar collector

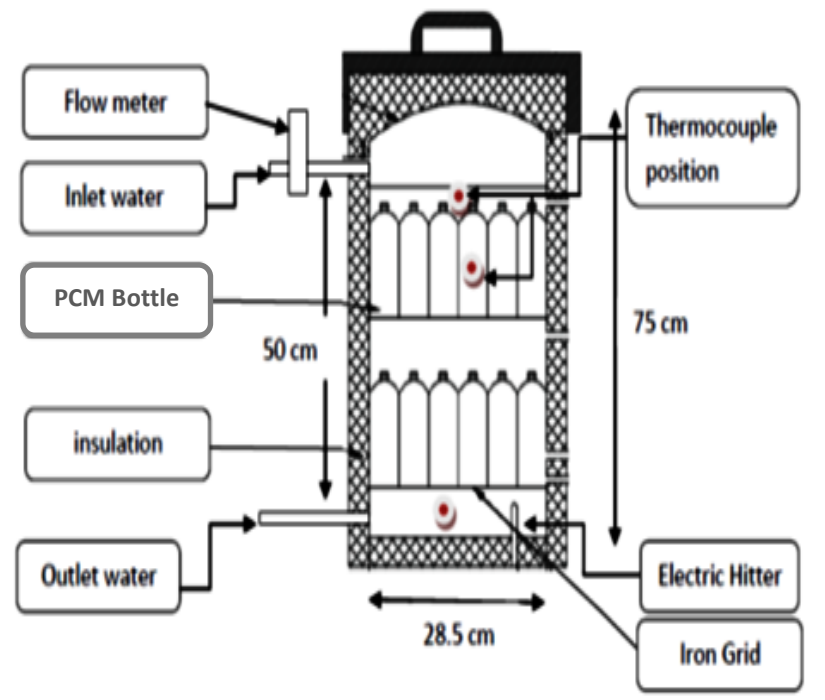


Figure 4-9. Schematic diagram of storage tank

4.4.3. Solar power meter

The Digital Make-**TES** Solar Model 1333 is installed on one side of the solar collector to measure the total solar radiation in the inclined plane. Figure 4-10 shows the digital solar meter. The device was calibrated at the Ministry of Science and Technology, Renewable Energies Directorate in Iraq, as listed in Appendix B.1.



Figure 4-10. solar power meter.

4.4.4. Flow meter

To measure the volumetric flow rate of heat transfer fluid (water), a flow meter (range 1-18) L/min is used, and the calibration of this apparatus is shown in Appendix B.3.



Figure 4-11. Water flow meter used in this study

4.5. Experimental procedure.

Various tests have carried out which can be divided into two types depending on the heat source used. The first one relies on the conversion of solar energy to heat using the solar collector, which includes two cases as:

- ❖ Case 1, only 32 litres of water were used, without PCM. The test was carried out at different flow rates (1,3,5) L/min, to highlight the effect of flow rate on system efficiency, heat gain, heat transfer coefficient, and stored heat.
- ❖ Case 2, 22 litres of water, equivalent to 69% and 32 bottles filled with 8 kg paraffin wax, 9.92 litres, equal to 31%, are used for flow rates (1,3, 5) L / min, to be compared with the first case and find its effect on the melting time of the wax and the amount of heat stored.

For both cases, the following steps were performed:

- 1- Changing the angle of the solar collector one time every single day, to ensure a maximum amount of solar radiation is applied to the solar collector.
- 2- Monitoring, measuring and recording temperature every 10 minutes.
- 3- Starting the water pump and adjusting the required flow rate.
- 4- Starting the solar collector from 9 am to 3 pm, for sunny days only, because in the test experiments observed that the water temperature in the tank becomes higher than the exit temperature of the solar collector after 3 pm, despite the presence of solar radiation.
- 5- The water pump is then switched off, and the inlet, outlet valves of the water tank are turned off to isolate the solar collector.
- 6- Reading solar radiation data manually using the solar meter every 10 minutes from 9 am to 3 pm.
- 7- Temperature recording continues until 8 am the next morning.
- 8- Temperature data is transferred to the computer and water is replaced with new water, for the next test.

In the second type of test, a 1kW electric heater is used as a heat source, and four different cases were carried out as:

- a. Case - 1, only 32 litres, of water were used, 100%, without PCM.
- b. Case – 2, 78 % water 25.2 L, 22 % PCM 6.8 L, 5.5 kg PCM.
- c. Case – 3, 69 % water 22.1 L, 31 % PCM 9.9 L, 8 kg PCM.
- d. Case – 4, 69 % water 22 L, 31 % PCM with copper mesh 9.6 L, 7.2 kg PCM.

4.6. Governing equations.

4.6.1. Flat-plate solar collector

1) The tilted angle of the flat-plate collector, β

For the greatest amount of solar radiation, the solar collector must be directed southward at an appropriate slope, the angle of inclination can be found from the following relationship [60]:

$$\beta = | \varphi - \delta | \quad \dots\dots\dots (4.3)$$

φ , refers to, a latitude angle = 32.5°

δ , refers to, a declination angle which has a variable value, based on the date, can be found from the relationship[60] :

$$\delta = 23.45 \sin\left[\frac{360}{365} (284+n) \right] \quad \dots\dots\dots (4.4)$$

Where, n, represents the number day in the year, starting from, 20 March to 20 April. Solar angles are illustrated in Appendix A.3.

Changing the tilted angle of the flat-plate collector, one time every single day, to ensure the highest amount of solar radiation on the solar collector, and to make all experiments days convergent in the amount of solar radiation.

2) Energy balance

By applying the first law of thermodynamics, for the flat plate collector in steady-state energy balance, as follows [58]:

Useful energy gain (Q_u) = collector energy absorbed - surroundings heat loss

$$Q_u = Q_i - Q_{loss} \quad \dots\dots\dots (4.5)$$

$$Q_u = A_C \cdot I_T \cdot (\tau\alpha) - A_C \cdot U_L (T_P - T_a) \quad \dots\dots\dots (4.6)$$

- A_C = Collector absorbing plate area (m^2).
- I_T = Total solar radiation which is incident on the tilted Collector (W/m^2), the data is taken from the solar meter radiation.
- τ = Glazing transition coefficient, for normal cases, is [1]:

$$\tau = \frac{(4n)2N_g}{(1+n)4N_g} \dots\dots\dots (4.7)$$

- N_g = the number of glass sheets, and $n = 1.5$ =the refractive index of windows glass, then, $\tau = 0.85$, for $N_g = 2$
- α = plate absorption coefficient = 0.9
- U_L = Overall heat loss coefficient ($W/m^2 \text{ } ^\circ C$).
- T_p = The mean absorber plate temperature ($^\circ C$).
- T_a = Ambient temperature ($^\circ C$).

3) The overall loss coefficient collector U_L is equal to the sum of the top, back, and edge losses, as follows [58].

$$U_L = U_t + U_b + U_e \dots\dots\dots (4.8)$$

U_t represents the most significant losses, which are the energy losses through the upper part of the solar collector to the surrounding environment as a result of convection and radiation from the absorption plate to the glass cover.

The heat transfer coefficient between the glass cover and the atmosphere can be obtained from the following equation [57] :

$$h_w = 5.7 + 3.8 * V \dots\dots\dots (4.9)$$

V represents the velocity of wind in m/s, the air speed in Iraq ranges between 5 to 10 km/h, and from the Iraqi Weather Bulletin estimated airspeed at 5 km/h.

$$h_w = 10.9777 \sim 11 \text{ w/m}^2 \cdot ^\circ C$$

Calculation of the top loss coefficient of the solar collector (U_t) attached in Appendix A.2.

$$U_{t32} = 2.496 \sim 2.5 \text{ W/m}^2 \cdot ^\circ\text{C}$$

U_b , represents back losses, can be obtained as follows [58]:

$$U_b = \frac{K}{L} \quad \dots\dots\dots (4.10)$$

Where k , represents the thermal conductivity of the insulator = 0.045 W/ m $^\circ\text{C}$, and L represents the insulation thickness = 0.08 m.

$$U_b = 0.5625 \text{ W/m}^2 \cdot ^\circ\text{C}$$

U_e represents edge losses; if the heat transfer is one-way, around the perimeter of the collector, the collector edge losses can be expressed as follows [58]:

$$U_e = \frac{(UA)_{\text{edge}}}{Ac} \quad \dots\dots\dots (4.11)$$

$$U_e = 0.638 \text{ W/m}^2 \cdot ^\circ\text{C}$$

From equation (4.8) we get:

$$U_L = 3.7 \text{ W/m}^2 \cdot ^\circ\text{C}$$

- 4) The thermal efficiency of a solar collector is the ratio between the total useful gain over a given period to the total solar energy dropped during that period, as equation (4.12) [61]:

$$\eta_{th} = \frac{\int Q_u dt}{AC \int I dt} \quad \dots\dots\dots (4.12)$$

- 5) The instantaneous thermal efficiency of the collector[61]:

$$\eta_i = \frac{Q_{ui}}{Ac.I} \quad \dots\dots\dots (4.13)$$

when $Q_{ui} = \dot{m} \cdot cp_w \cdot (T_i - T_o) \quad \dots\dots\dots (4.14)$

6) Not all of the useful energy that the absorbent plate has gained, the actual energy that will be transferred to the heat transfer fluid, the ratio between them is called the (F_r), heat removal factor as in the following

$$\text{equation[58]: } F_r = \frac{Q_{ui}}{AC[I\tau\alpha - UL(T_p - T_a)]} \quad \dots\dots\dots (4.15)$$

$$\eta_i = F_r \left[(\tau\alpha) - \frac{UL(T_p - T_a)}{I} \right] \quad \dots\dots\dots (4.16)$$

7) η_o represents the overall thermal efficiency of the solar heat system is[58].

$$\eta_o = \frac{m \cdot C_p \cdot \Delta T_w}{AC \cdot I_{avg} \cdot \text{time}} \quad \dots\dots\dots (4.17)$$

3.6.2. Thermal storage equations, during the charging process

1) The case of using water only, the amount of heat stored (E_{storeg}), is a sensible heat, which can be obtained from the equation (1.1):

$$E_{storege} = \rho \cdot V \cdot C_p \cdot (T_f - T_i) \quad \dots\dots (4.18)$$

The water properties (ρ , C_p), depends on the average water temperature in the tank T_{min} .

2) The case of using water and paraffin wax.

The total amount of energy stored is equal to the sum, amount of heat stored in water and the amount of heat stored in PCM.

$$E_{storeg} = E_{storeg, water} + E_{storeg, PCM} \quad \dots\dots (4.19)$$

The amount of heat stored in PCM, which can be obtained from the equation (1.2), (4.18) [62]:

$$E_{storege, PCM} = m_{pcm} [Cp_s \cdot (T_i - T_{melt}) + L + Cp_l \cdot (T_f - T_{melt})] \quad (4.20)$$

- 3) The case of using water and paraffin wax with copper mesh:
replace the paraffin mass, In equation 4.20, with the paraffin mesh
mixture mass[47]:

$$m_{mixture} = m_p + m_{mesh} \quad \dots\dots (4.21)$$

Also, replace the specific heat of the PCM with the specific heat of the
paraffin mesh mixture[47]:

$$Cp_{mixture} = \frac{(m_p \cdot Cp_p + m_{mesh} \cdot Cp_{mesh})}{m_{mixture}} \quad \dots\dots (4.22)$$

4.7.Repeatability Check

Each case was retested several times during the same period and under the same conditions, to increase the reliability of the experimental test results of the water heating system used in our current study. Results were recorded to measure compatibility between results[70].

The PCM material temperature was chosen during the charging process, using the electric heater as a power source. The data obtained from the repeat test three times were graphically represented in Figure 4.12.

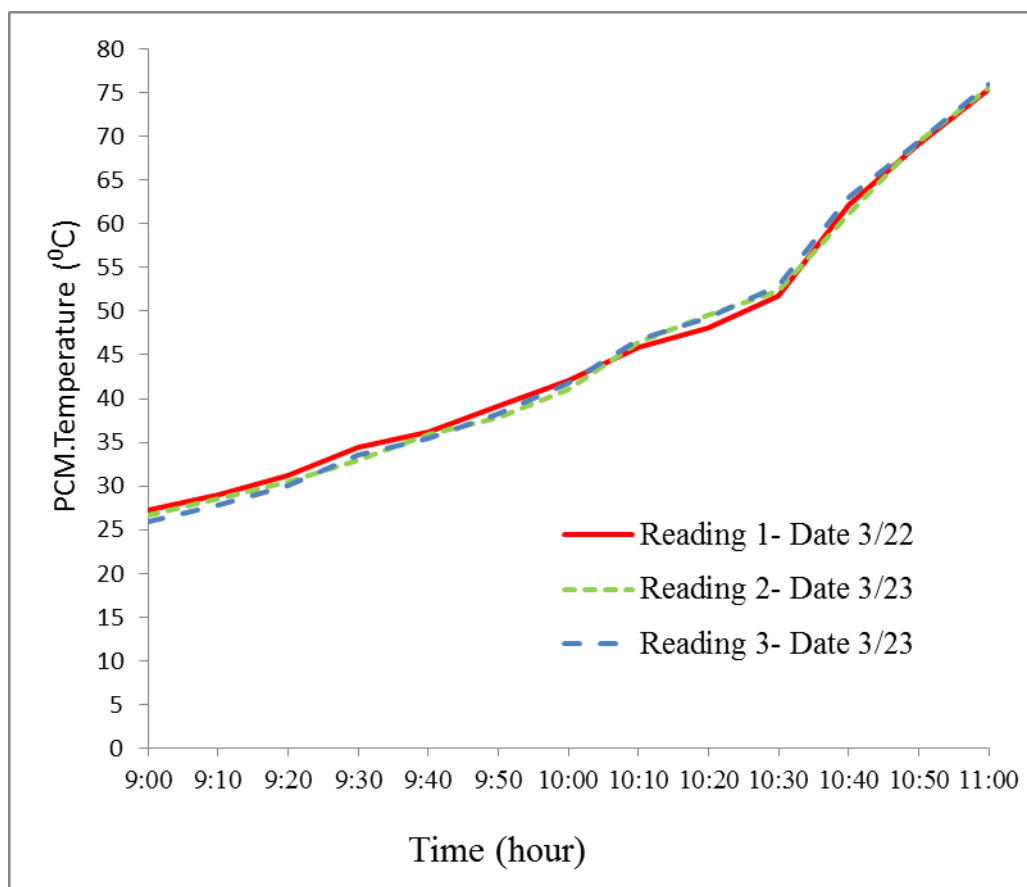


Figure. 4.12 Repeatability of PCM-temperature

Figure 4.12 shows the amount of convergence between the results and that there is a slight difference between them. The mean and the mean, standard deviation are calculated for this series of effects.

**C
H
A
P
T
E
R**

5

RESULTS AND DISCUSSION

Chapter Five

RESULTS AND DISCUSSION

This chapter presents the experimental and numerical results and discusses them in details. The study aims to highlight the effect of using phase change materials on the performance of the solar heater system designed in Chapter 4.

5.1. Experimental Results

Various experiments were carried out which be divided into two types depending on the heat source used, manufactured flat plate solar collector, and electric heater. The heating process in the first type in which the flat plate collector is the source of heat continues for six hours from (9 am to 3 pm) for three water flow rates 1, 3 and 5 L/m. Then the cooling process starts until eight o'clock in the morning of the next day for two cases (water only, 31% PCM + 69% water). All temperatures and solar radiation were recorded every 10 minutes. The heating process in the second type in which the electric heater is the source of heat continues for two hours from (9 am to 11 am), after which the cooling process starts until eight o'clock in the morning of the next day and for four cases as explained in the fourth chapter.

5.1.1. The solar collector, as heat source

In this type, several experiments were carried out during the test period; however, the data were taken only for sunny days to make a good comparison.

The solar collector tilt angle is calculated theoretically using equation (4.3), with one daily adjustment so that the beam of solar radiation is perpendicular to the collector surface at noon every day, to get maximum solar radiation. The data obtained are graphically represented in Figure 5-1.

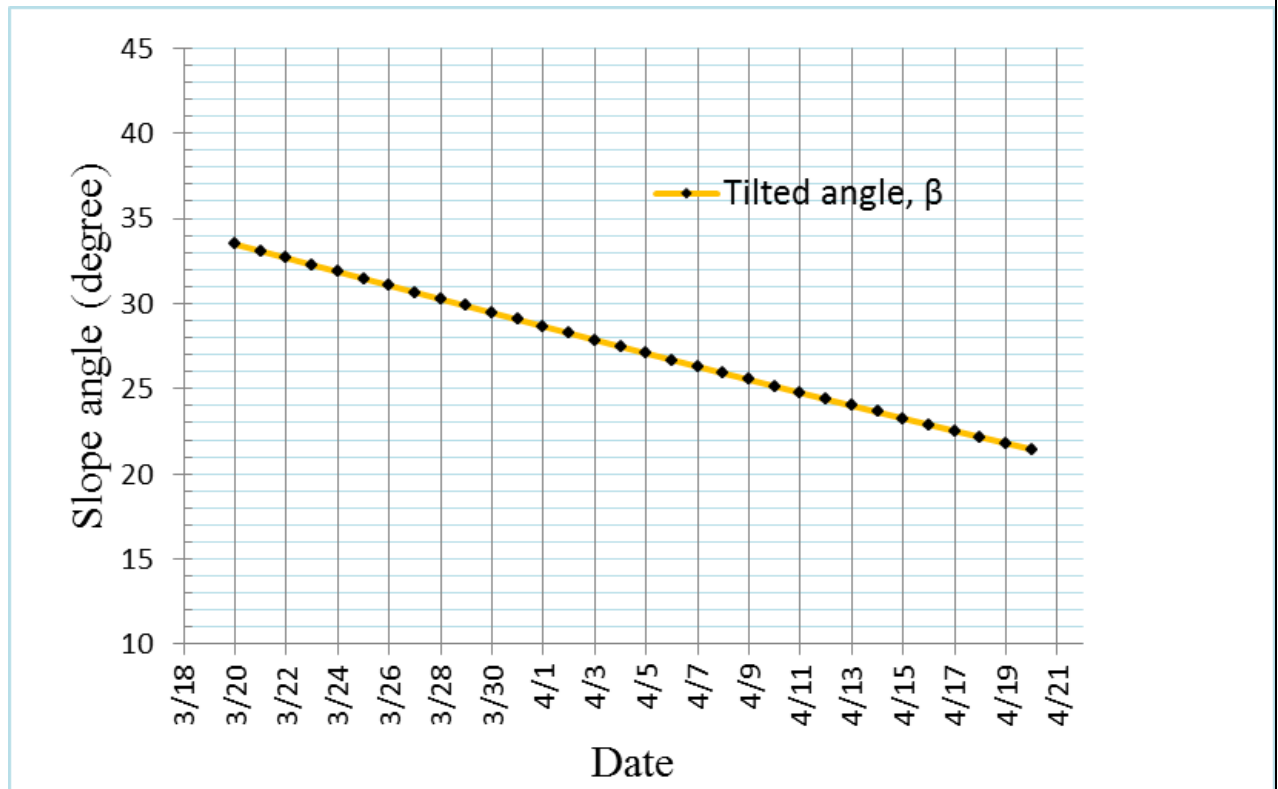


Figure 5-1: Daily tilt angle (β) used in this study

Figure 5.1 shows the variation in the tilt angle during the test. Solar radiation data is measured using the solar radiation meter and recorded manually every 10 minutes from 9 am to 3 pm, and three different dates were selected, as shown in Figure 5.2.

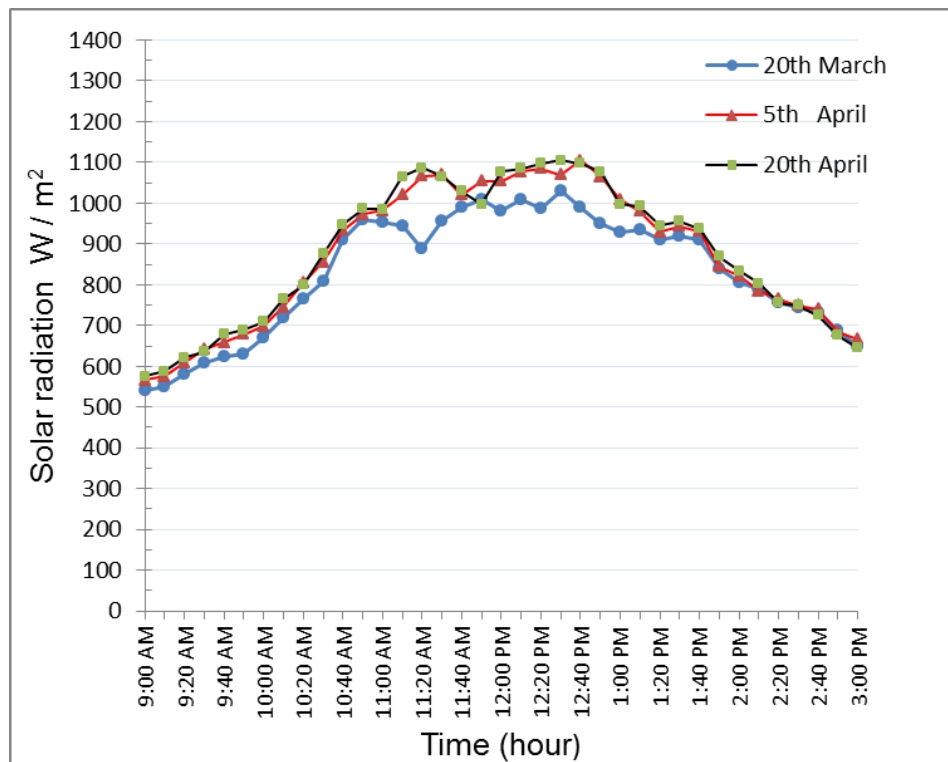


Figure 5.2: The solar radiation in the city of Karbala between 9 AM and 3 PM for three different dates

Figure 5-2 shows that solar irradiance values were close to each other, and this is, due to the selection of test days in clear sky conditions and the daily adjustment of the tilt angle. The value of solar radiation gradually increases to the maximum value at midday (12:15 to 12:30) and then begins to decrease this is because the solar radiation falls perpendicularly to the surface of the collector whenever we get close to noon. The average values for 6 hours for a day (20/3, 5/4, 20/4) were (794.88, 831.9, 838.97) W/m^2 respectively.

5.1.1.1. Case 1 (without PCM)

In this case, 32 litres of water were used without PCM. Tests were carried out at different flow rates, including 1, 3, and 5 L/min. The inlet, outlet, all temperatures, and solar radiation were recorded every 10 minutes. The change in the flow rate of water during the charging process has a significant impact on several factors, which will be discussed in this section.

1. Inlet/outlet temperature difference in the collector

Figure 5.3 shows that the water temperature difference in the solar collector using three different flow rate values of 1, 3 and 5 L/min during the charging process. As the flow rate of water increases, the temperature difference decreases, because the remaining time of the fluid in the collector is less. Therefore the heat transfer from the absorbent plate to the heat transfer fluid is less as well. The maximum difference temperatures at flow rate 1, 3, and 5 L/min, is 5.8, 3.1, and 2.1°C, respectively.

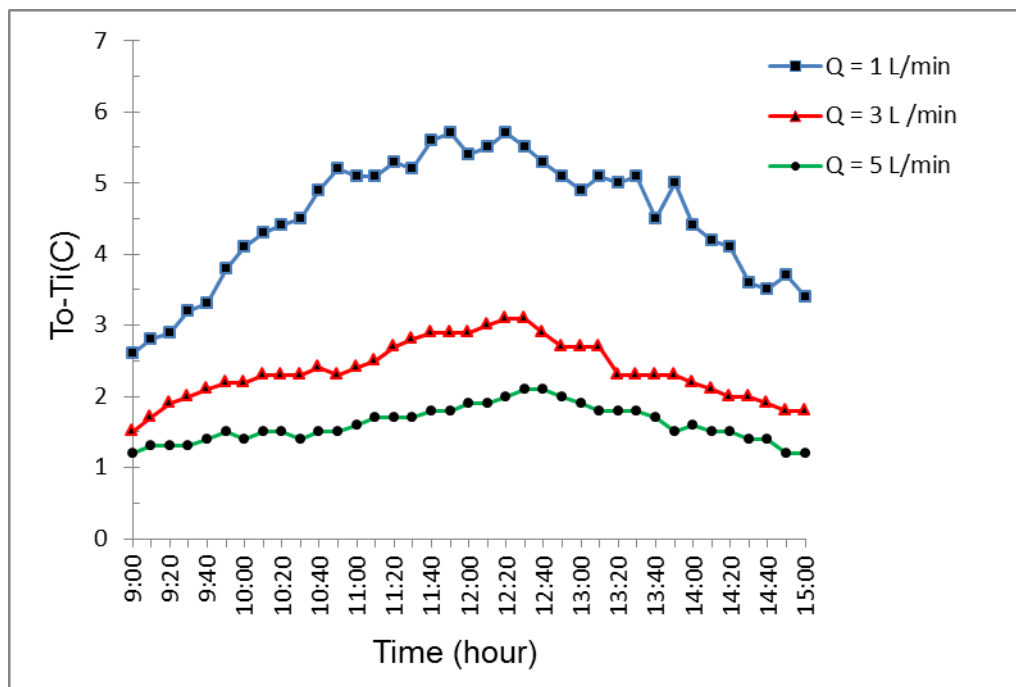


Figure 5.3: Hourly temperature difference in solar collector using three different flow rates

2. Time of heat charging

Figure 5.4 shows that as the water flow rate increases, the time required to reach the design temperature decreases. Increasing the water flow rate has a positive effect on reducing the time of heat charging, for example reaching the water temperature of 70 °C would have required 340, 290, and 255 min, at flow rate 1, 3, and 5 L/min, respectively.

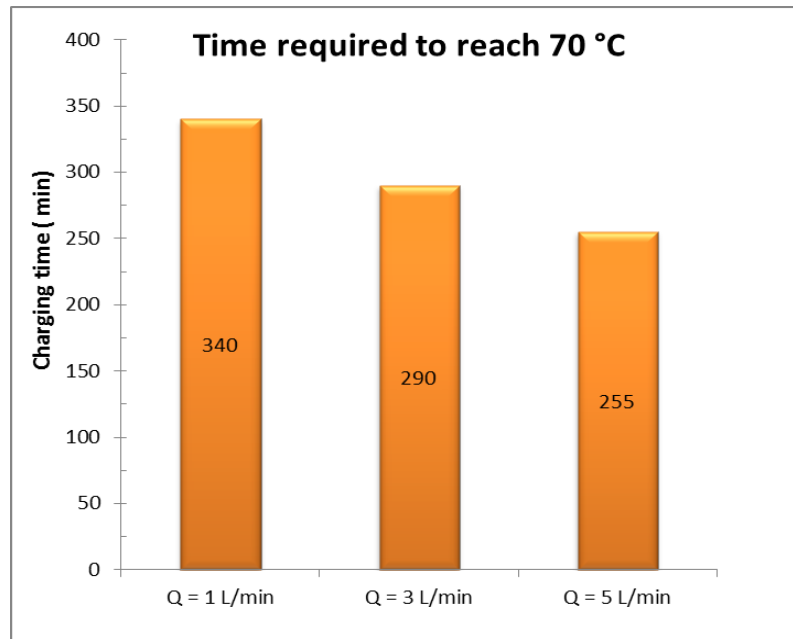


Figure 5.4: Time required to reach the temperature of 70 °C using three different mass flow rates

At the end of the charging process using 1, 3, and 5 L/min, the water temperature was 70.3, 71.4, and 72.3 °C, respectively. Figure 5.5 shows the Hourly water tank temperature for case 1 (without PCM) during the charging process with different water flow rates.

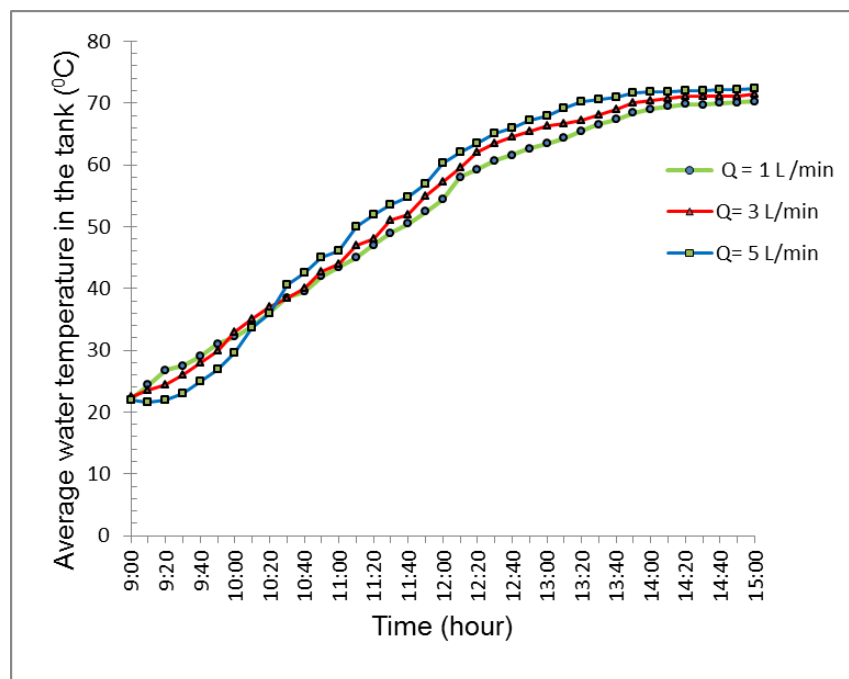


Figure 5.5: Hourly water tank temperature for case 1 (without PCM) during charging process with different water flow rates

3. Heat gain from the collector

Figure 5.6 shows that the instantaneous useful heat increases gradually over time until reaching the maximum value 377.162, 636.5, and 717.6 W at 1, 3, and 5 L/min, respectively at midday and then it decreases again depending on the amount of solar radiation falling on the solar collector. Also, Figure 5.6 shows that the maximum amount of useful heat is achieved when a flow rate of at 5 L/min is used.

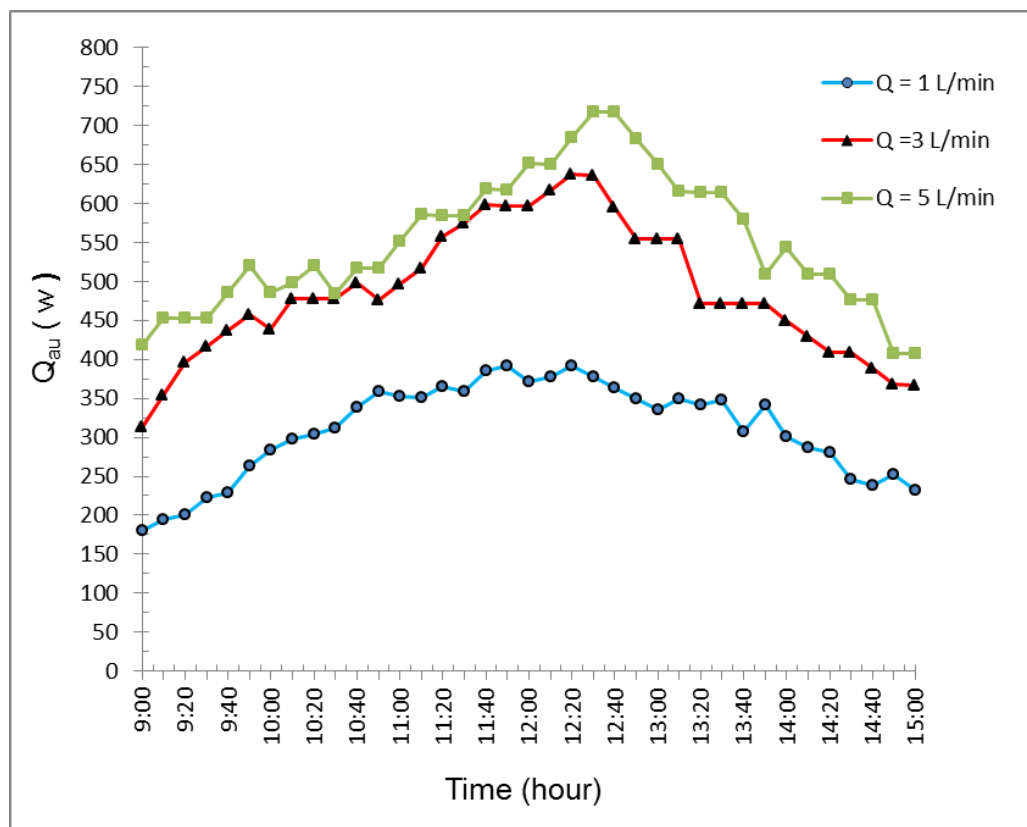


Figure 5.6: Instantaneous useful thermal energy with different flow rates

4. Instantaneous thermal efficiency of the collector, η_i

The instantaneous efficiency of the solar collector is calculated using Eq. 4.13, as shown in Figure 5.7.

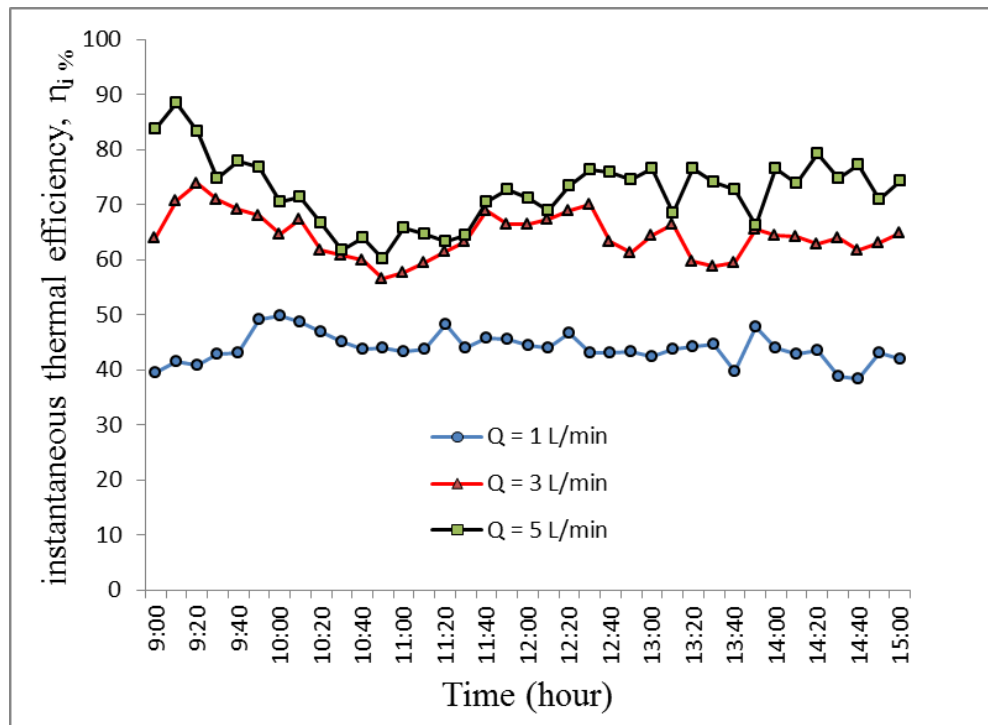


Figure 5.7: The instantaneous thermal efficiency of the collector with daylight time at a variable flow rate

Also, Figure 5.7 shows the effect of using different flow rates on the immediate thermal efficiencies of the solar collector. The higher the flow rate, the greater the instantaneous thermal efficiency, which happens at 5 L/min.

5. The thermal efficiency of a solar collector, η_{th} %

The thermal efficiency of the solar collector can be calculated using Eq. (4.12), and the maximum value is about 67% using a flow rate of 5 L/min is used.

6. Amount of heat stored (E_{stored}), and the overall thermal efficiency η_o %.

The amount of heat stored in the water is sensible heat. The overall thermal efficiency can be calculated using equations (4.18), (4.17), respectively, at

the flow rate 1, 3, and 5 L/min, and the properties ρ and C_p of pure water are taken from table C.1 in Appendix C and results for different flow rates are listed in Table 5.1.

Table 5.1: The amount of heat stored and the overall thermal efficiency results

	$Q = 1 \text{ L/min}$	$Q = 3 \text{ L/min}$	$Q = 5 \text{ L/min}$
E_{stored} , kJ	6393.448761	6484.8276	6670.241
η_O %	43.33	43.51	43.67

Table 5.1 shows, the amount of heat stored in the water and the overall efficiency increase with increasing water flowrate. The improvement rate of thermal storage is 1.3%, and 4.3% at 3 L/min, and 5 L/min, respectively.

The final average water temperatures in the tank at the end of the three tests were 39.1, 39.6 and 40.3 °C utilizing flow rates of 1, 3 and 5 L/min.

5.1.1.2. Case 2 (with PCM)

In this case, a mixture of water and paraffin wax was used to store heat utilizing 22.2 litres of water which is equivalent to 69% of the total volume and 9.9 litres of paraffin wax (32 bottles) which is equal to 31% of the total volume. Also, three different water flow rates of 1,3 and 5 L/min were used. The inlet, outlet, all temperatures, and solar radiation were recorded every 10 minutes.

This case focuses on the behaviour of paraffin wax, the final water temperature, and heat stored.

1. PCM behaviour during the charging process

The charging process of the system was graphically represented, in figures 5.8, 5.9, and 5.10, for flow rates 1, 3, and 5 L/min, respectively.

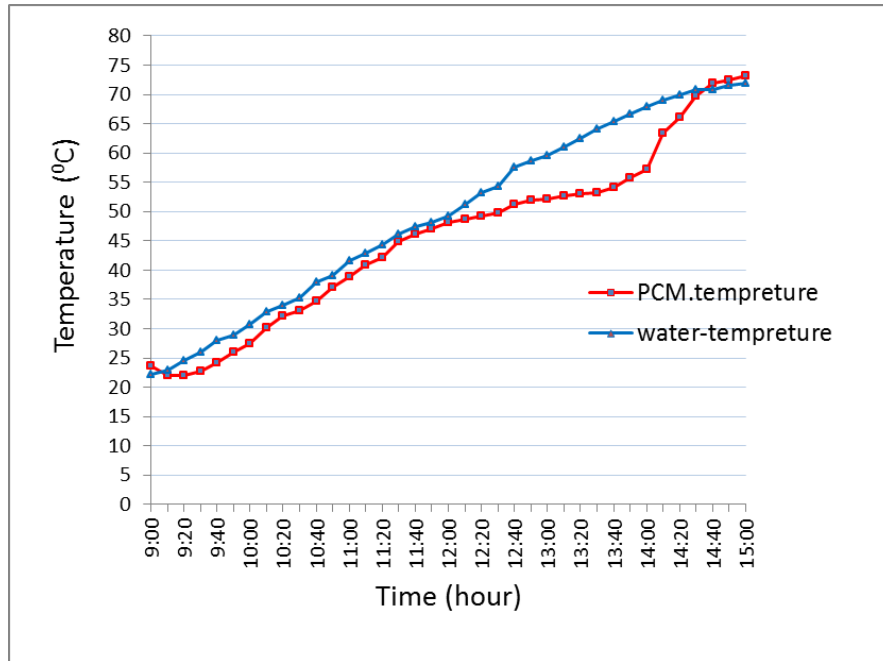


Figure 5.8: Average water temperature and PCM temperature with flow rate of 1 L/min

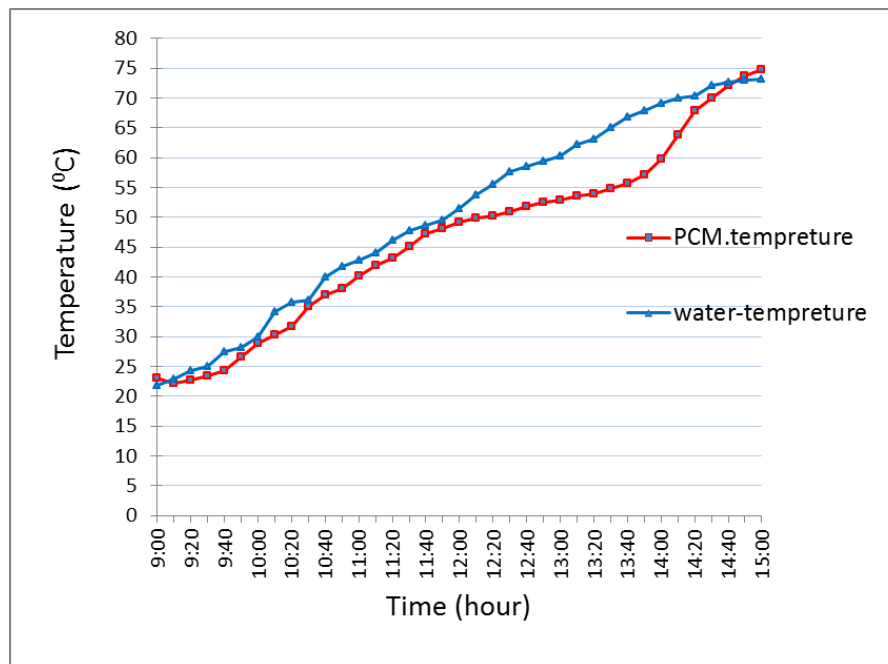


Figure 5.9: Average water temperature and PCM temperature with flow rate of 3 L/min

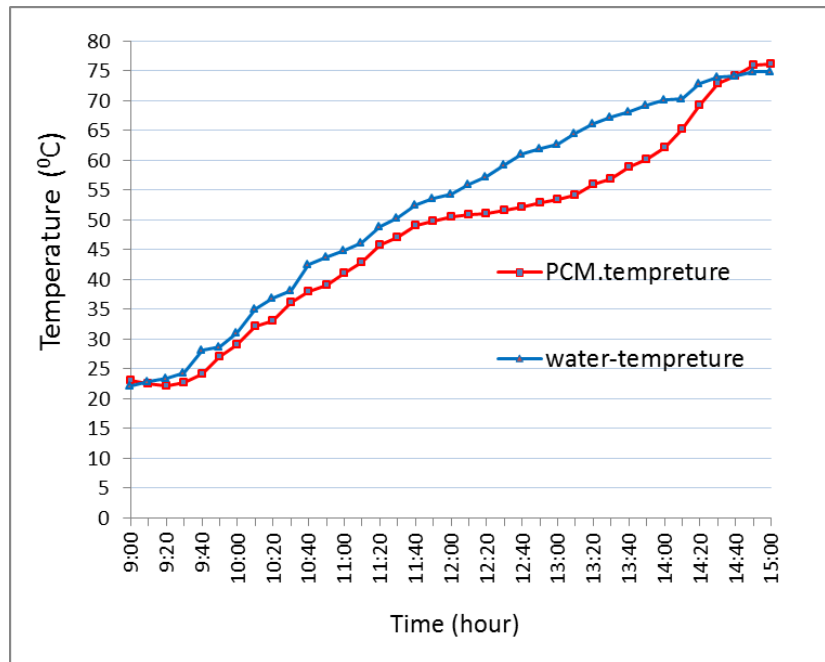


Figure 5.10: Average water temperature and PCM temperature with flow rate of 5 L/min

From Figure 5.8, 5.9, and 5.10, the following observations can be obtained:

- ❖ During the charging process, distributed storage heat between the water and PCM material.
- ❖ At first, the water temperature rises more than the temperature of the PCM, until we reach the melting temperature range, because of the low thermal conductivity of PCM.
- ❖ The range melting of PCM was about (51 to 53) °C, conforms to the specifications of PCM.
- ❖ At a temperature of about 51° C, which is close to the liquefy temperature, the PCM material temperature remains slightly increases until it reaches 53 °C. This can be explained as the PCM at this stage undergoes a phase change, and therefore large amounts absorb heat at a constant temperature. Then, the PCM temperature starts to rise at a quicker rate to catch up with the water temperature.
- ❖ The increased flow rate (HTF) had a significant effect on the melting time of paraffin wax. The melting time was 4.334, 4.166, and 4 hour at the flow rate of 1, 3, and 5 l / min. The rate of improvement at the time of melting (3.84%, 7.7%) was at 3 and 5 L/ min compared to the melting time at 1 L / min.

- ❖ At the end of the heating process, the temperature of the PCM is higher than the temperature of the water.
- ❖ The increase in the flow rate (HTF) leads to a rise in the rate of heat flow from the collector to the storage system.
- ❖ The maximum PCM-temperatures, at the end of the charging process, is 73.2, 74.8, and 76.2 °C, at flow rate 1, 3, and 5 L/min, respectively.
- ❖ The maximum average water temperature in the tank T_{ms} , at the end of the charging process, is 72, 73.2, and 74.8 °C, at flow rate 1, 3, and 5 L/min, respectively.

Figure 5.11 shows the PCM temperature during the charging process with time using different water flow rates.

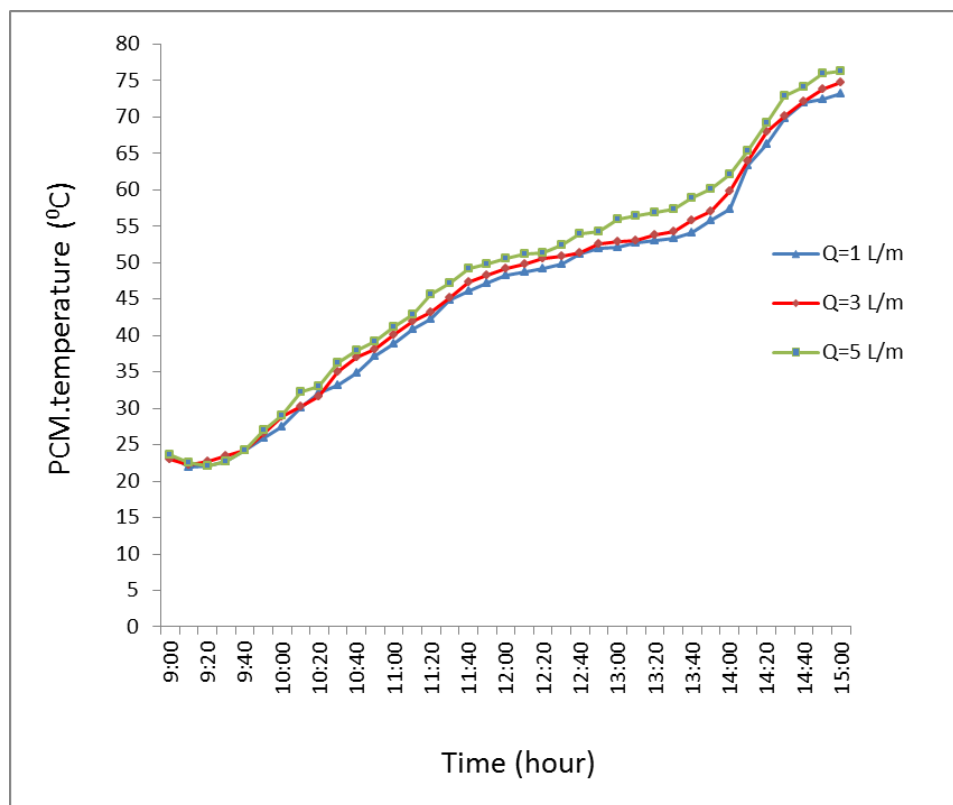


Figure 5.11: Temperature variation of PCM with time using three different flow rates

2. Storage tank average temperature

The final average water temperatures in the tank at the end of the three tests were 46.9, 48.9 and 49.1 °C utilizing flow rates of 1, 3 and 5 L/min.

3. Heat stored, and overall thermal efficiency of the solar heating system

The type of heat stored in this case (case 2) differs from the first case, because it contains latent heat and sensible heat, as a result of the use of PCM. The total amount of energy stored is equal to the summation of the heat stored in water and the amount of heat stored in PCM.

From the application of the equations 4.18, 4.20, 4.19 and 4.17 we find the amount of stored heat and the total thermal efficiency η_o , to heat 22 litres of water and 8 kg PCM from the initial temperature to the final temperature (T_i to T_f) within six hours, using flow rate 1, 3, 5 l / min.

The properties of pure water (ρ , C_p) can be taken from table C.1 in Appendix C, at T_{min} . The thermophysical properties of the PCM can be made from Table 4.2. The results of heat stored, and overall thermal efficiency is listed in Table 5.2.

Table 5.2: Stored heat and total thermal efficiency of case 2 with three different water flow rates

	Q = 1 L /min	Q = 3 L /min	Q = 5 L /min
$E_{\text{stored,water}}$, kJ	4542.6818	4660.7916	4817.9866
$E_{\text{stored,PCM}}$, kJ	2739.52	2779.84	2789.92
$E_{\text{stored,total}}$, kJ	7282.2018	7440.6316	7607.9066
η_o %	47.467	48.41	49.39

Table 5.2 shows a significant increase in the amount of heat stored and the overall-thermal efficiency of the solar water heating system.

5.1.1.3. Comparison between case 1(without PCM) and case 2 (with PCM)

As mentioned earlier in Chapter 1, the advantage of using the phase change materials in thermal heating systems is to store the most significant amount of excess thermal energy, to maintain the water temperature within the required range in the absence of solar energy. Figure 5.12, and 5.13 shows the main advantage obtained from using the PCM, which keeps the water temperature at about 9.3 °C higher than that of without PCM. The hot water temperature improved in tests of the solar heating system due to the use of PCM and increased HTF flow rate.

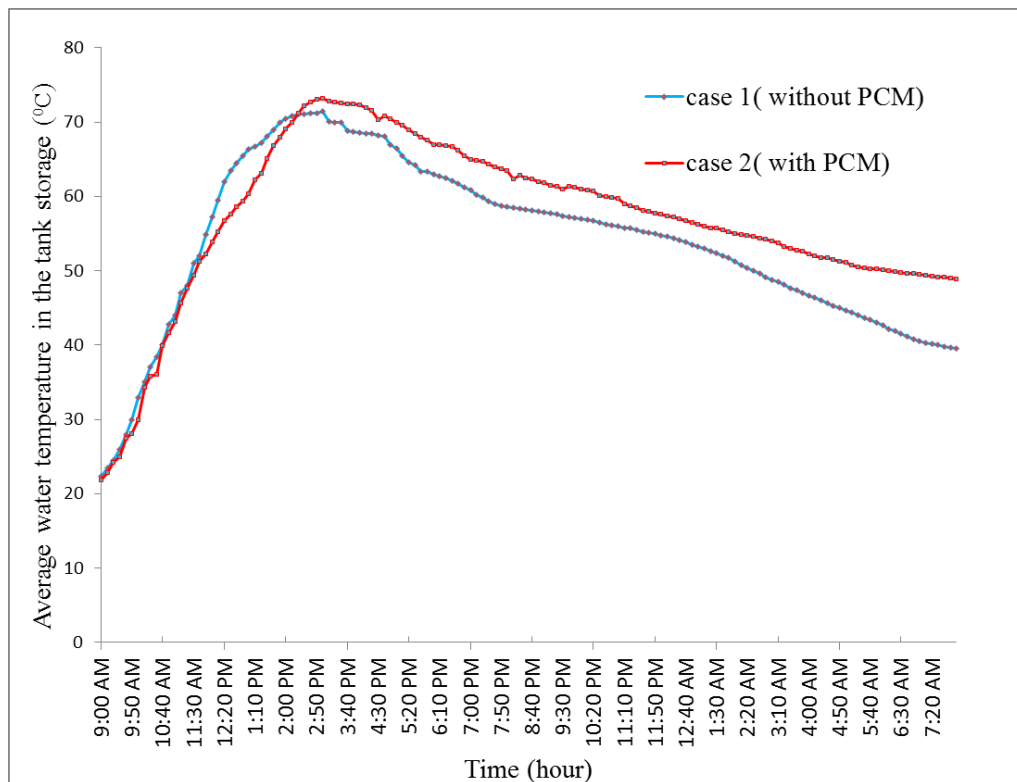


Figure 5.12: Average water temperature in the storage tank, for the cases of with and without PCM, using $Q = 5$ L/min vs time.

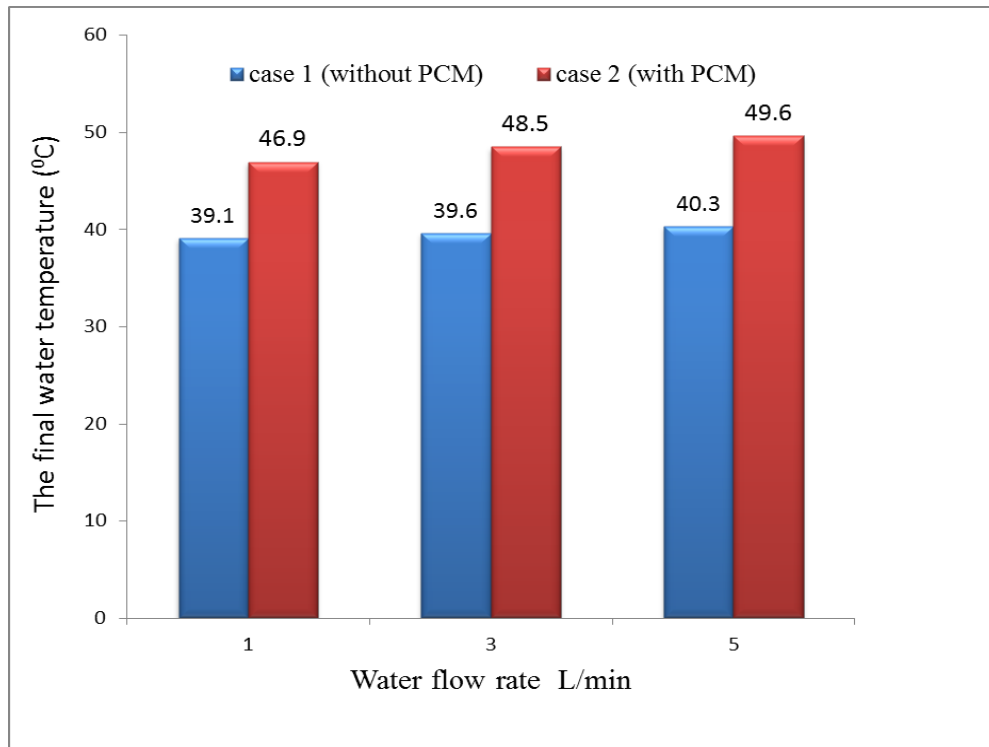


Figure 5.13: Final midpoint storage tank water temperature, for the cases of with and without PCM utilizing three different mass flow rates

Table 5.3 shows the improved hot water temperature in Case 2 (with PCM) for variable flow rates.

Table 5.3: Improvement in hot water temperature in case 2 (with PCM)

Volume flow rate (Lpm)	Improved water temperature
1	19.95 %
3	22.47 %
5	23.1 %

Figure 5.14 shows the amount of heat stored (E_{storeg}) for the cases of with and without PCM utilizing three different mass flow rates. The cases with PCM give more heat storage than those of without PCM. This highlighted the advantage of using PCM materials to store more heat in the current study of the solar heater system.

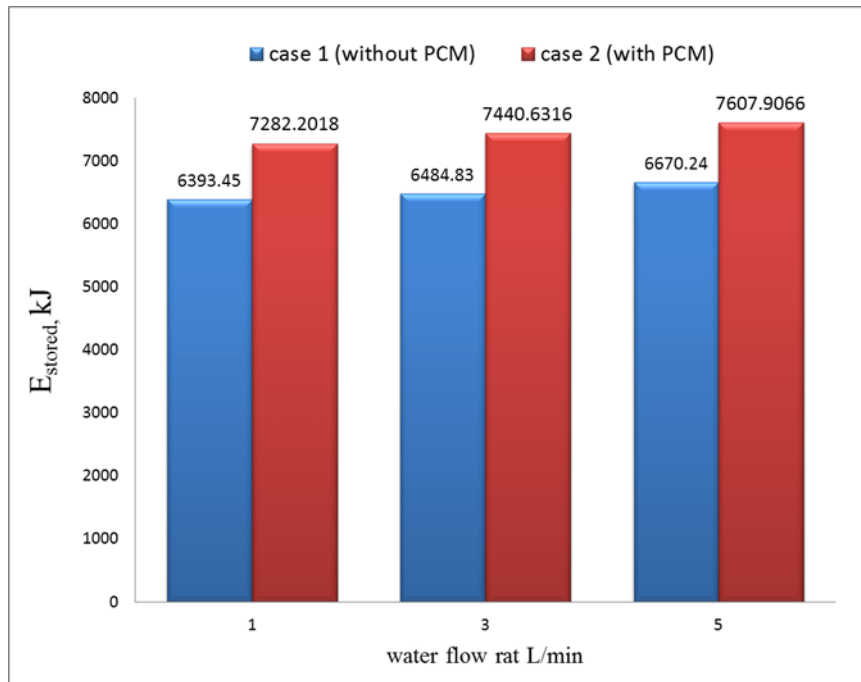


Figure 5.14 The amount of heat stored (E_{stored}) for the cases of with and without PCM utilizing three different mass flow rates

Table 5.4 shows the amount of heat storage improvement due to the use of PCM for variable flow rates.

Table 5.4: The amount of heat stored, at solar system tests, due to use PCM.

Volume flow rate (L/min)	Improved heat stored
1	13.9 %
3	14.74 %
5	14.05 %

5.1.2 Electric driven heat storage system (using 1 kW heater element).

To further verify the improvement results obtained as a result of using PCM in a solar water heating system. In addition to avoid the effect of variable solar radiation intensity during the day, and to operate in controlled conditions, the same test was repeated in similar surrounding terms, 1 kW of heater element is used as a heat source.

Four cases were tested:

- a. Case- 1, only 32 litres of water were used, without PCM.
- b. Case- 2, 78 % water 25.2 L, 22 % PCM 6.8 L, 5.5 kg PCM.
- c. Case- 3, 69 % water 22 L, 31 % PCM 9.9 L, 8 kg PCM.
- d. Case- 4, 69 % water 22 L, 31 % PCM with copper mesh 9.9 L, 8 kg.

In this case, the storage water tank was disconnected from the solar collector by closing the input, output line valves. Test start by turning on the electrical source that feeds the electric heater for two hours. Temperature meter is used to record temperatures every 10 minutes, beginning at 9 am until 8 am the next morning. Key parameters studied in this case are discussed as:

1. The behaviour of the PCM using an electric heating element as a heat source

Figure 5.15 shows the variation in temperature of the water, PCM and ambient air, during the processes of charging and discharging of heat.

The behaviour was similar to the case where the solar collector was the source of energy. The slight difference that the heating process was running more smoothly due to the stability of the amount of heat generated from the heater. At the beginning of the discharging heat process, we note that the temperature difference between PCM and water is about 3 °C, until the

temperature approaches 51 °C (solidification temperature), as the temperature difference drops to 1.5 °C.

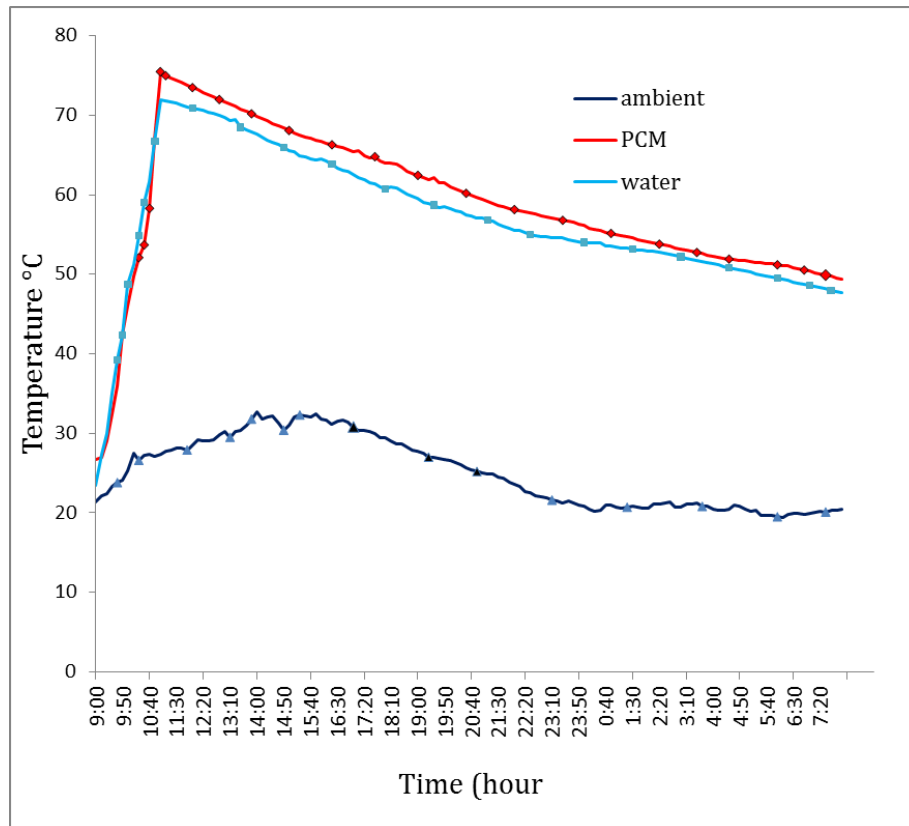


Figure 3.15. Variation in temperature of the water, PCM and ambient air, for case-3

2. Final water temperatures for different cases

Figure 5-16. shows the main advantage obtained from using 8 kg of PCM, which keeps the water temperature at about 7.4 °C higher than that of without PCM.

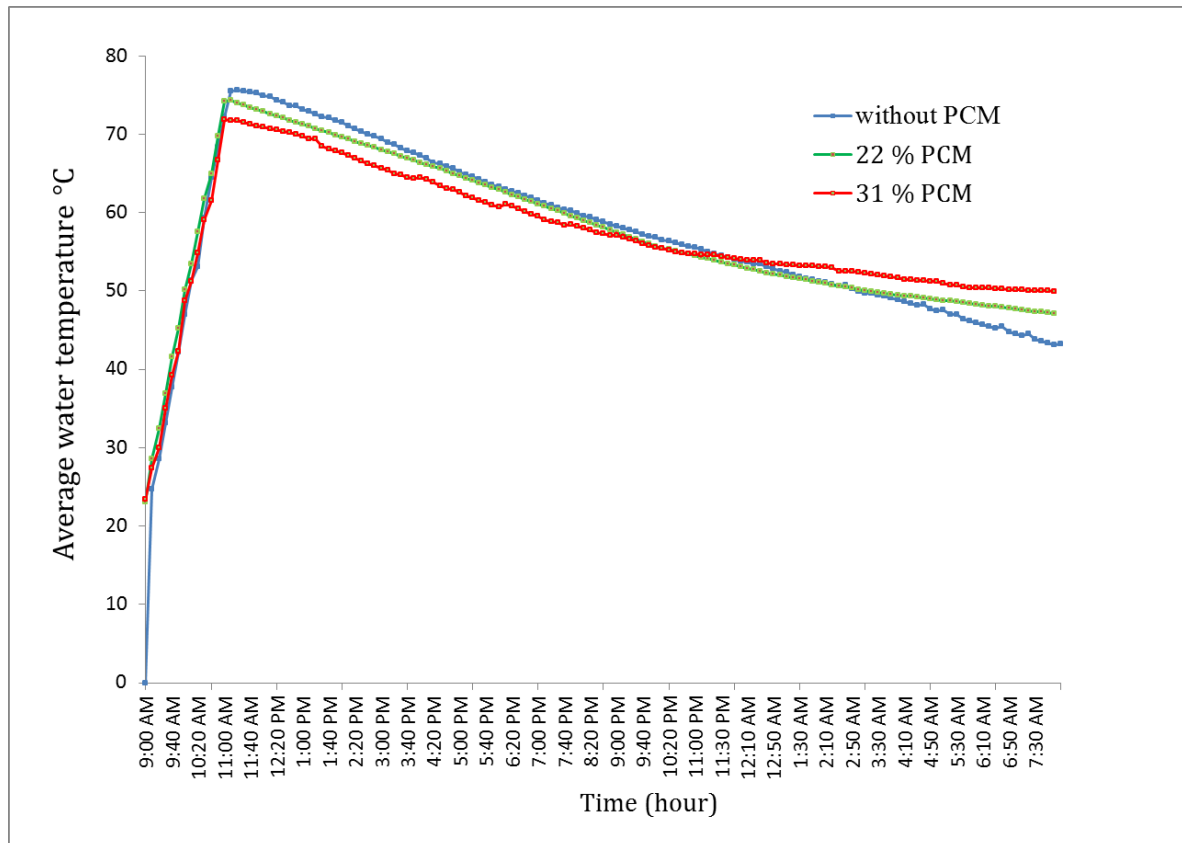


Figure 5-16. Average water temperature in the storage tank, for the cases of without PCM, 22% PCM and 31% PCM using a heater element

Figure 5-17. shows the final average water temperatures in the tank at the end of the three tests, case-1, case-2, and case-3, were 40.3, 46.5, and 47.7 °C, respectively. In other words, the higher the proportion of the amount of PCM used in the storage tank, the water kept its temperature and was hotter.

Table 5.5: Improvement in hot water temperature using external heater element and two different ratios of PCM

The proportion of the PCM in the tank water %	Improvement in water temperature
22	15.38 %
31	18.3 %

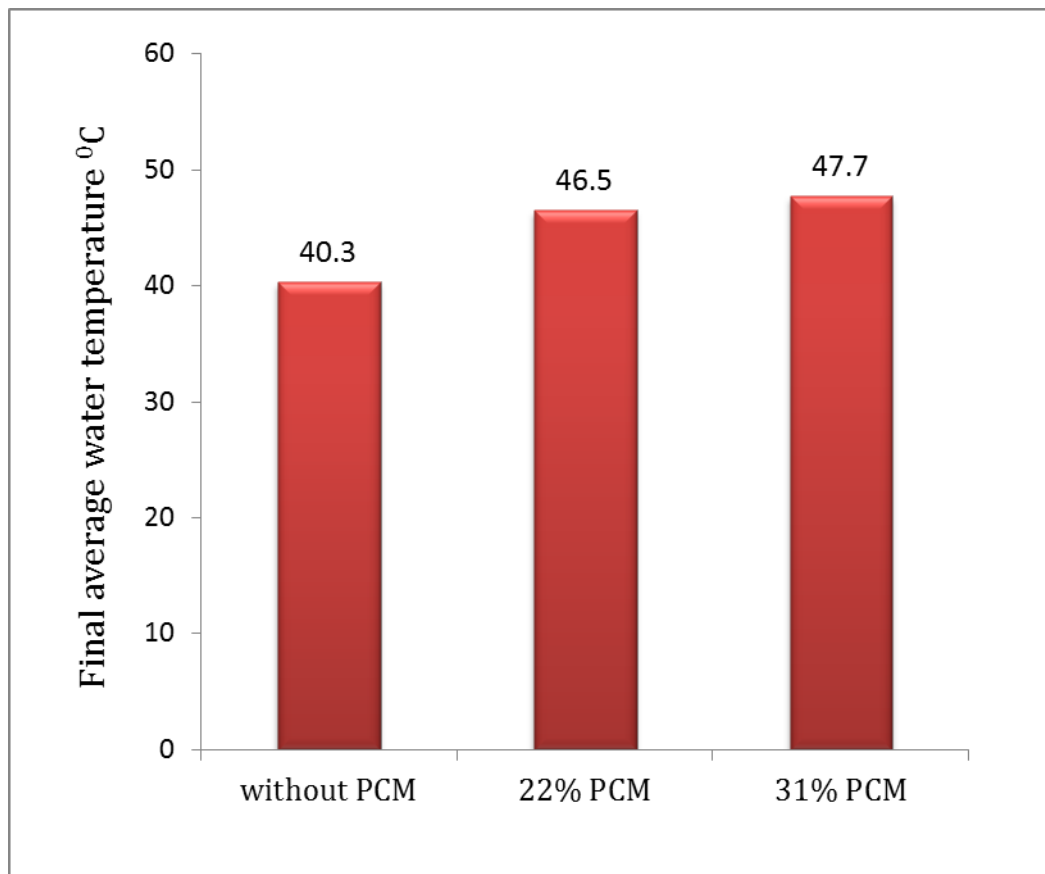


Figure 5.17. Final average water temperature, for the cases of without PCM, 22% PCM and 31% PCM using a heater element

2. The amount of heat stored (E_{storeg})

The amount of heat stored can be calculated using Eqs. 4.18, 4.19, and 4.20. The properties of ρ and C_p of pure water are taken from Table C-1 in Appendix C, and the results are listed in Table 5.6.

Figure 5.18, and Table 5.6, shows the amount of heat stored (E_{stored}) for the cases of with and without PCM. The cases with PCM give more heat storage than those without PCM. The higher a proportion of the amount of PCM used in the storage tank was given more heat storage than those of without PCM.

Table 5.6: Heat stored, and overall thermal efficiency of without PCM, 22% PCM and 31% PCM using a heater element

	without PCM	with 22 % PCM	with 31 % PCM
$E_{\text{stored,water}}$, kJ	6729.66	5325.66	4414.6043
$E_{\text{stored,PCM}}$, kJ	0	1590.245	2684.32
$E_{\text{stored,total}}$, kJ	6729.66	6915.905	7098.9243

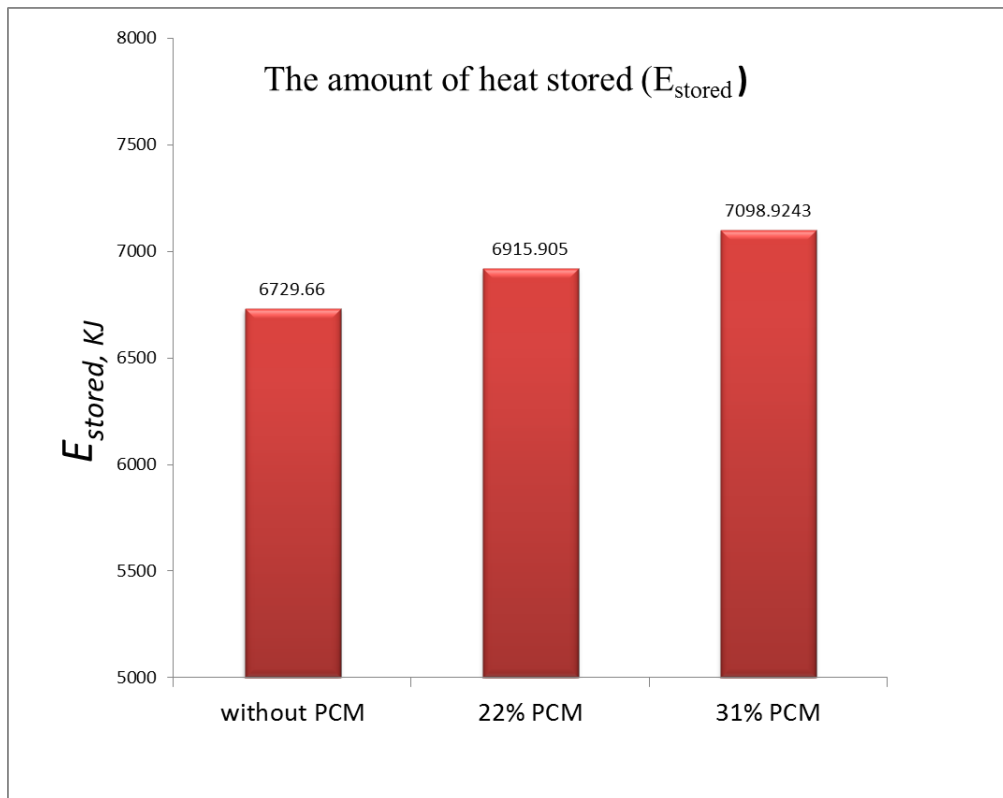


Figure 5.18 The amount of heat stored (E_{storeg}) for the cases of with and without PCM.

Table 5.7: The Improved in the amount of heat stored (E_{storeg}), at heater system tests, due to use PCM.

The proportion of the PCM in the tank water %	Improved heat stored temperature
22	2.8 %
31	5.5 %

Figure 5-19 shows that the water remained hot, at about 25.5, and 27.9 °C more than the ambient temperature, as a result of using 22, and 31 % PCM, respectively.

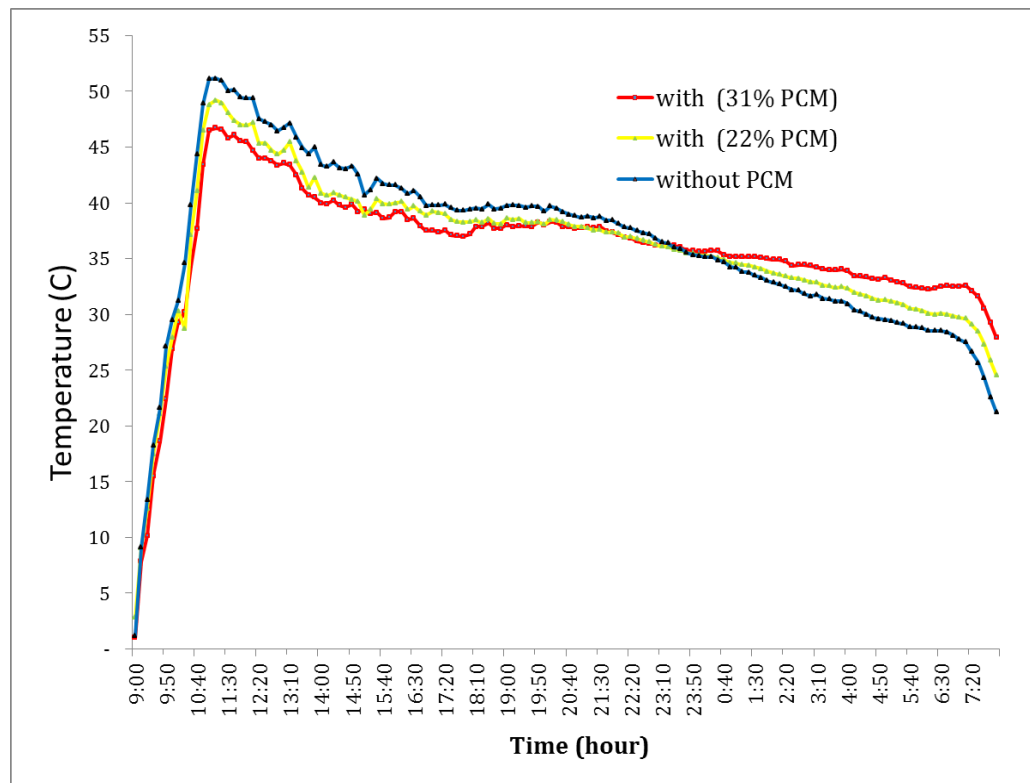


Figure 5-19: Difference between the water temperature and the ambient temperature, for the cases of without PCM, 22% PCM and 31% PCM

5.1.2.1. Case 4: Improving the thermal conductivity of the paraffin wax by adding copper mesh

All studies conducted by researchers previously indicated that the thermal conductivity of paraffin wax is weak. Moreover, it is one of the most important defects that are characterized by it because it affects the heat transfer process to and from paraffin wax and thus reduces the benefit of using it as PCM materials for thermal storage. Therefore, an investigation will be made to improve the thermal conductivity of paraffin wax by adding a substance with high conductivity. In this state, 25 g of copper mesh is added to each aluminium container that contains wax material, while

reducing the amount of paraffin wax material in the container in the same proportion to avoid leakage during the phase change from solid to liquid. Some parameters are studied:

1. Time of heat charging

Figure 5-20 shows the effect of adding the copper mesh on the paraffin wax temperature during the charging process.

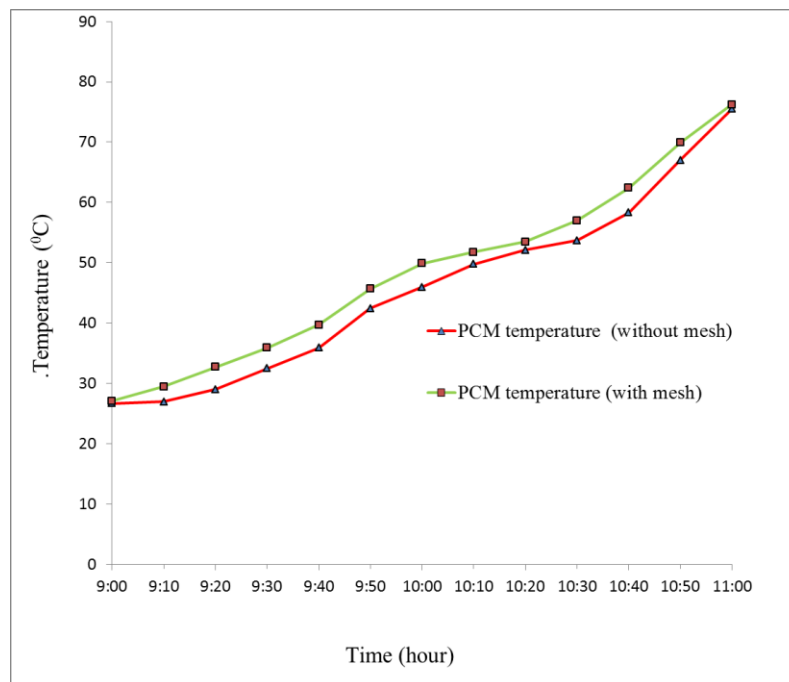


Figure 5-20. Variation in temperature of the PCM with and without mesh during charging process.

Also, Figure 5-20 shows how the behaviour of paraffin wax is changed when adding the copper mesh, as its ability to acquire heat before reaching the melting point is improved during the process of charging the heat. This reduces the time needed to reach the melting temperature, by 10 minutes. The improvement rate in melting time is 12.5%. After the melting process is complete, the effect of the adding copper mesh material becomes less, because the heat transfer method inside the liquid PCM is switched to convection. The maximum temperature at the end of the charging process of paraffin wax without and with mesh copper were 75.5 and 76.1 °C,

respectively. The maximum water temperature was at the end of the charging process, in the case of with or without a copper mesh, was 72.5 and 71.9 ° C, respectively.

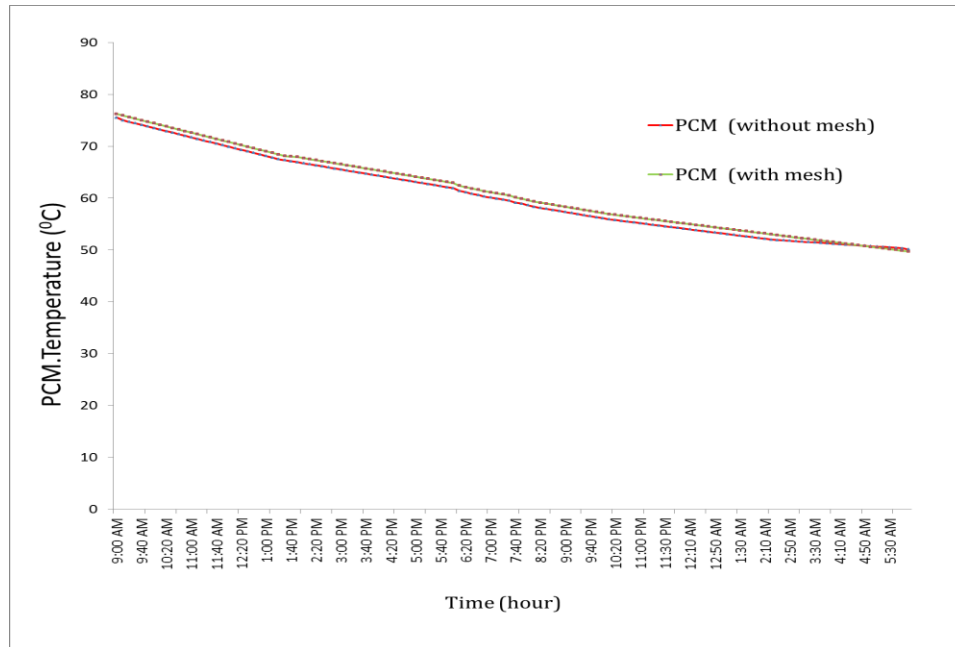


Figure 5-21. Variation in temperature of the PCM with and without mesh during discharging process.

In the discharge process, the effect of adding the copper mesh was slight on the solidification time as shown in figure 5-21.

The final average water temperatures in the tank at the end of the two tests, without and with copper mesh were 47.7, and 47.1 °C, respectively. The reason for this is that the amount of paraffin wax used for latent thermal storage was less when adding the copper mesh, causing water to lose a part of its heat.

2. The amount of heat stored (E_{stored})

The amount of heat stored can be calculated using Eqs. (4.18), (4.19), and (4.20). In the case of adding the copper mesh, must replace the paraffin mass, and the specific heat of the PCM in equation (4.19), with the paraffin

mesh mixture mass, and specific heat using equations (4.21), and (4.22). The results are listed in Table 5.8.

Table 5.8: Experimental energy stored for the cases of using 31% PCM without copper mesh and 31% PCM with copper mesh

	31 % PCM without mesh	31 % PCM with mesh
$E_{\text{stored,water}}$, kJ	4414.6043	4380.97
$E_{\text{stored,PCM}}$, kJ	2684.32	2651.22
$E_{\text{stored,total}}$, kJ	7098.9243	7032.199

Table 5-8, shows that the amount of heat stored in the case of using paraffin wax with copper mesh was less than the case without mesh because the amount of wax used as thermal storage was less.

5.2. The numerical results

The 24-hour simulation time results of the charge and discharge operations performed for a 2-dimensional water tank containing aluminium PCM containers that are heated by a constant heat flux showed the benefit of using PCM in the heat storage. It also showed the heat transfer process through the system, the behaviour of the PCM material during the charging and discharging process, and a weak thermal conductivity of it.

5.2.1 Heat transfer in the water tank

Figures 5-22, and 5-23, shows the velocity vectors, and velocity streamlines, during the charging process (heat adding process), in the numerical modelled system for case 1 (without PCM) and case 2 (with PCM), respectively. This visualizes the speed of water molecules during the heating process and

shows the directions of natural convection flow currents that circulate inside the water tank.

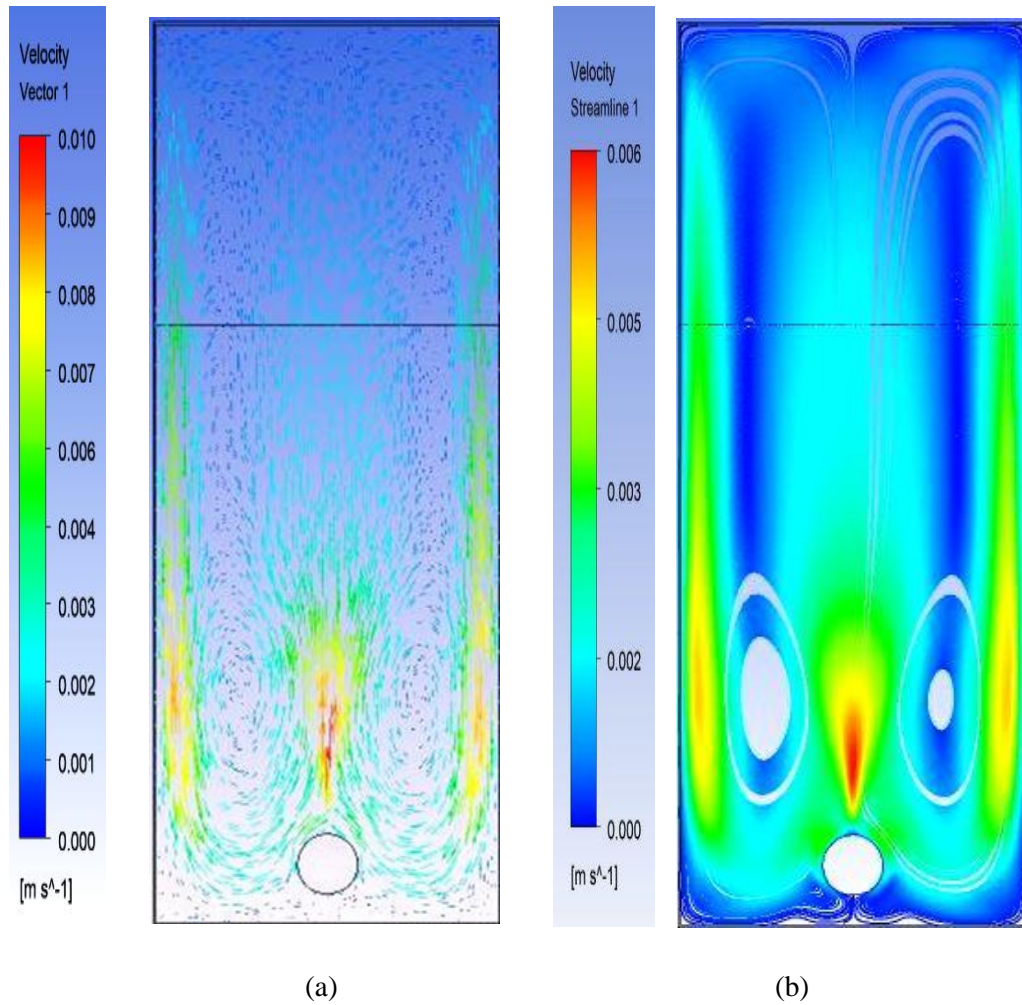


Figure 5-22: (a) Velocity vectors (b) velocity streamline during the charging process for the numerical modeled system, for case 1 (without PCM)

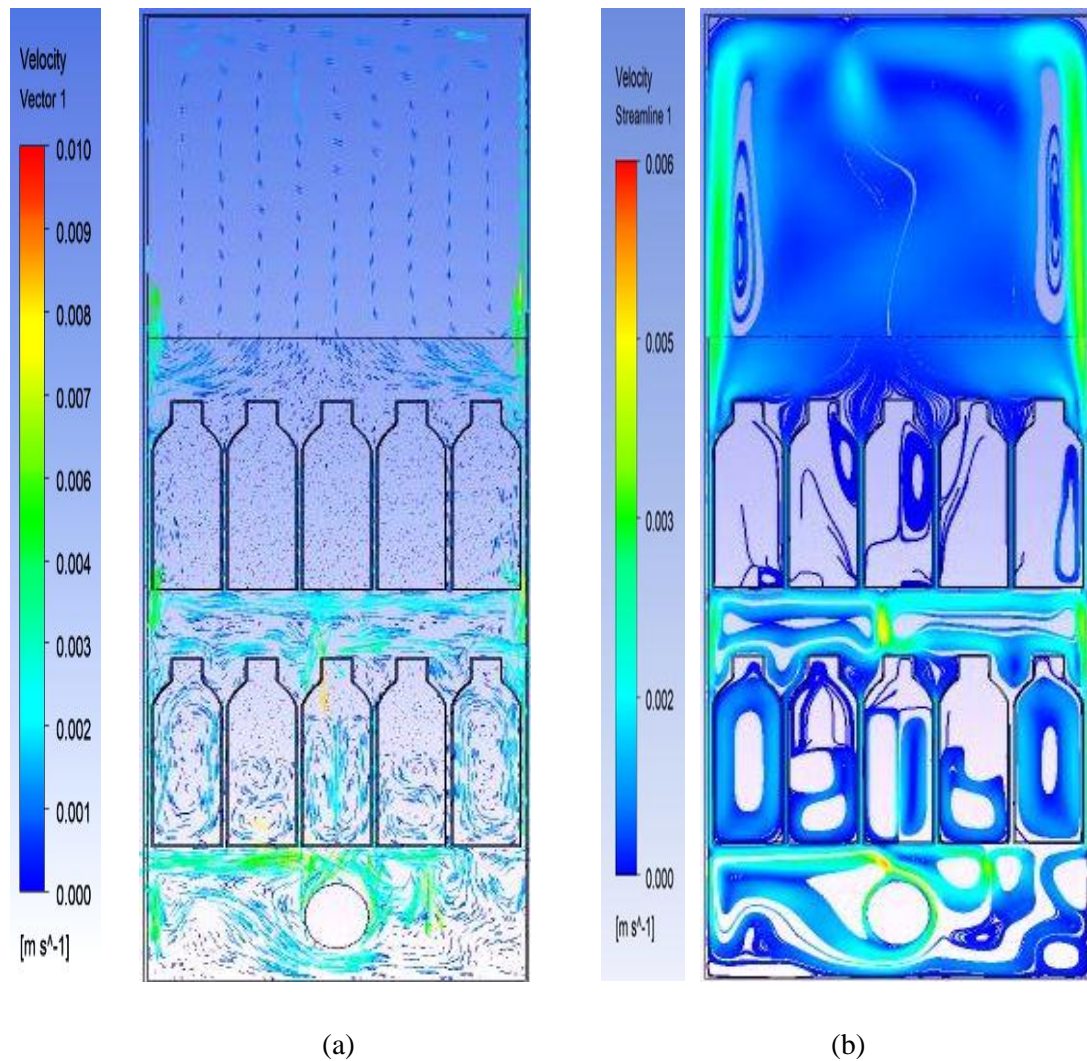


Figure 5-23: (a) Velocity vectors (b) velocity streamline during the charging process for the numerical modeled system, for case 2 (with PCM)

The temperature rises during the two-hour charging process, as a result of the heat flow generated by the heater placed at the bottom of the water tank. The heat transfer occurs via the natural water circulation inside the tank. The natural convection currents inside the system occur, when the layers of water surrounding the heater receive heat, expand thermally, less their density, rising vertically to the top, and lowering the heavier and denser water layers due to gravity. The situation with PCM was different due to the presence of rows of PCM containers. It served as barriers to convection currents. It was observed that temperatures rise in the water layers below the first row of

PCM containers was faster than the rest of the water layers, Especially in the centre of the tank water. That will lead to an increase in the water layer temperature that contact with the bottom of PCM containers in the lower row.

5.2.2. Temperature distribution and thermal energy storage

Figures 5-24, and 5-25 shows the temperature distribution contours for the case-1 (without PCM) numerical modelled system.

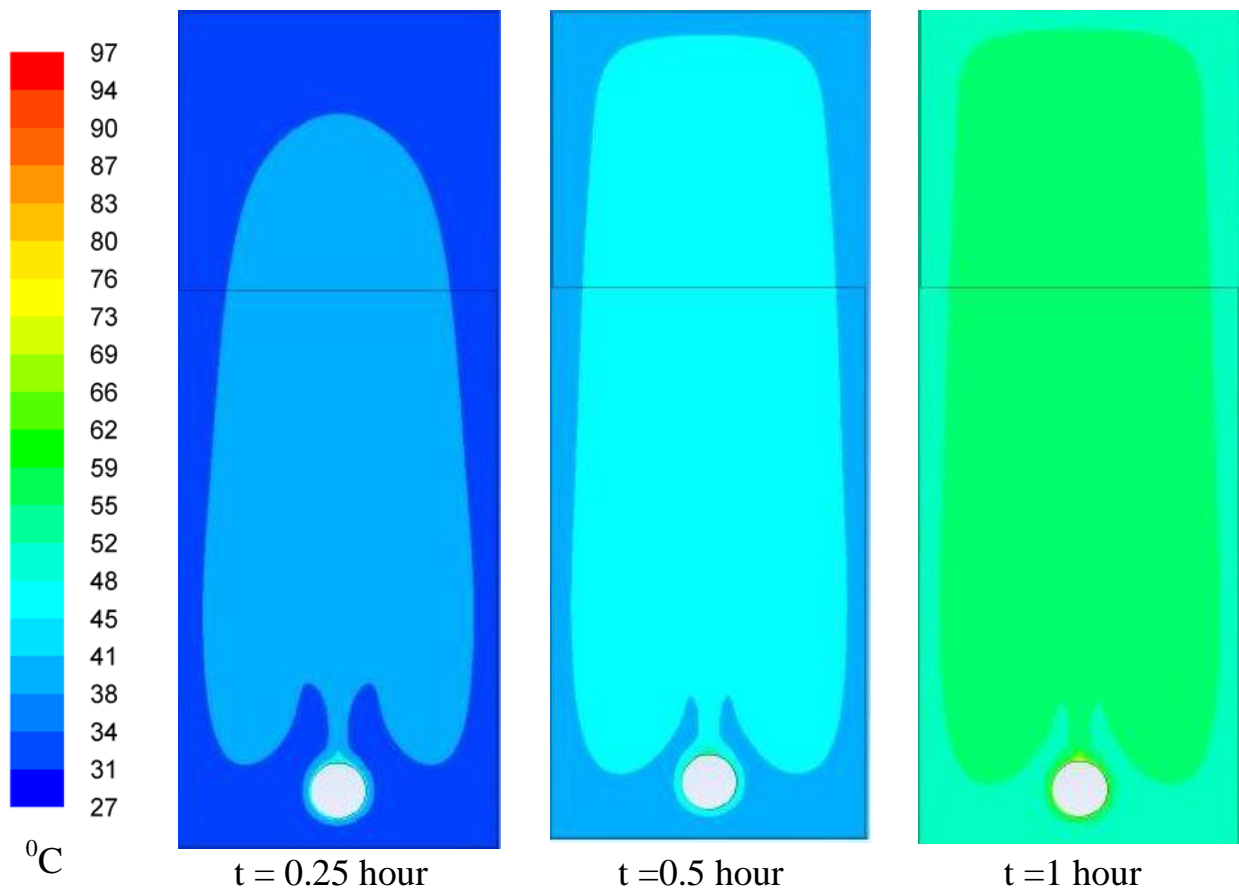


Figure 5-24. Temperature distribution contours during the first hour of charging process, for case 1 (without PCM)

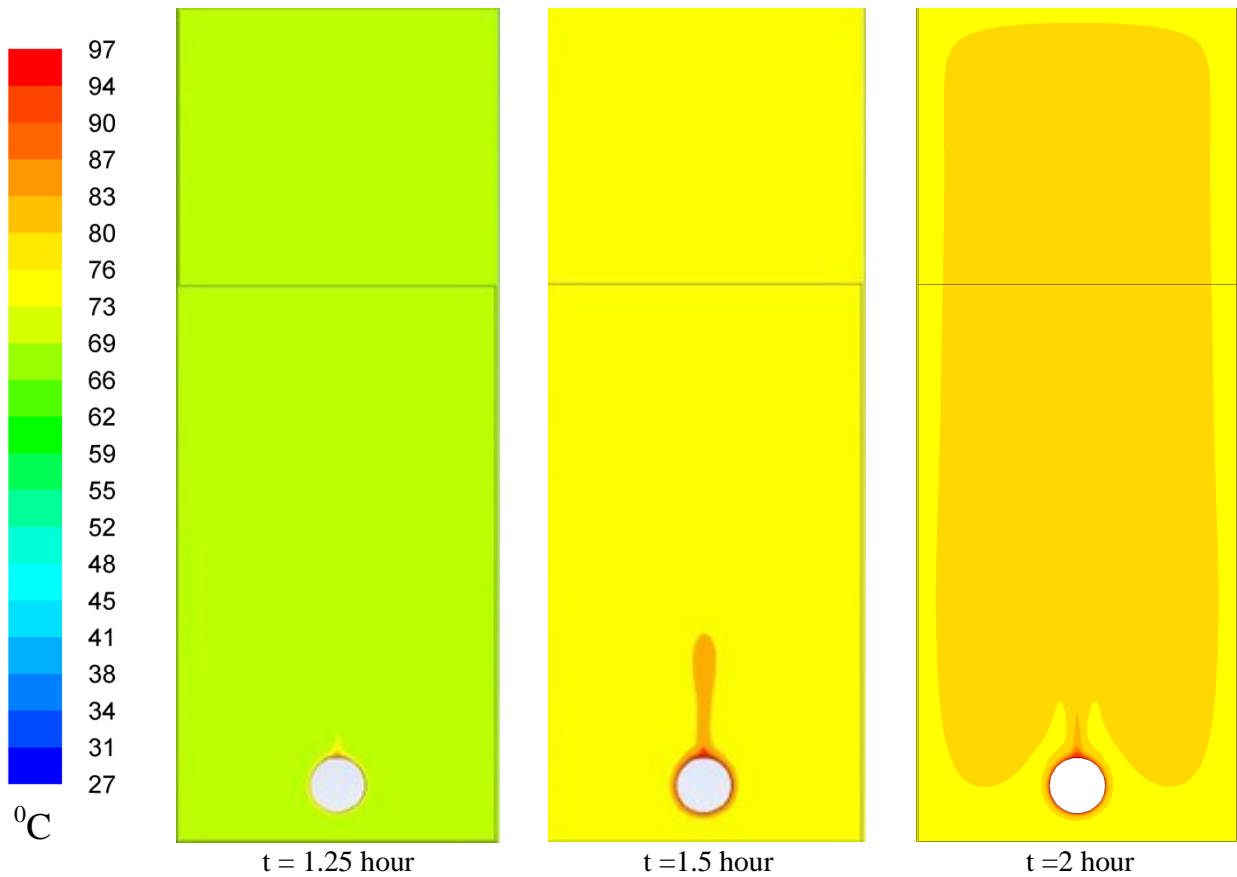


Figure 5-25. Temperature distribution contours during the second hour of charging process, for case 1 (without PCM)

In this case, the convection currents were running smoothly, and the (SHS) is the only possibly thermal storage. At the end of the heating process, the maximum water temperature is 76.3°C .

After removing the heat flux, the discharging process begins. The discharging process in without PCM went smoothly, and at the end of the simulation process, the final water temperature is 39.7°C . It is less than the required temperature water for home use.

Figures 5-26, and 5-27, shows the temperature distribution contours for the case2 (with using PCM) for the modelled system, during the charging process.

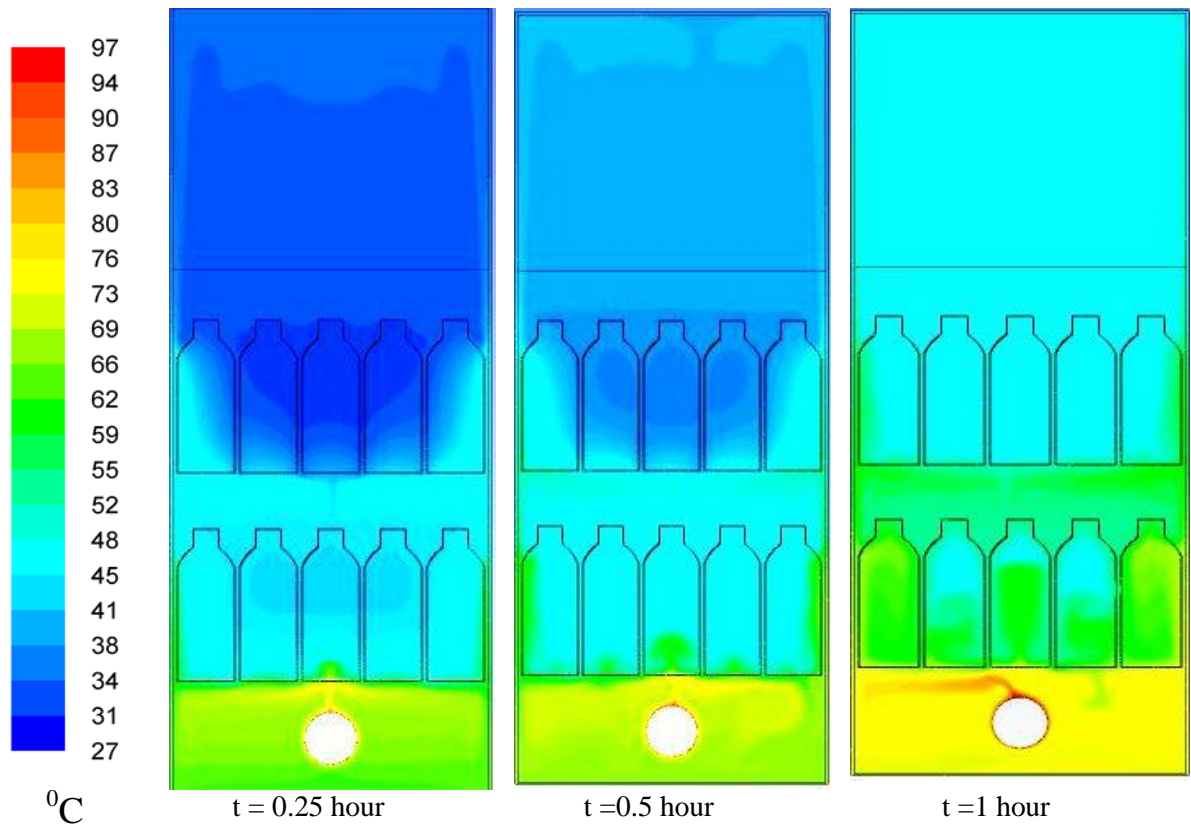


Figure 5-26. Temperature distribution contours during the first hour of charging process, for case 2 (with PCM)

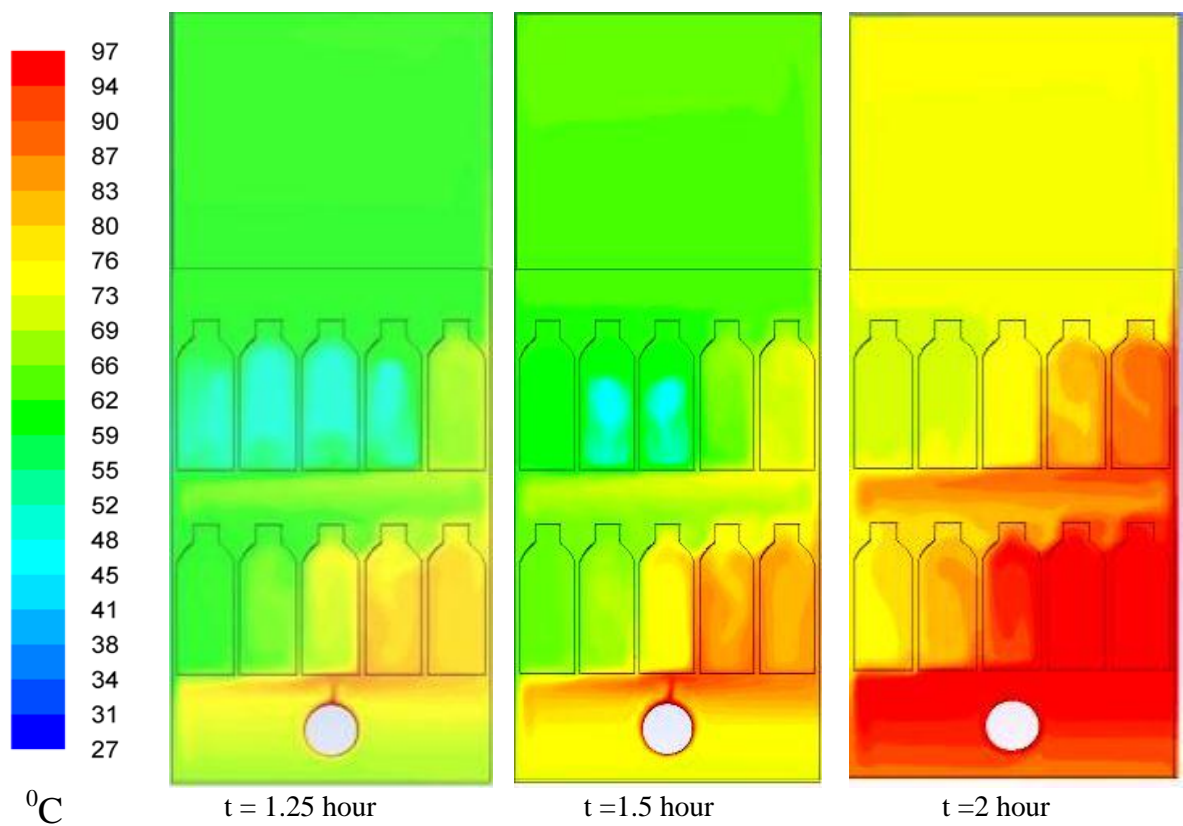


Figure 5-27. Temperature distribution contours during the second hour of charging process, for case 2 (without PCM)

The case2 (with PCM), was different, because the rows of PCM containers, act as barriers to convection currents, this led to an increase the water layer temperature that contact with the bottom of PCM containers in the below row, especially in the centre of the tank water.

The effect of the convection currents on both sides of the water tank is more clear, due to the gap between the inner side surface of the tank and the PCM containers are higher than the gap between the PCM containers. This caused to escapes the hot water to the side tank gap, and warm up the sides of the containers facing the side of the water tank before the rest parts of these containers.

In this case, the (SHS) and (LHS) is the possibly thermal storage. At the beginning of the heating period, the water temperature rises faster than the solid PCM, due to the poor thermal conductivity of PCM, and the thermal storage is the (SHS) type for water and PCM.

When the PCM temperature approaches the melting temperature ($T_{\text{melt}} = 52^{\circ}\text{C}$), the phase change of the PCM begins in the lower row containers after approximately 0.25 hour have passed. However in the upper row, we did not show the fusion process until 0.4861 hour of simulation and in the foamed, not a liquid phase. Figure 5-28, displays the liquid-fraction contours for case 2 (with PCM), during the charging process.

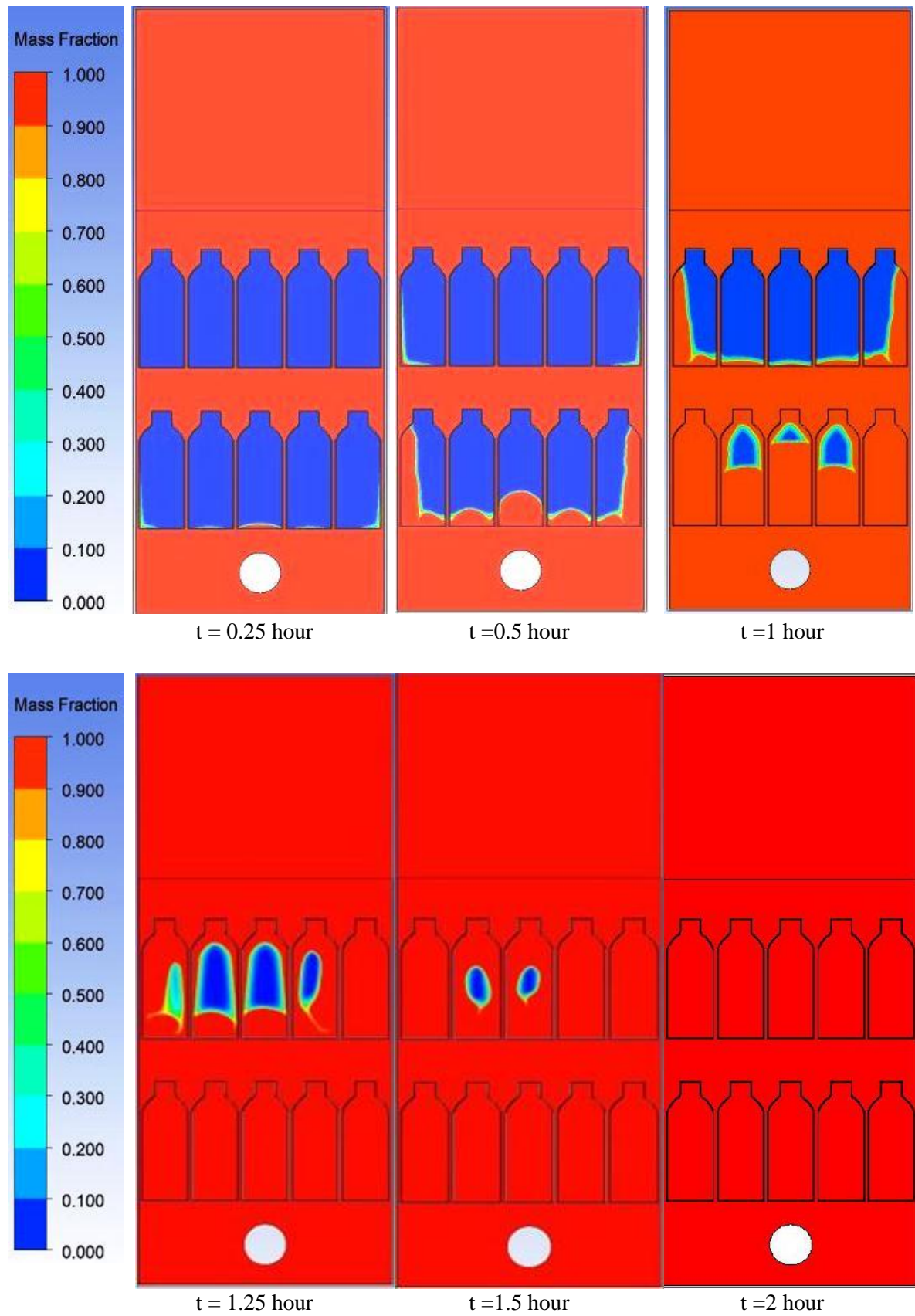
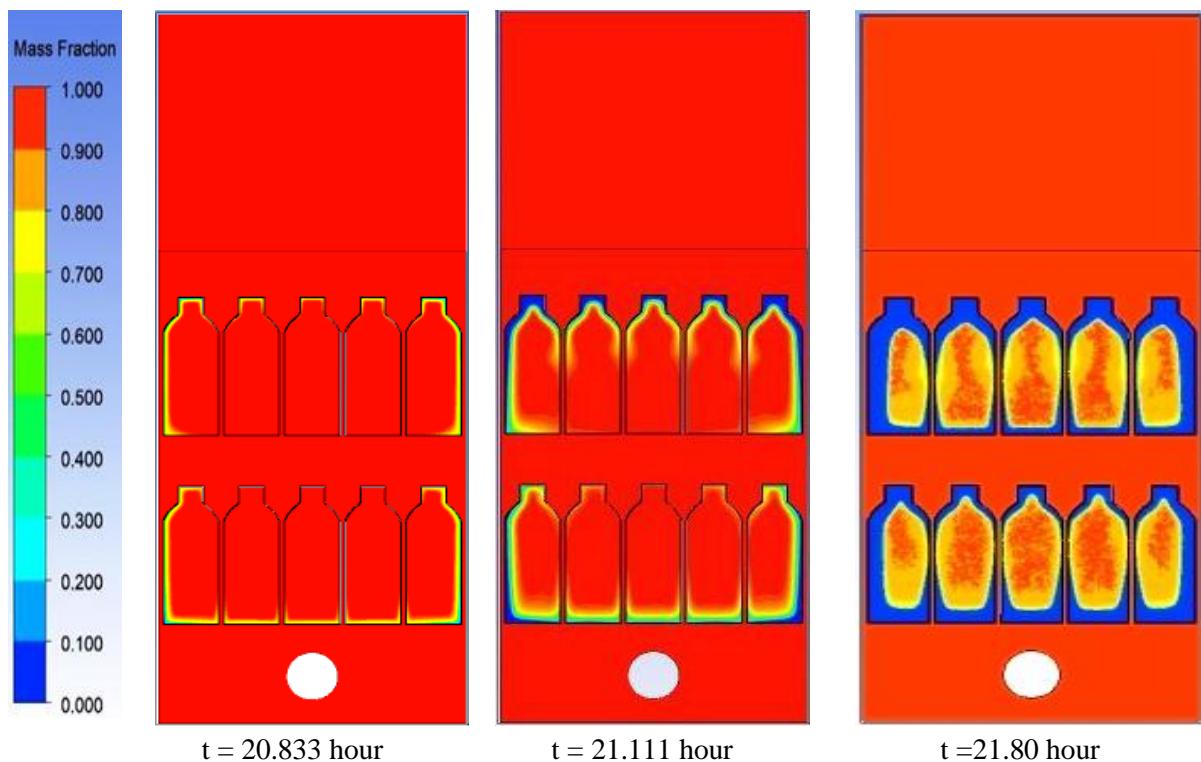


Figure 5-28. Liquid-fraction contours during the charging process for case-2 with PCM

The phase change process ends when the last amount of paraffin wax is melted in the container placed in the middle of the upper row after approximately 1.722 hour. During this time, the thermal storage in the PCM is (LHS) type. After this, the (SHS) is the only storage until the end of the heating process. The maximum of water, PCM temperatures are 73.19, and 76.87 °C, respectively. The difference in the maximum water temperature between the two cases (with or without PCM) is because of that part of the heat energy has been stored in the PCM material.

Also, in case 2 (using PCM), the effect of having a PCM material was visible when the PCM temperature approaches the solidification temperature ($T_{\text{solid}} = 51$ °C), the latent heat stored in the PCM, begins to release to the water.

Figure 5-29, shows the liquid-fraction contours for case 2 (with PCM) for the modelled system, during the discharging process.



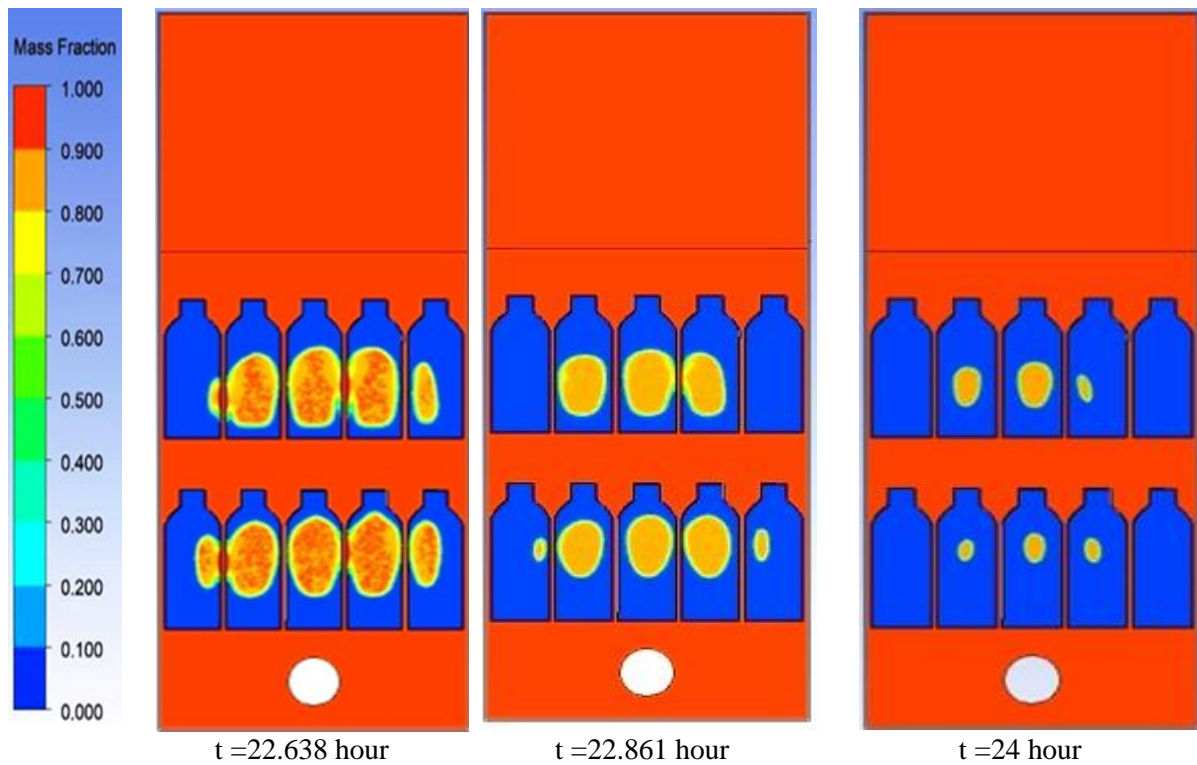


Figure 5-29. Liquid-fraction contours during the discharging process for case 2 (with PCM)

Figure 5-29 shows that the PCM change its phase, and return to the solid-state, begins approximately 20.833 hour from the start of the simulation. At the end of the simulation process, the final temperatures are 48.22, and 50.12 °C for water, and PCM, respectively, and that 1% fraction of the PCM did not solidify.

Figure 5-30 shows, the numerical average temperatures of water, and PCM, with time for case 2 (with PCM).

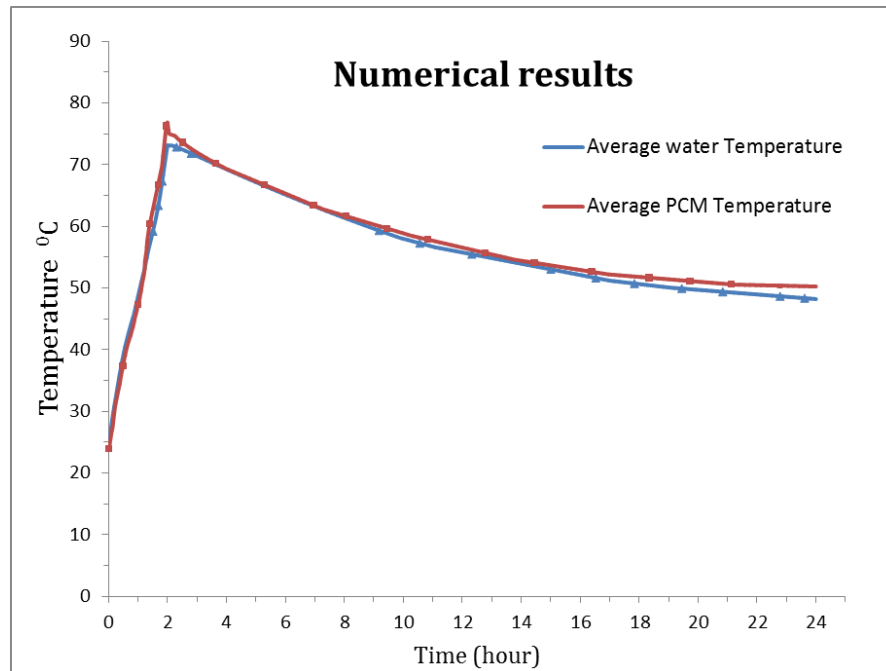


Figure 5- 30. Numerical average temperatures of water and PCM with time for case 2 (with PCM).

At the end of the heating process, the water temperature T_{maximum} is 76.3 °C. While, at the end of the simulation process, the final temperatures are 48.22, and 50.12 °C for water, and PCM, respectively.

Figure 5-31 shows that using PCM can maintain the water temperature at a higher temperature which remains within the required hot range for home use. The difference in the final water temperature between the two cases is 8.5 °C, with a temperature gain of 21.46%.

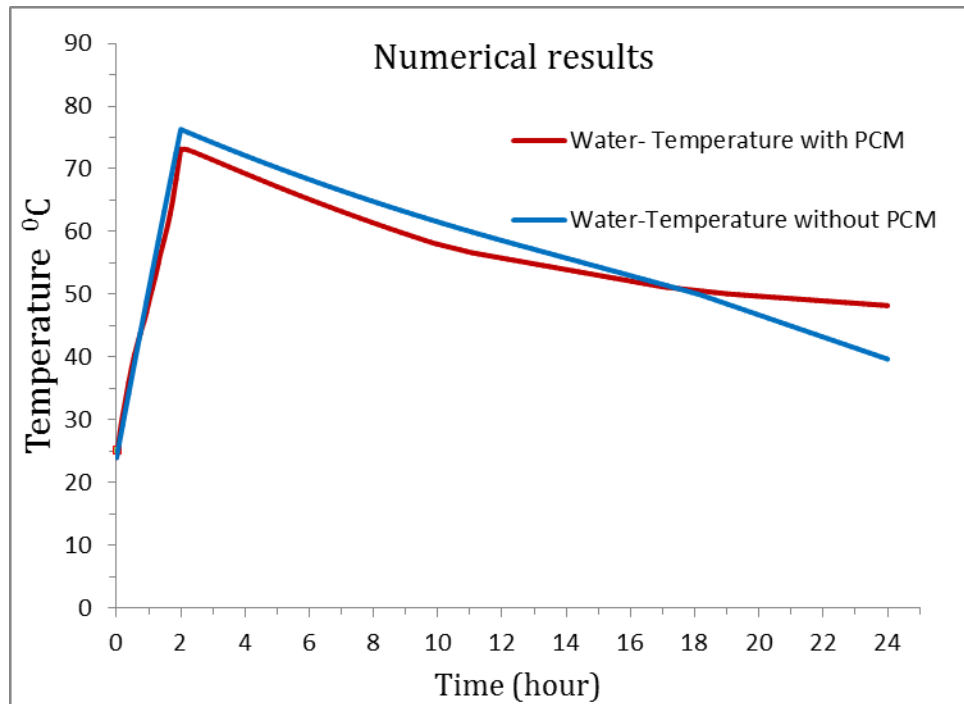


Figure 5-31. Numerical average water temperature with time for cases with and without PCM

5.3. Validation numerical results with the experimental work

Figure 5-32 shows numerical and experimental temperatures of water and PCM during heat charging and heat discharging processes. A good agreement between the experimental and numerical is obtained with a maximum deviation rate of 5.17%.

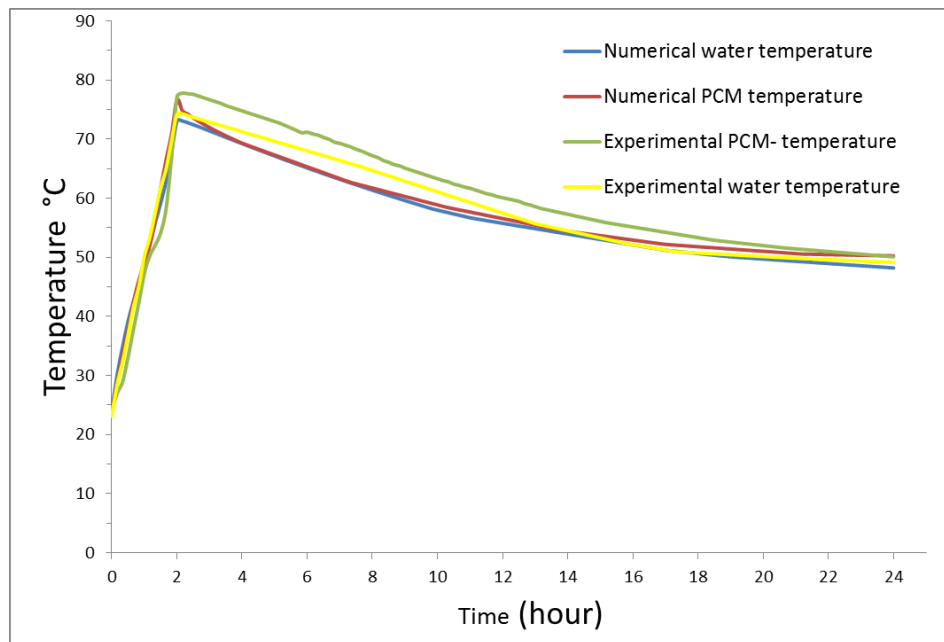


Figure 5-32: Numerical and experimental temperature results for water and PCM during charging and discharging heat process.

Figure 5-33 shows the results of the experimental and numerical heat charge to the PCM.

The Experimental results were better in explaining the behaviour of the PCM material than the numerical results, especially in the phase change period from solid to liquid. The reason for that is in experimental tests, one of the thermocouples is installed inside the central PCM container. Where, is placed on the top row, so that only this temperature of the container is measured. In contrast, the PCM temperature in the numerical solution represents the average temperatures of all PCM containers. We do not have a mechanism for photographing the process of melting in the experimental tests. Not to use another location to measure the PCM temperature to

increase the accuracy of the results is to avoid leakage of liquid PCM material into the water tank.

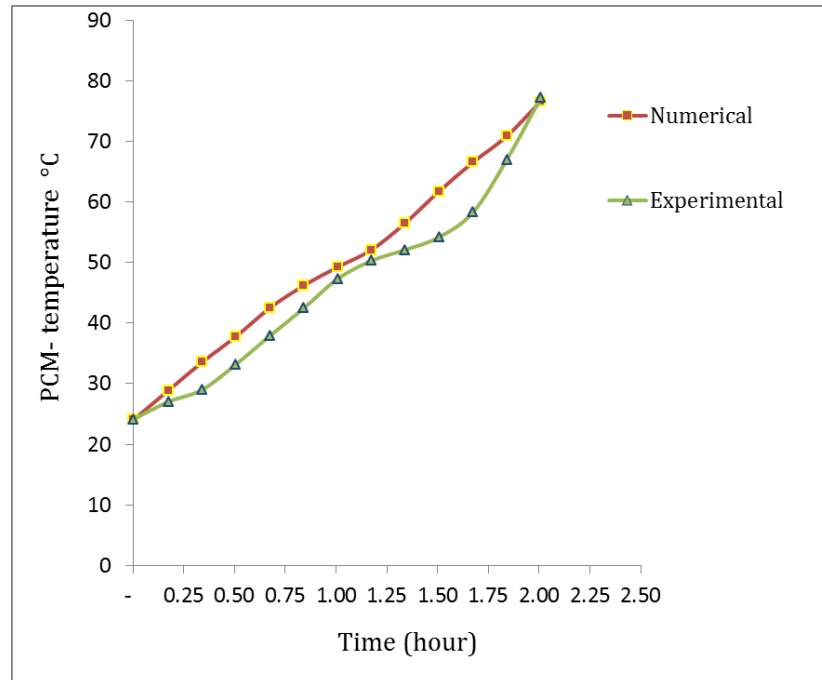


Figure 5-33. Numerical and experimental temperatures results for PCM during charging heat process

Figure 5-34 shows another acceptable agreement between the numerical and experimental results recorded for the PCM temperatures during the heat discharge process. The results showed that the period of changing the phase of the PCM material from the liquid to solid phase state in the numerical solution was longer than in the experimental tests, due to the different way to measure temperature, and not having a mechanism for photographing in the experimentally tests as well. The total error rate during the heating process is (4.12 %).

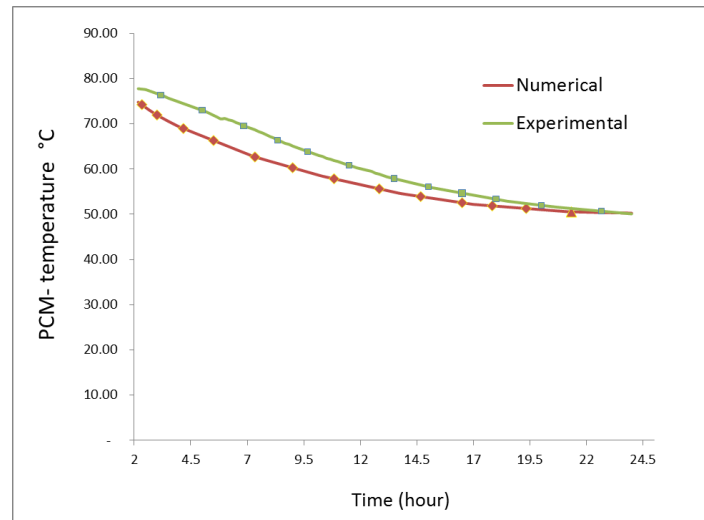


Figure 5-34. Numerical and experimental temperatures result for 31% PCM during discharging heat process.

Figure 5-35 shows, a good agreements between the results of the numerical solution and the results of the experimental tests of water temperatures again during the charging and discharging heat process. This is because of all results values, whether numerical or experimental, represented the average water temperature in the tank. The total error rate during the heating process is (1.33 %).

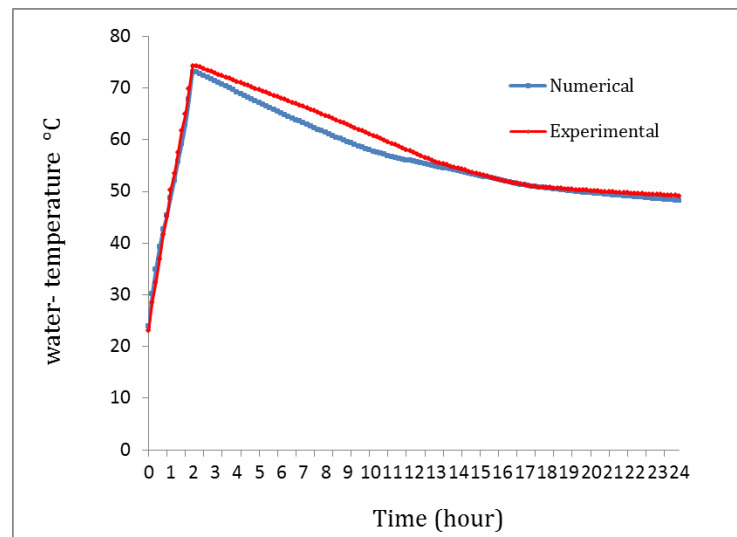


Figure 5-35. Numerical and experimental temperatures result for water, during charging and discharging heat process.

5.4. Validation with similar work

To ensure the validity of the results of our experimental research, the current work is verified to a similar experimental study by Al-Hinti et al. [31]. A preliminary investigation was conducted in Amman - Jordan during April of 2008. Thirty-eight cylindrical aluminium containers filled with paraffin wax with a melting temperature of 52 °C were used. The total amount of paraffin wax used is 38 kg. The volume of paraffin wax containers represents 47% of the water tank volume. The water was heated using an electric heater of 2kw for 3 hours, and the highest water temperature was 76 °C. Results showed that PCM material could keep the water temperature by up to 13 °C higher than that of without PCM, and the water remained hot at a level 36, and 22 °C above the ambient temperature, in the cases with, and without using PCM, respectively. In the present research, an amount of 8 kg of paraffin wax was used, the number of wax containers was 32 with a volume of 0.31 litre. The volume of wax containers accounts for 31% of the water volume in the tank. Results showed that the hot water temperature at the end of the testes was about 7.4 °C higher than the water temperature without PCM. Furthermore, the water is still hotter about 27.9 and 21.2 ° C above the ambient temperature, in the cases with and without using PCM, respectively.

Figure 5-36, shows a comparison between the current work and reference [31] in terms of the temperature difference between the water and the ambient, for the cases of with and without PCM.

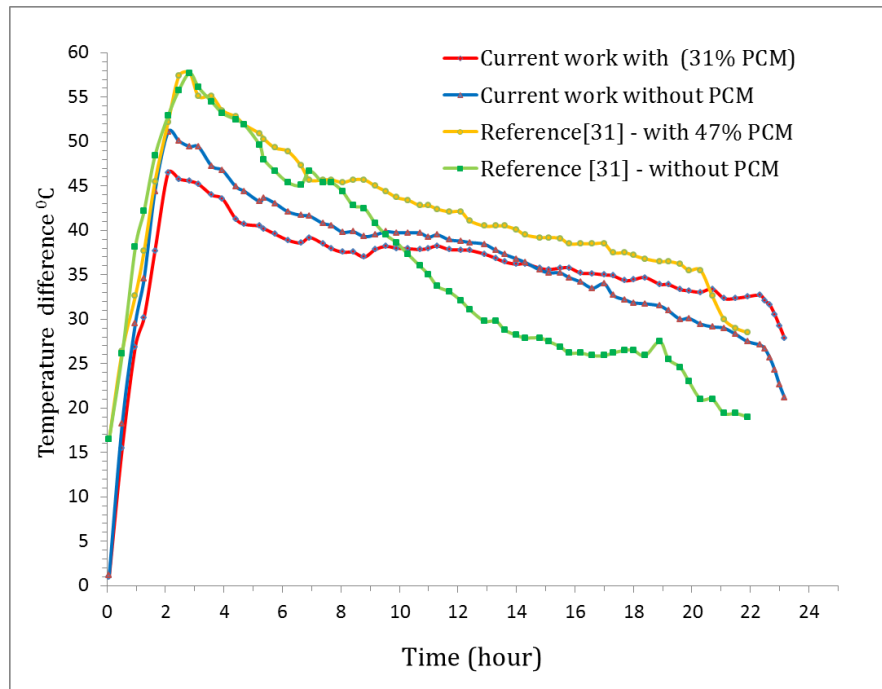


Figure 5-36. Comparison between the current work and [31] in terms of temperature difference between the water and the ambient for the cases of with and without PCM.

The difference in the results between the current work and the previous reference[31], is due to the difference in the percentage of paraffin wax quantities used, the size of the different packaging used, and the effect of totally different weather conditions between the Jordanian and Iraqi airs.

**C
H
A
P
T
E
R**

6

Conclusions and recommendation

Chapter Six

Conclusions and Recommendation

This research aims to highlight the effect of using phase change materials on the performance of a solar water heating system. This system is experimentally tested under the climatic conditions of the city of Karbala in Iraq from March 20 to 20 April 2019. Also, a numerical model of the proposed solar water heating system was carried out using ANSYS Fluent. The experimental and numerical results are validated against each other, and similar previous work and good agreements are achieved. This chapter summarizes the principal conclusions of this work and the future recommendations related to this work.

6.1 Conclusions

The main conclusions obtained from this research can be summarized in the following points:

1. The proposed PCM solar heating system can achieve a water temperature of about 9.3 °C higher than that of without using PCM.
2. The improvement in hot water temperature due to the use of PCM is 19.95, 22.47, and 23.1 % utilizing flow rates of 1, 3 and 5 L/min, respectively using real solar energy.
3. The improvement in heat storage due to use PCM is 13.9, 14.74, and 14.05 % utilizing flow rates of 1, 3 and 5 L/min, respectively.
4. As the solar radiation increases the temperature difference between the inlet and the outlet of the collector rises to reach its maximum value at noon.
5. As the water flow rate increases, the temperature difference between the inlet and the outlet of the collector decreases. Maximum temperature differences of 5.8, 3.1, and 2.1°C using flow rate 1, 3, and 5 L/min, respectively. Also, the overall thermal efficiency increases and the

improvement rate of thermal storage is 1.3%, and 4.3% at 3 L/min, and 5 L/min respectively.

6. As the water flow rate increases, the PCM melting time decreases. The melting time of paraffin wax was 4.334, 4.166 and 4 hour utilizing flow rate of 1, 3 and 5 L/min, respectively. The rate of improvement in the melting time was 3.84% and 7.7% using 3 and 5 L/min compared to the melting time at 1 L/ min.
7. Adding copper mesh (25 g) reduces the melting time by 12.5%, while there has a limited effect on the solidification time. Also, it affects the heat stored negatively as a result of reducing the amount of paraffin wax.
8. A good agreements are achieved between the experimental and numerical results with an average deviation of about 5.17%.

6.2. Recommendations

The recommendations for future work as follow:

1. Studying the designed solar water heating system in a real application for providing hot water for a specified period.
2. Studying other types of PCM materials with different arrangements and packaging types.
3. Using other metal additives or other technologies to improve the thermal conductivity of the PCM materials.

REFERENCE

Reference

- [1] C. Julian Chen, "PHYSICS OF SOLAR ENERGY". Copyright © 2011 by John Wiley & Sons, Inc. All rights reserved Published by John Wiley & Sons, Inc., Hoboken, New Jersey Published simultaneously in Canada, 2011.
- [2] Hussein A. Kazem and Miqdam T. Chaichan, "Status and future prospects of renewable energy in Iraq," *Renewable and Sustainable Energy Reviews* 16 (2012) 6007–6012 Contents
- [3] Fadhil Abdulrazzaq Kareem, Noor Samir Lafta and Doaa Zaid Khalaf, "Energy and Exergy Analysis of the Solar Radiation Incident over Iraq," *IOP Conf. Ser. Mater. Sci. Eng.*, vol. 518, no. 3, 2019.
- [4] Y. Al-Douri and Fayadh M. Abed, "Solar energy status in Iraq: Abundant or not - Steps forward," *Journal. Renewable Sustainable Energy* vol. 8, no. 2, 2016.
- [5] R. Senthilkumar, N.Sithivinayagam N. Shankar, "Experimental Investigation of Solar Water Heater Using Phase Change Material.," *International Journal of Research in Advent Technology*, Vol.2, No.7, July 2014.
- [6] Yangzhuoran Liu, "Design a Solar Water Heat System for Pony Club " *Faculty of Engineering and Sustainable Development.*, June, 2012.
- [7] Sunil.K.Amrutkar, Satyshree Ghodke and. K. N. Patil, "Solar Flat Plate Collector Analysis," *IOSR Journal of Engineering.*, vol. 02, no. 02, pp. 207–213, 2013.
- [8] Soteris A. Kalogirou, *Solar energy engineering: processes and systems*, Second Edition. *Journal of Chemical Information and Modelin.*vol. 53, no. 9. 2013.
- [9] L. M. Ayompe, A. Duffy, M. Mc Keever, M. Conlon, and S. J. McCormack, "Comparative field performance study of flat plate and heat pipe evacuated tube collectors (ETCs) for domestic water heating systems in a temperate climate," *Energy*, vol. 36, no. 5, pp. 3370–3378, 2011.
- [10] Zanis.Jesko, "Classification of solar collectors," *Journal Engineering for Rural Development.*, pp. 22–27, 2008.
- [11] Anna Heimsath, "Concentrating solar collectors for process heat and electricity generation," *IOSR Journal of Engineering*, vol. 44, no. 8, pp. 61–65, 2009.

- [12] Edina Milisic, "Modelling of energy storage using phase-change materials (PCM materials)," Master's Thesis Submission date: July 2013, Norwegian University of Science and Technology Department of Energy and Process Engineering.
- [13] Robynne Murray, "Simultaneous Charging and Discharging of a Latent Heat Energy Storage System for Use With Solar Domestic Hot Water," Master's Thesis, Dalhousie University Halifax, Department Of Mechanical Engineering, The Nova Scotia July 2012.
- [14] A. Shukla, D. Buddhi, and R. L. Sawhney, "Solar water heaters with phase change material thermal energy storage medium: A review," *Renew. Sustain. Energy Rev.*, vol. 13, no. 8, pp. 2119–2125, 2009.
- [15] T. E. Alam, "Experimental Investigation of Encapsulated Phase Change Materials for Thermal Energy Storage," *Brook. Pap. Econ. Act.*, no. January, p. 54, 2015.
- [16] R. M. Patil and C. Ladekar, "Experimental Investigation for Enhancement of Latent Heat Storage using Heat pipes in Comparison with Copper Pipes," *Int. Ref. J. Eng. Sci.*, vol. 3, no. 9, pp. 44–52, 2014.
- [17] Davide Lora, "Phase change material product design. Market and business development assessment in the food industry," Master's Thesis, Universities Politecnica De catalunya, July 2014.
- [18] R. Senthilkumar and N. S. N. Shankar, "Experimental Investigation of Solar Water Heater Using Phase Change Material," *International Journal of Research in Advent Technology*, Vol.2, No.7, July 2014 .
- [19] J. M. P. Q. Delgado, J. C. Martinho, A. Vaz Sá, A. S. Guimarães, and V. Abrantes, "Thermal Energy Storage with Phase Change Materials," *J. Eng. Sci* ,no. 20, pp. 75–98, 2012.
- [20] Atul Sharma, V. V Tyagi, C. R. Chen, and D. Buddhi, "Review on thermal energy storage with phase change materials and applications," *Renewable and Sustainable Energy Reviews* vol. 13, pp. 318–345, 2009.
- [21] Ibrahim Dincer, and M. A. Rosen, THERMAL ENERGY STORAGE, SYSTEMS AND APPLICATIONS, SECOND EDITION, SECOND EDI. United Kingdom For: This edition first published 2011 Copyright © 2011, John Wiley & Sons, Ltd, 2011.
- [22] Manish K. Rathod, "Thermal stability of phase change materials used in latent heat energy storage systems," *Renewable and Sustainable Energy*

Reviews, Volume 18, February 2013, Pages 246-258.

- [23] Ruijun Pan, “Energy density and volume expansion in solid-liquid phase change , for energy applications,” Master of Science Thesis KTH School of Industrial Engineering and Management Energy Technology EGI-2013-075MSC EKV965 pp. 5–6, 2013.
- [24] David MacPhee, “Performance Investigation of Various Cold Thermal Energy Storages,” Master Thesis of Applied Science in Mechanical Engineering. University of Ontario Institute of Technology July 2008.
- [25] S. D. Sharma and K. Sagara, “Latent Heat Storage Materials and Systems: A Review,” *Int. J. Green Energy*, vol. 2, no. 1, pp. 1–56, 2005.
- [26] Thomas Hasenöhrl, “An Introduction to Phase Change Materials as Heat Storage Mediums,” Dept. of Energy Sciences, Faculty of Engineering, Lund University, Box 118, 22100 Lund, Sweden. May 09, 2009.
- [27] E. Oró, A. de Gracia, A. Castell, M. M. Farid, and L. F. Cabeza, “Review on phase change materials (PCMs) for cold thermal energy storage applications,” *Appl. Energy*, vol. 99, pp. 513–533, 2012.
- [28] A. Heinz and W. Streicher, “Application of phase change materials and PCM-slurries for thermal energy storage,” *Ecstock Conf.*, p. 8, 2006.
- [29] E. B. S. Mettawee and G. M. R. Assassa, “Experimental study of a compact PCM solar collector,” *Energy*, vol. 31, no. 14, pp. 2958–2968, 2006.
- [30] H. Benli and A. Durmuş, “Performance analysis of a latent heat storage system with phase change material for new designed solar collectors in greenhouse heating,” *Sol. Energy*, vol. 83, no. 12, pp. 2109–2119, 2009.
- [31] I. Al-Hinti, A. Al-Ghandoor, A. Maaly, I. Abu Naqeera, Z. Al-Khateeb, and O. Al-Sheikh, “Experimental investigation on the use of water-phase change material storage in conventional solar water heating systems,” *Energy Convers. Manag.*, vol. 51, no. 8, pp. 1735–1740, 2010.
- [32] Mohammad Ali Fazilati, Ali Akbar Alemrajabi, “Phase change material for enhancing solar water heater, an experimental approach,” *Energy Convers. Manag.*, vol. 71, pp. 138–145, 2013.
- [33] Miqdam T. Chaichan, Khalil I. Abaas, and Humam M. Salih, “Practical Investigation for Water Solar Thermal Storage System Enhancement Using Sensible and Latent Heats in Baghdad-Iraq Weathers,” *Journal of*

- Al Rafidain University College 158 ISSN (1681 – 6870). 33, pp. 158–182, 2014.
- [34] K.Kavitha¹, S.Arumugam, “A Study on Phase Change Material (PCM) For Insitu Solar Thermal Energy Collection and Storage,” *International Journal of Innovative Research in Science, Engineering and Technology*, vol. 4, no. 2, pp. 350–354, 2015.
- [35] L Mongibello, M Atrigna, N Bianco, M Di Somma, G Graditi¹ and N Risi, “Experimental test of a hot water storage system including a macro-encapsulated phase change material (PCM),” *J. Phys. Conf. Ser.*, vol. 755, no. 1, 2017.
- [36] R. Senthil and M. Cheralathan, “Effect of the phase change material in a solar receiver on thermal performance of parabolic dish collector,” *J.Therm. Sci.*, vol. 21, no. 6, pp. 2803–2812, 2017.
- [37] K. Nasir, M. Ali, and A. AL Mamoori, “Thermal Characteristics of Phase Change Material Used As Thermal Storage System By Using Solar Energy,” *Kufa J. Eng.*, vol. 9, no. 1, pp. 1–22, 2018.
- [38] K. K. Gupta and M. Ramachandran, “Effect of Ethylene glycol as Phase Change Material in a Cold Storage Unit on retention of cooling,” *IOP Conf. Ser. Mater. Sci. Eng.*, vol. 377, no. 1, 2018.
- [39] P. C. Eames and P. W. Griffiths, “Thermal behaviour of integrated solar collector/storage unit with 65 °C phase change material,” *Energy Convers. Manag.*, vol. 47, no. 20, pp. 3611–3618, 2006.
- [40] P. Sarafraz, “Thermal optimization of flat Plate PCM capsules in natural convection solar water heating systems,” p. 182, 2013.
- [41] A. Kumar, G. Kumar, and S. A. I. Nath, “Design and Fabrication of Hot Water Tank Using Phase Change Material With Ansys Model,” *Int. J. Chem. Sci*, vol. 14, no. 4, pp. 3037–3045, 2016.
- [42] W. M. Asyraf, A. Vasu, F. Y. Hagos, M. M. Noor, and R. Mamat, “Transient modelling of heat loading of phase change material for energy storage,” *MATEC Web Conf.*, vol. 90, p. 01078, 2017.
- [43] K. Chintakrinda, R. J. Warzoha, R. D. Weinstein, and A. S. Fleischer, “Quantification of the impact of embedded graphite nanofibers on the transient thermal response of paraffin phase change material exposed to high heat fluxes,” *J. Heat Transfer*, vol. 134, no. 7, 2012.
- [44] C. L. Saw, H. H. Al-Kayiem, and A. L. Owolabi, “Experimental investigation on the effect of PCM and Nano-enhanced PCM of

- integrated solar collector performance,” *WIT Trans. Ecol. Environ.*, vol. 179 VOLUME, pp. 899–909, 2013.
- [45] F. Kenfack and M. Bauer, “Innovative Phase Change Material (PCM) for heat storage for industrial applications,” *Energy Procedia*, vol. 46, pp. 310–316, 2014.
- [46] R. A. Hassan, A. K. Shyaa and B. M. Kadim , “Experimental Study on the Effect of Using Metallic Brushes on the Charging” *Journal of Engineering*, vol. 21, no. December, pp. 1–15, 2015.
- [47] B. M. H. Hammendy, “Experimental Study on the Effect of Insertion of Copper Lessing Rings in Phase Change Material (PCM) on the Performance of Thermal Energy Storage " *Al-Khwarizmi Engineering Journal*, vol. 11, no. December 2017, pp. 60–72, 2015.
- [48] N Beemkumar, A Karthikeyan, A Manoj, J S Keerthan, Joseph Paul Stallan, Amithkishore P, “Investigation of Sensible and Latent Heat Storage System using various HTF,” *IOP Conf. Series: Materials Science and Engineering* 197 (2017).
- [49] A. R. Abdulmunem, “Passive Cooling By Utilizing The Combined Pcm / Aluminum Foam Matrix To Improve Solar Panels Performance ” *The Iraqi Journal For Mechanical And Material Engineering*, Vol.17, No4, Dec. 2017.
- [50] Agbanigo, A. Olubunmi and Ajayi, I. S. “Performance Evaluation of Solar Water Heating System with PCM Thermal Storage,” *Journal of Multidisciplinary Engineering Science and Technology (JMEST) ISSN: 2458-9403 Vol. 4 Issue 10, October - 2017*
- [51] A. A. Khudhair, F. F. Hatem and D. A. M. Ridha, “Enhancement of Thermal Storage Properties of Phase Change Material by Using Metallic Swarf,” *Eng. Technol. J.*, vol. 36, no. 5A, 2018.
- [52] A. Mahmud, K. Sopian, M. A. Alghoul, M. Sohif, and A. M. Graisa, “Using a paraffin wax-aluminum compound as a thermal storage material in a solar air heater,” *J. Eng. Appl. Sci.*, vol. 4, no. 10, pp. 74–77, 2009.
- [53] K. Joudi and A. Taha, “Simulation of Heat Storage and Heat Regeneration in Phase Change Material,” *J. Eng.*, vol. 18, no. 9, 2012.
- [54] S. F. Hosseinizadeh, A. A. R. Darzi, and F. L. Tan, “Numerical investigations of unconstrained melting of nano-enhanced phase change material (NEPCM) inside a spherical container,” *Int. J. Therm. Sci.*, vol.

51, no. 1, pp. 77–83, 2012.

- [55] S. Mat, A. A. Al-Abidi, K. Sopian, M. Y. Sulaiman, and A. T. Mohammad, “Enhance heat transfer for PCM melting in triplex tube with internal-external fins,” *Energy Convers. Manag.*, vol. 74, pp. 223–236, 2013.
- [56] K. D. Reddy, P. Venkataramaiah, and T. R. Lokesh, “Parametric Study on Phase Change Material Based Thermal Energy Storage System,” *Energy Power Eng.*, vol. 06, no. 14, pp. 537–549, 2014.
- [57] J. P. Solano, F. Roig, F. Illán, and A. García, “Conjugate Heat Transfer in a Solar-Driven Enhanced Thermal Energy Storage System Using PCM,” Proceedings of the 4th World Congress on Mechanical, Chemical, and Material Engineering (MCM'18) Madrid, Spain – August 16 – 18, 2018 pp. 1–8, 2018.
- [58] T. L. Bergman, D. Of M. E. U. Of Connecticut, A. S. Lavine, And M. P. Incropera, *"Introduction to Heat Transfer" Sixth Edition by John Wiley & Sons, Inc.* 2011.
- [59] A. Sharma, *"Introduction to Computational Fluid Dynamics", ISBN: 978-0-13-127498-3 British Library Cataloguing-in-Publication Data*, vol. M. 2016.
- [60] G. Ziskind, *Modelling of heat transfer in phase change materials (PCMs) for thermal energy storage systems.* Woodhead Publishing Limited, 2014.
- [61] Ibrahim Dincer and Mehmet Akif Ezan, *"Heat storage: A unique solution for energy systems" Green Energy and Technology.* ISSN 1865-3529 ISSN 1865-3537 (electronic) ISBN 978-3-319-91892-1 ISBN 978-3-319-91893-8 (eBook) Library of Congress Control Number: 2018942212, 2018.
- [62] I. I. Rikoto and M. M. Garba, “Design , Construction and Installation of 250-Liter Capacity Solar Water Heating System at Danjawa Renewable Energy Model Village,” *International Journal of Engineering Sciences* www.tijournals.com ISSN:no. 4, pp. 39–44, 2015.
- [63] E. Ekramian, S. G. Etemad, and M. Haghshenasfard, “Numerical Analysis of Heat Transfer Performance of Flat Plate Solar Collectors,” *J. Fluid Flow, Heat Mass Transf.*, vol. 1, 2014.
- [64] N. Ghimire and R. Pokhrel, “Analysis of Parameters of Locally Manufactured Flat Tube Solar Water Heater to Increase the Efficiency,”

Rentech Symposium Compendium, Volume 3, September 2013 vol. 520, pp. 26–29, 2013.

- [65] N. G. E. John, “Performance Optimization Of A Thermosyphon Flat Plate Solar Water Heater,” , Master of Thesis, Jomo Kenyatta University Of Agriculture And Technology, 2019.
- [66] G. IORDANOU, “Flat-Plate Solar Collectors for Water Heating with Improved Heat Transfer for Application in Climatic Conditions of the Mediterranean Region,” *Durham E-Theses Onlin*, 2009.
- [67] N. Arslanogla, “Optimization of Tili Angle for Solar Collectores,” *Int. J. Energy Power Eng.*, vol. 10, no. 5, pp. 500–503, 2016.
- [68] A. Klevinskis and V. Bučinskas, “Analysis of a Flat-Plate Solar Collector,” *Moksl. - Liet. ateitis*, vol. 3, pp. 39–43, 2011.
- [69] Datacolor International, “Colour repeatability and reproducibility,” *Text. Technol. Int.*, pp. 138–139, 1996.
- [70] J. A. Duffie, W. A. Beckman, and J. McGowan, "*Solar Engineering of Thermal Processes*"*Fourth Edition*, vol. 53, no. 4. 1985.

APPENDIX. A

Appendix A

A.1 Calculations of the Rayleigh number (Ra) [50]

Transition in a free convection boundary layer depends on the relative magnitude of the buoyancy and viscous forces in the fluid. It is customary to correlate its occurrence in terms of the Rayleigh number, which is simply the product of the Grashof and Prandtl numbers [50].

For The Long Horizontal Cylinder, the critical Rayleigh number is:

$$Ra = Gr.Pr = \frac{g.\beta(T_f-T_i)x^3}{\nu.\alpha} \sim 10^9 \quad (A.1)$$

Ra = Rayleigh number

Gr = Grashof number

Pr = Prandtl number

g = Gravitational acceleration (9.81), m/s²

β = Thermal expansion coefficient, 1/k

T_F = Final temperature, °C

T_i = Initial temperature, °C

ν = Kinematic viscosity, m²/s

α = water thermal diffusivity, kg.m³/J

x = Characteristic length (The diameter of the heater) = 0.05 m

if $Ra \geq 10^9$ the flow permit transition to turbulence.

Water properties (ρ , C_p , ν , β , K), are taken at the average water temperature in the tank T_{min}, from tables C1 in Appendix C.

$$T_{min} = \frac{(T_f+T_i)}{2} \quad (A.2)$$

$$T_{min} = \frac{(351+295)}{2} = 323 \text{ K} = 50 \text{ }^\circ\text{C}$$

$$\alpha = \frac{K}{\rho.C_p} = 1.5575 * 10^{-7} \text{ m}^2/\text{s} \quad (A.3)$$

Ra = 3.27*10⁸ the flow is laminar

A.2 Calculation of the top loss coefficient of solar collector [63]

$$U_t = \frac{1}{N_g} + \frac{\sigma(T_p^2 + T_a^2)(T_p + T_a)}{\frac{1}{\varepsilon_p + 0.00591N_g h_w} + \frac{2N_g - f + 0.133\varepsilon_p}{\varepsilon_g} - N_g} \quad (\text{A.4})$$

$$\frac{C}{T_p} \left[\frac{T_p - T_a}{N_g + f} \right]^{0.33} + \frac{1}{h_w}$$

The wind loss coefficient given by:

$$h_w = \frac{8.6V_w^{0.6}}{L^{0.4}} \quad (\text{A.5})$$

$$\text{When } 0 < \beta < 70 \quad \text{then} \quad C = 520(1 - 0.000051\beta^2) \quad (\text{A.6})$$

$$f = (1 + 0.089h_w - 0.1166h_w\varepsilon_p)(1 + 0.078N_g) \quad (\text{A.7})$$

Where, ε_p the emissivity of plate (0.1)

ε_g the emissivity of glass (0.88)

N_g the number of glass , $\sigma = 5.67 * 10^{-8}$

A.3 The declination angle

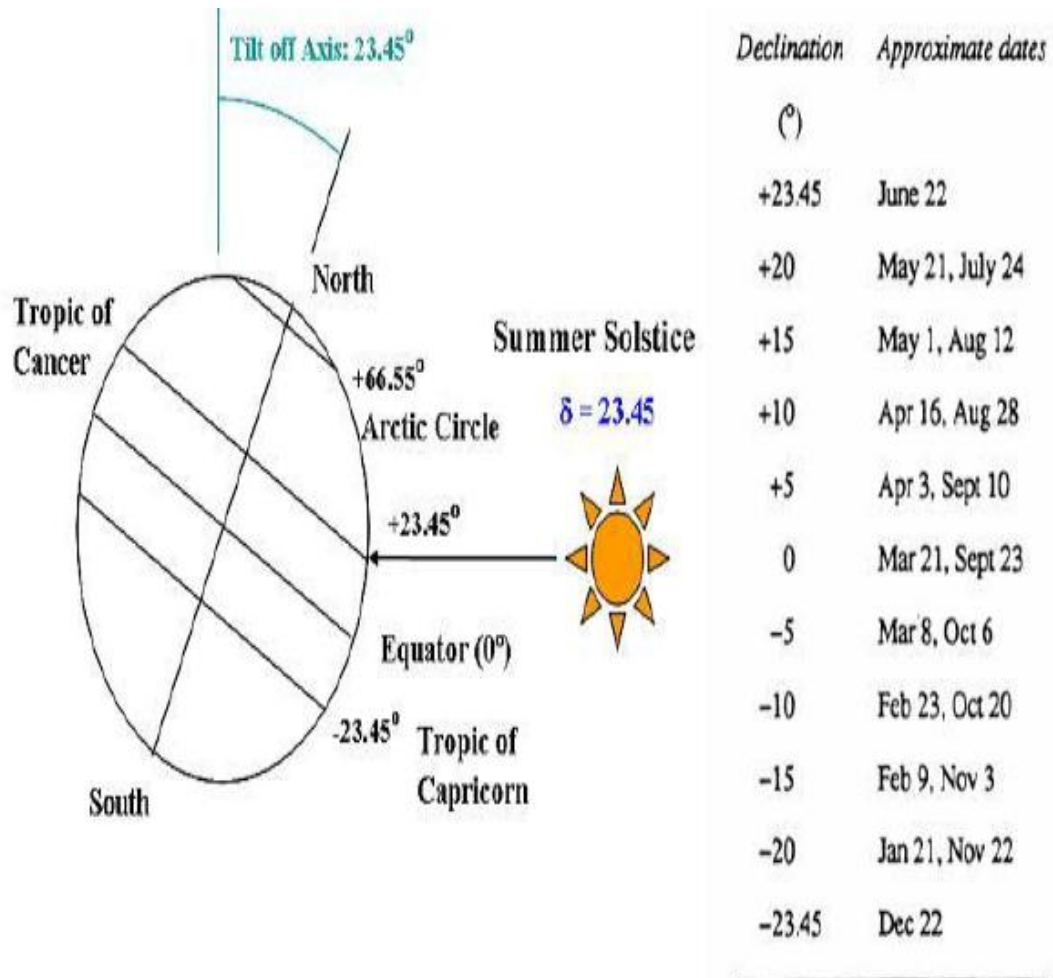


Fig. (A.1). The declination angle

A.4. Solar angles for horizontal, inclined and vertical surfaces

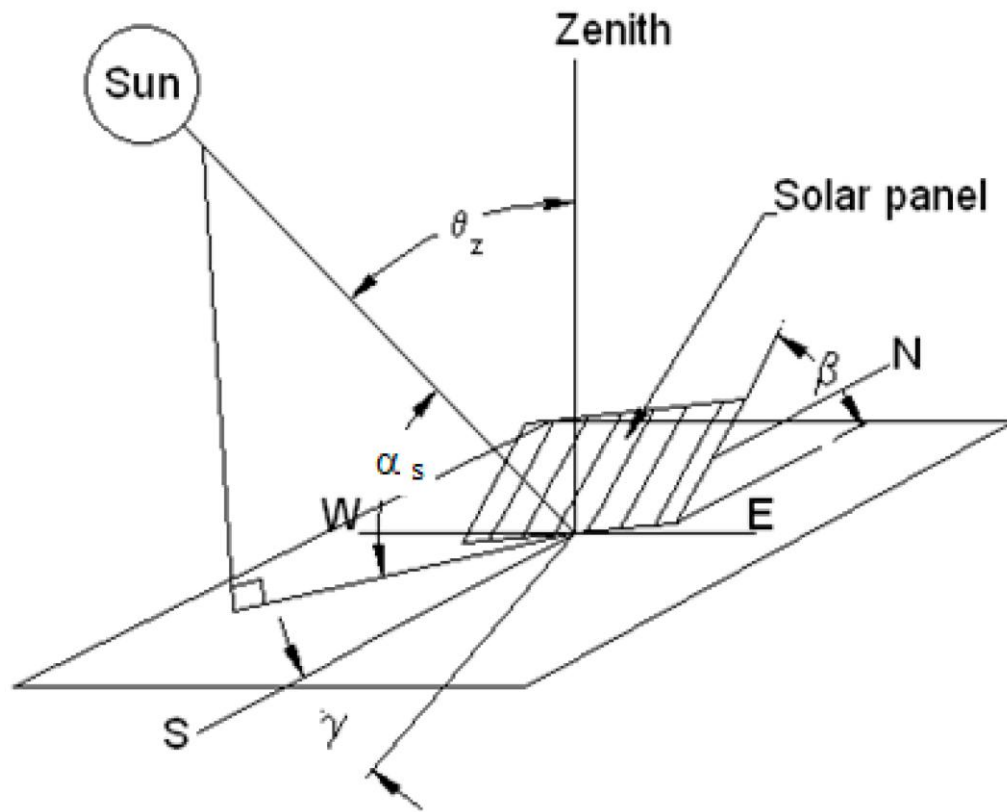


Fig. (A.2). Solar angles for horizontal, inclined and vertical surfaces

APPENDIX. B

Appendix (B)

The Calibration of Instruments used in Thesis:

B.1. The temperature meter and thermocouple and Solar power meter

REPUBLIC OF IRAQ
MINISTRY OF SCIENCE & TECHNOLOGY
RENEWABLE ENERGY DIRECTORATE

جمهورية العراق
وزارة العلوم والتكنولوجيا
دائرة الطاقات المتجددة
معاً لمساعدة جوازنا المصلحة الواملة لحجر الإرماب
العدد: ط م / ١٩١٤
التاريخ: ٢٠١٨ / ١٢ / ١٩

وزارة العلوم والتكنولوجيا
Ministry Of Science & Technology

الى / جامعة كربلاء / كلية الهندسة
م / نتائج

تحية طيبة....

اشارة الى كتابكم المرقم (٤٥٣٤) بتاريخ ٢٠١٨/١٢/٤ الخاص بطالب الماجستير حسن فتحي علوان , نرفق لكم طيا نتائج الفحص والمعايرة مع البيانات والمخطط لكل مما يلي:

١. فحص ومعايرة لمزدوج حراري (Thermo - couple) عدد (١)
٢. فحص ومعايرة لجهاز قراءة وتسجيل بيانات (Data logger)
٣. فحص ومعايرة لجهاز (Solar member)

للتفضل بالاطلاع... مع التقدير.

وزارة العلوم والتكنولوجيا
دائرة الطاقات المتجددة

وزارة العلوم والتكنولوجيا
Ministry Of Science & Technology

المرفقات
- نتائج الفحص
- بيانات ومخطط

ضياء جليل حسين
معاون المدير العام
٢٠١٨ / ١٢ / ١٩

نسخة منه الى /
- قسم التخطيط والمتابعة / شعبة المعلومات والاحصاء ... مع الاوليات.

نتائج الفحص والمعايرة:

١. تم اجراء فحص ومعايرة بين مزدوج حراري (Thermo couple) نوع k قياسي مع مزدوج حراري مصنع عدد (١) ولمدى درجة حرارة (٣٢,٩- ١٦٥,٨) سيليزي من خلال استخدام فرن حراري بمواصفات خاصة. حيث كان اعلى فرق مسجل اعلى من المزدوج القياسي هو (١.١) سيليزي وكما موضح في البيانات و المخطط المرفق واعلى فرق مسجل اقل من المزدوج القياسي هو (٤,٣) سيليزي وكما موضح في البيانات والمخطط المرفق.

٢. تم مقارنة القراءات بين جهاز (channel SD card Data Logger) الذي يحمل الرقم (١.٣٨٣٢٥٥) المطلوب فحصه مع جهاز مماثل له معتمد لدينا حيث وجد ان القراءات كانت متقاربة الى حد ما والفرق البسيط يعزى الى الاختلاف في مدى نسبة الخطأ من جهاز الى اخر علما ان نتائج هذا النوع من الاجهزة يخضع لمعايير دولية قياسية .

٣. تم اجراء معايرة لجهاز قياس شدة الاشعاع الشمسي المطلوب معايرته :
(TES ١٣٣٣ Solar power meter) والذي يحمل الرقم التسلسلي (١٥٠٨٠٨٥٧٧) وذلك من خلال للمقارنة القراءات مع جهاز قياسي معتمد لدينا.



Figure (B.1): Temperature meter, thermocouples and Solar power meter calibration

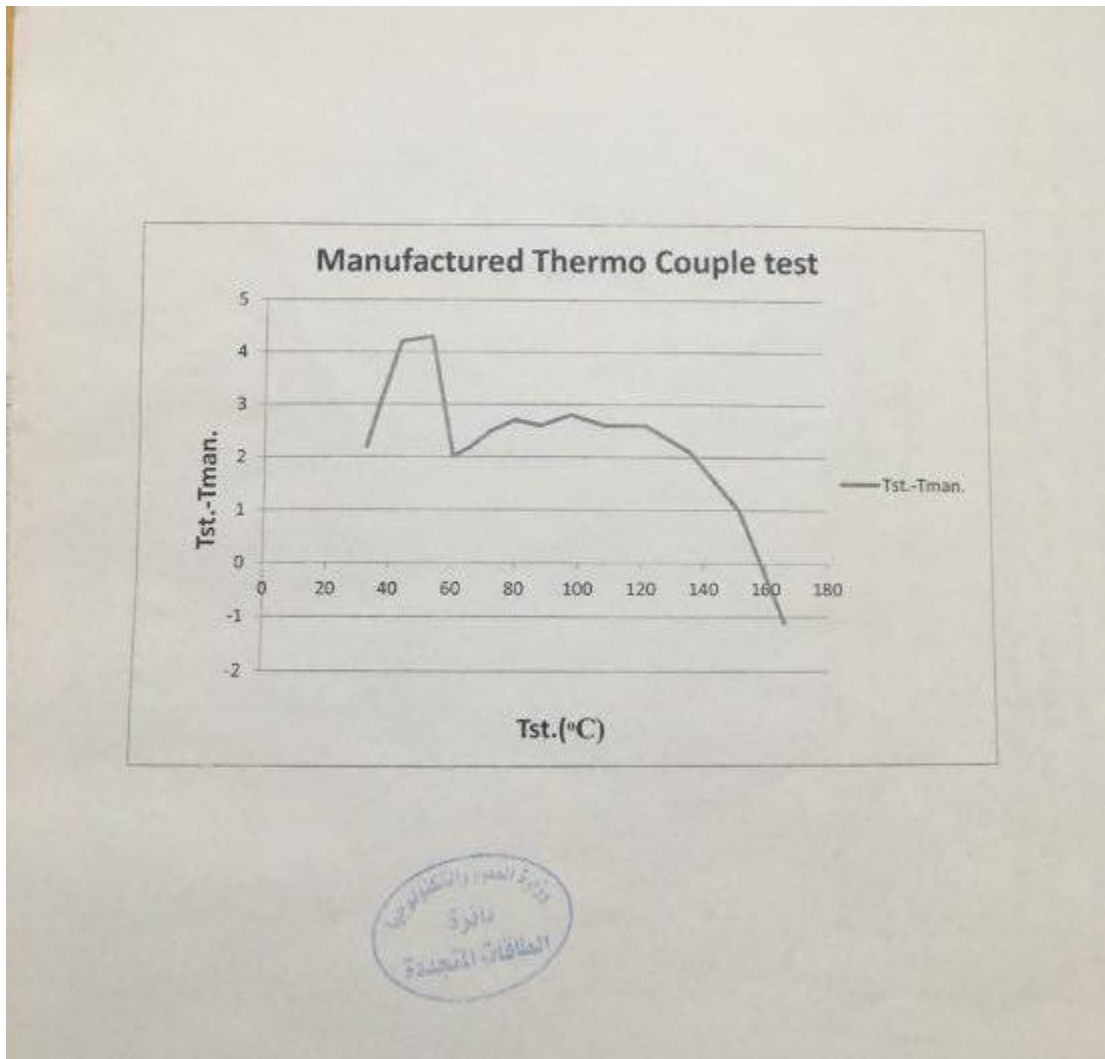


Figure (B.2): The Calibration of thermocouples

B.2. The Phase Change Material Specifications



Central Drug House (P) Ltd.

AN ISO 9001:2008 CERTIFIED COMPANY

Manufacturers of : Laboratory Fine Chemicals & Dehydrated Culture Media

www.cdhfinechemical.com

Product Specification	
PARAFFIN WAX 52-54 ⁰ C FOR HISTOLOGY	
PRODUCT CODE	184235
SYNONYMS	--
C.I. NO.	--
CASR NO.	(8002-74-2)
ATOMIC OR MOLECULAR FORMULA	--
ATOMIC OR MOLECULAR WEIGHT	--
PROPERTIES	Combustible
--	
PARAMETER	LIMIT
Description	White to off white translucent waxy, odourless smooth mass.
Solubility	Soluble in benzene and chloroform.
Congealing point	52 - 54 ⁰ C
Clarity	Passes test.
Free acid	To pass the test.
MAXIMUM LIMIT OF IMPURITY	
Sulphated ash	Not more than 0.1%
Note(s) : Assay (if applicable) method mentioned.	
WARNING	
Hazard statements : May cause respiratory irritation. Causes skin irritation. Causes serious eye irritation.	
Precautionary statements	
Prevention: Avoid breathing dust/fume/gas/mist/vapours/spray. Wash thoroughly after handling. Use only outdoors or in a well-ventilated area. Wear protective gloves/protective clothing/eye protection/face protection.	
Response: IF INHALED: Remove to fresh air and keep at rest in a position comfortable for breathing. IF IN EYES: Rinse cautiously with water for several minutes. Remove contact lenses, if present and easy to do. Continue rinsing. Call a POISON CENTER or doctor/physician if you feel unwell. If eye irritation persists: Get medical advice/attention.	
Disposal: Dissolve the chemical to be disposed, in water and allow it to run to waste, diluting with large quantities of water. The quantities greater than 10g should be dissolved in water and transferred to heavy metal waste drums for collection by specialist disposal company.	
Hazard Pictogram(s) :	
 GHS07	

Figure (B.3): Paraffin wax specification

B.3. Calibration of flowmeter

The flow meter (range 1-18) L/min is calibrated with using a stopwatch and graded glass cylinder. The volume flow rate was utilized in the calibration of flow meter is 1000, 1500, 2000 and 2500 mL with the following steps, as shown in Figure B.4.

- A volume of water was heaped up in graded glass cylinder after override through the flowmeter which reads 1 L/min
- The period was registered by using the stopwatch for 60 seconds.
- The volume flow rate was gotten it with dividing the volume on time.

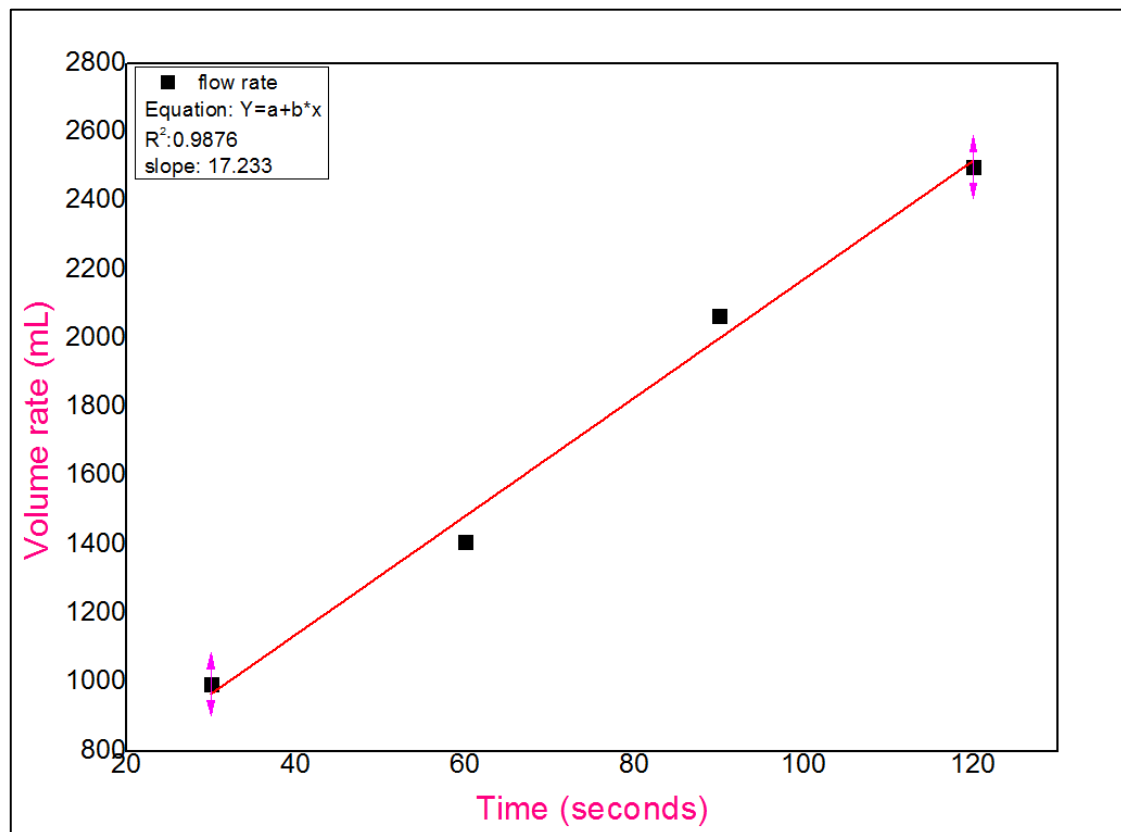


Figure (B.4): Calibration of flowmeter

APPENDIX. C

Appendix (C)

C.1. Thermophysical properties of pure water

Table C.1 shows thermophysical properties of pure water at atmospheric pressure[21].

Table C.1. Thermophysical properties of pure water at atmospheric pressure[21]

T(°C)	$\rho(\text{kg/m}^3)$	$\mu \times 10^3(\text{kg/m}\cdot\text{s})$	$\nu \times 10^6(\text{m}^2/\text{s})$	k(W/m·K)	$\beta \times 10^5(1/\text{K})$	Cp(J/kg·K)	Pr
0	999.84	1.7531	1.7533	0.5687	-6.8140	4209.3	12.976
5	999.96	1.5012	1.5013	0.578	1.598	4201	10.911
10	999.7	1.2995	1.2999	0.5869	8.79	4194.1	9.286
15	999.1	1.136	1.137	0.5953	15.073	4188.5	7.991
20	998.2	1.0017	1.0035	0.6034	20.661	4184.1	6.946
25	997.07	0.8904	0.893	0.611	20.57	4180.9	6.093
30	995.65	0.7972	0.8007	0.6182	30.314	4178.8	5.388
35	994.3	0.7185	0.7228	0.6251	34.571	4177.7	4.802
40	992.21	0.6517	0.6565	0.6351	38.53	4177.6	4.309
45	990.22	0.5939	0.5997	0.6376	42.26	4178.3	3.892
50	988.04	0.5442	0.5507	0.6432	45.78	4179.7	3.535
60	983.19	0.4631	0.471	0.6535	52.33	4184.8	2.965
70	977.76	0.4004	0.4095	0.6623	58.4	4192	2.534
80	971.79	0.3509	0.3611	0.6698	64.13	4200.1	2.201
90	965.31	0.3113	0.3225	0.6759	69.62	4210.7	1.939
100	958.35	0.2789	0.2911	0.6807	75	4221	1.729

Source: D.J. Kukulka, Thermodynamic and Transport Properties of Pure and Saline Water, MSc Thesis, State University of New York at Buffalo (1981).

C.2. Thermophysical properties of air at atmospheric

Table C.2 shows thermophysical properties of air at atmospheric pressure[21].

Table C.2. Thermophysical properties of air at atmospheric pressure [21]

T(K)	$\rho(\text{kg/m}^3)$	$C_p(\text{J/kg}\cdot\text{K})$	$\mu \times 10^7(\text{kg/m}\cdot\text{s})$	$\nu \times 10^6(\text{m}^2/\text{s})$	$k \times 10^3(\text{W/m}\cdot\text{K})$	$\alpha \times 10^6(\text{m}^2/\text{s})$	Pr
200	1.7458	1.007	132.5	7.59	18.1	10.3	0.737
250	1.3947	1.006	159.6	11.44	22.3	15.9	0.72
300	1.1614	1.007	184.6	15.89	26.3	22.5	0.707
350	0.995	1.009	208.2	20.92	30	29.9	0.7
400	0.8711	1.014	230.1	26.41	33.8	38.3	0.69
450	0.774	1.021	250.7	32.39	37.3	47.2	0.686
500	0.6964	1.03	270.1	38.79	40.7	56.7	0.684
550	0.6329	1.04	288.4	45.57	43.9	66.7	0.683
600	0.5804	1.051	305.8	52.69	46.9	76.9	0.685
650	0.5356	1.063	322.5	60.21	49.7	87.3	0.69
700	0.4975	1.075	338.8	68.1	52.4	98	0.695
750	0.4643	1.087	354.6	76.37	54.9	109	0.702
800	0.4354	1.099	369.8	84.93	57.3	120	0.709
850	0.4097	1.11	384.3	93.8	59.6	131	0.716
900	0.3868	1.121	398.1	102.9	62	143	0.72
950	0.3666	1.131	411.3	112.2	64.3	155	0.723

Source: I. Dincer, Heat Transfer in Food Cooling Applications, Taylor & Francis, Washington, DC. (1997)

الملخص

تعد الطاقة الشمسية من أهم مصادر الطاقة المتجددة المستخدمة للحد من آثار التلوث والاحتباس الحراري نتيجة حرق الوقود الأحفوري، إلا أن هذه الطاقة تكون متقطعة ومتاحة خلال النهار فقط. يهدف هذا البحث إلى دراسة تجريبية ورقمية لإمكانية تحسين سعة تخزين الحرارة لنظام تسخين المياه بالطاقة الشمسية باستخدام مواد تغيير الطور (PCMs). حيث تم تصميم وتصنيع نظام تسخين للمياه بالطاقة الشمسية يحتوي على مادة البرافين يعمل في ظل الظروف المناخية لمدينة كربلاء في العراق، وتم اختبار النظام تجريبياً للفترة ما بين ٢٠ مارس إلى ٢٠ أبريل في عام ٢٠١٩.

تم استخدام مصدران رئيسيان للحرارة خلال الاختبار التجريبي، الأول هو مجمع الطاقة الشمسية ذو اللوحة المستوية والمتصلة مباشرة بخزان المياه. لهذا التكوين، تم اختبار النظام تجريبياً لحالتين، بدون PCM (يحتوي الخزان على الماء فقط) ومع ال PCM (تم تضمين حاويات PCM في خزان المياه). أما مصدر الحرارة الثاني فكان عنصر السخان الكهربائي، وقد تم استخدامه لتجنب تأثير التذبذب في كثافة الطاقة الشمسية على سلوك مادة ال PCM، وقد تكرر سيناريو مشابه لاختبار النوع الاول، للحالات بدون PCM ومعها. وقد تم استخدام شمع البارافين كمادة PCM معبأة في حاويات ألنيوم أسطوانية مغمورة داخل خزان المياه. علاوة على ذلك، فقد تم تنفيذ نمذجة رقمية باستخدام برنامج (ANSYS Fluent) (بما في ذلك عمليات ذوبان وتصلب شمع البارافين) لتسليط الضوء على سلوك مادة ال PCM أثناء عمليات الشحن / التفريغ.

وقد أظهرت النتائج أن دمج مواد ال PCM مع أنظمة تسخين المياه بالطاقة الشمسية أمر فعال ومفيد حيث يمكن لمواد ال PCM تخزين كمية إضافية من الحرارة ليتم توفيرها واستخدامها في الليل. كما أظهرت النتائج التجريبية أن نظام التسخين الشمسي PCM المقترح يمكن أن يحقق درجة حرارة ماء أعلى بنحو ٩.٣ درجة مئوية من دون استخدام PCM وان نسبة التحسن في درجة حرارة الماء الساخن بسبب استخدام PCM وصلت إلى ٢٣٪ تقريباً، في حين أن أقصى نسبة تحسن في التخزين الحراري بسبب استخدام PCM حوالي ١٤٪. كما أظهرت النتائج أن إضافة شبكة نحاسية الى مادة ال PCM قد قللت من وقت الذوبان بنسبة تصل إلى ١٢.٥٪، إلا أنها اثرت سلباً على كمية التخزين الحراري نتيجة تقليل كمية شمع البارافين. وأخيراً، تم التحقق من صحة البيانات التجريبية والعديدية وتحقيق اتفاقيات جيدة بمتوسط انحراف اجمالي بلغ حوالي ٥.١٧٪.



وزارة التعليم العالي والبحث العلمي
جامعة كربلاء
كلية الهندسة
قسم الهندسة الميكانيكية

تقصي استعمال البارافين كمادة متغيرة الطور مع الماء في أنظمة تسخين الماء بالطاقة الشمسية

رسالة مقدمة الى كلية الهندسة - جامعة كربلاء كجزء من متطلبات نيل
درجة الماجستير في علوم الهندسة الميكانيكية
(حراريات وموائع)

من قبل

حيدر سعدون ساجت

بكالوريوس ١٩٩٨

بإشراف

الاستاذ الدكتور عباس ساهي شريف

الدكتور فاضل نورالدين الموسوي

٢٠٢٠ م

١٤٤٠ هـ